

# IAEA TECDOC SERIES

IAEA-TECDOC-1991

## **Harmonization and Intercomparison of Models for Accidental Tritium Releases to the Atmosphere**

*Report of Working Group 7*

*Modelling and Data for Radiological Impact  
Assessments (MODARIA) Programme*



**IAEA**

International Atomic Energy Agency

# IAEA SAFETY STANDARDS AND RELATED PUBLICATIONS

## IAEA SAFETY STANDARDS

Under the terms of Article III of its Statute, the IAEA is authorized to establish or adopt standards of safety for protection of health and minimization of danger to life and property, and to provide for the application of these standards.

The publications by means of which the IAEA establishes standards are issued in the **IAEA Safety Standards Series**. This series covers nuclear safety, radiation safety, transport safety and waste safety. The publication categories in the series are **Safety Fundamentals**, **Safety Requirements** and **Safety Guides**.

Information on the IAEA's safety standards programme is available at the IAEA Internet site

[www.iaea.org/resources/safety-standards](http://www.iaea.org/resources/safety-standards)

The site provides the texts in English of published and draft safety standards. The texts of safety standards issued in Arabic, Chinese, French, Russian and Spanish, the IAEA Safety Glossary and a status report for safety standards under development are also available. For further information, please contact the IAEA at: Vienna International Centre, PO Box 100, 1400 Vienna, Austria.

All users of IAEA safety standards are invited to inform the IAEA of experience in their use (e.g. as a basis for national regulations, for safety reviews and for training courses) for the purpose of ensuring that they continue to meet users' needs. Information may be provided via the IAEA Internet site or by post, as above, or by email to [Official.Mail@iaea.org](mailto:Official.Mail@iaea.org).

## RELATED PUBLICATIONS

The IAEA provides for the application of the standards and, under the terms of Articles III and VIII.C of its Statute, makes available and fosters the exchange of information relating to peaceful nuclear activities and serves as an intermediary among its Member States for this purpose.

Reports on safety in nuclear activities are issued as **Safety Reports**, which provide practical examples and detailed methods that can be used in support of the safety standards.

Other safety related IAEA publications are issued as **Emergency Preparedness and Response** publications, **Radiological Assessment Reports**, the International Nuclear Safety Group's **INSAG Reports**, **Technical Reports** and **TECDOCs**. The IAEA also issues reports on radiological accidents, training manuals and practical manuals, and other special safety related publications.

Security related publications are issued in the **IAEA Nuclear Security Series**.

The **IAEA Nuclear Energy Series** comprises informational publications to encourage and assist research on, and the development and practical application of, nuclear energy for peaceful purposes. It includes reports and guides on the status of and advances in technology, and on experience, good practices and practical examples in the areas of nuclear power, the nuclear fuel cycle, radioactive waste management and decommissioning.

HARMONIZATION AND  
INTERCOMPARISON OF MODELS  
FOR ACCIDENTAL TRITIUM  
RELEASES TO THE ATMOSPHERE

The following States are Members of the International Atomic Energy Agency:

AFGHANISTAN	GEORGIA	OMAN
ALBANIA	GERMANY	PAKISTAN
ALGERIA	GHANA	PALAU
ANGOLA	GREECE	PANAMA
ANTIGUA AND BARBUDA	GRENADA	PAPUA NEW GUINEA
ARGENTINA	GUATEMALA	PARAGUAY
ARMENIA	GUYANA	PERU
AUSTRALIA	HAITI	PHILIPPINES
AUSTRIA	HOLY SEE	POLAND
AZERBAIJAN	HONDURAS	PORTUGAL
BAHAMAS	HUNGARY	QATAR
BAHRAIN	ICELAND	REPUBLIC OF MOLDOVA
BANGLADESH	INDIA	ROMANIA
BARBADOS	INDONESIA	RUSSIAN FEDERATION
BELARUS	IRAN, ISLAMIC REPUBLIC OF	RWANDA
BELGIUM	IRAQ	SAINT LUCIA
BELIZE	IRELAND	SAINT VINCENT AND THE GRENADINES
BENIN	ISRAEL	SAMOA
BOLIVIA, PLURINATIONAL STATE OF	ITALY	SAN MARINO
BOSNIA AND HERZEGOVINA	JAMAICA	SAUDI ARABIA
BOTSWANA	JAPAN	SENEGAL
BRAZIL	JORDAN	SERBIA
BRUNEI DARUSSALAM	KAZAKHSTAN	SEYCHELLES
BULGARIA	KENYA	SIERRA LEONE
BURKINA FASO	KOREA, REPUBLIC OF	SINGAPORE
BURUNDI	KUWAIT	SLOVAKIA
CAMBODIA	KYRGYZSTAN	SLOVENIA
CAMEROON	LAO PEOPLE'S DEMOCRATIC REPUBLIC	SOUTH AFRICA
CANADA	LATVIA	SPAIN
CENTRAL AFRICAN REPUBLIC	LEBANON	SRI LANKA
CHAD	LESOTHO	SUDAN
CHILE	LIBERIA	SWEDEN
CHINA	LIBYA	SWITZERLAND
COLOMBIA	LIECHTENSTEIN	SYRIAN ARAB REPUBLIC
COMOROS	LITHUANIA	TAJIKISTAN
CONGO	LUXEMBOURG	THAILAND
COSTA RICA	MADAGASCAR	TOGO
CÔTE D'IVOIRE	MALAWI	TRINIDAD AND TOBAGO
CROATIA	MALAYSIA	TUNISIA
CUBA	MALI	TURKEY
CYPRUS	MALTA	TURKMENISTAN
CZECH REPUBLIC	MARSHALL ISLANDS	UGANDA
DEMOCRATIC REPUBLIC OF THE CONGO	MAURITANIA	UKRAINE
DENMARK	MAURITIUS	UNITED ARAB EMIRATES
DJIBOUTI	MEXICO	UNITED KINGDOM OF GREAT BRITAIN AND NORTHERN IRELAND
DOMINICA	MONACO	UNITED REPUBLIC OF TANZANIA
DOMINICAN REPUBLIC	MONGOLIA	UNITED STATES OF AMERICA
ECUADOR	MONTENEGRO	URUGUAY
EGYPT	MOROCCO	UZBEKISTAN
EL SALVADOR	MOZAMBIQUE	VANUATU
ERITREA	MYANMAR	VENEZUELA, BOLIVARIAN REPUBLIC OF
ESTONIA	NAMIBIA	VIET NAM
ESWATINI	NEPAL	YEMEN
ETHIOPIA	NETHERLANDS	ZAMBIA
FIJI	NEW ZEALAND	ZIMBABWE
FINLAND	NICARAGUA	
FRANCE	NIGER	
GABON	NIGERIA	
	NORTH MACEDONIA	
	NORWAY	

The Agency's Statute was approved on 23 October 1956 by the Conference on the Statute of the IAEA held at United Nations Headquarters, New York; it entered into force on 29 July 1957. The Headquarters of the Agency are situated in Vienna. Its principal objective is "to accelerate and enlarge the contribution of atomic energy to peace, health and prosperity throughout the world".

# HARMONIZATION AND INTERCOMPARISON OF MODELS FOR ACCIDENTAL TRITIUM RELEASES TO THE ATMOSPHERE

REPORT OF WORKING GROUP 7

MODELLING AND DATA FOR RADIOLOGICAL IMPACT  
ASSESSMENTS (MODARIA) PROGRAMME

## COPYRIGHT NOTICE

All IAEA scientific and technical publications are protected by the terms of the Universal Copyright Convention as adopted in 1952 (Berne) and as revised in 1972 (Paris). The copyright has since been extended by the World Intellectual Property Organization (Geneva) to include electronic and virtual intellectual property. Permission to use whole or parts of texts contained in IAEA publications in printed or electronic form must be obtained and is usually subject to royalty agreements. Proposals for non-commercial reproductions and translations are welcomed and considered on a case-by-case basis. Enquiries should be addressed to the IAEA Publishing Section at:

Marketing and Sales Unit, Publishing Section  
International Atomic Energy Agency  
Vienna International Centre  
PO Box 100  
1400 Vienna, Austria  
fax: +43 1 26007 22529  
tel.: +43 1 2600 22417  
email: [sales.publications@iaea.org](mailto:sales.publications@iaea.org)  
[www.iaea.org/publications](http://www.iaea.org/publications)

For further information on this publication, please contact:

Radiation Safety and Monitoring Section  
International Atomic Energy Agency  
Vienna International Centre  
PO Box 100  
1400 Vienna, Austria  
Email: [Official.Mail@iaea.org](mailto:Official.Mail@iaea.org)

© IAEA, 2022  
Printed by the IAEA in Austria  
January 2022

### IAEA Library Cataloguing in Publication Data

Names: International Atomic Energy Agency.  
Title: Harmonization and intercomparison of models for accidental tritium releases to the atmosphere / International Atomic Energy Agency.  
Description: Vienna : International Atomic Energy Agency, 2022. | Series: IAEA TECDOC series, ISSN 1011-4289 ; no. 1991 | Includes bibliographical references.  
Identifiers: IAEAL 21-01474 | ISBN 978-92-0-144221-5 (paperback : alk. paper) | ISBN 978-92-0-144121-8 (pdf)  
Subjects: LCSH: Tritium — Environmental aspects. | Nuclear facilities — Accidents. | Environmental impact analysis.

## FOREWORD

Models are essential tools in evaluating radiological impacts within the safety assessment process and regulatory control of facilities as well as of activities in planned exposure situations, existing exposure situations and emergency exposure situations. Modelling the transfer of radionuclides in the environment and assessing the resulting radiation exposure of people and the environment is needed in the evaluation of the radiological impact of routine releases and accidental releases of radionuclides from such facilities and activities.

The IAEA has been organizing programmes of international model testing since the 1980s. These programmes have contributed to a general improvement in models, both in the transfer of data and in the capabilities of modellers in Member States. IAEA publications on this subject over the past three decades demonstrate the comprehensive nature of the programmes and record the associated advances that have been made.

From 2012 to 2015 the IAEA organized a programme entitled Modelling and Data for Radiological Impact Assessments (MODARIA), which focused on testing the performance of models, developing and improving models for particular environments, reaching consensus on datasets that are generally applicable in environmental transfer models and providing an international forum for the exchange of experience, ideas and research information.

Different aspects were addressed by ten working groups within MODARIA covering four thematic areas. Thematic Area 1 on the remediation of contaminated areas consisted of three working groups covering (i) remediation strategies and decision aiding techniques, (ii) exposures in contaminated urban environments and the effect of remedial measures and (iii) the application of models for assessing radiological impacts arising from naturally occurring radioactive material and contaminated legacy sites to support remediation management. Thematic Area 2 on uncertainties and variability consisted of four working groups that focused on (i) analysis of radioecological data for human and wildlife exposure assessment, (ii) uncertainty and variability analysis for assessments of radiological impacts from routine radioactive discharges, (iii) a framework for environmental change in long term safety assessments of radioactive waste disposal facilities and (iv) modelling of accidental tritium releases. Thematic Area 3 on exposures and effects on biota consisted of two working groups on (i) biota modelling of radionuclide transfer and exposure and (ii) modelling radiation effects on the wildlife population. Thematic area 4 on marine modelling consisted of one working group on the modelling of radionuclide dispersion and transfer following accidental release from land based facilities to marine environments. This publication describes the work of MODARIA Working Group 7, which focused on the harmonization and intercomparison of models for accidental releases of tritium to the atmosphere.

The IAEA wishes to express its gratitude to all those who participated in the work of the MODARIA programme and gratefully acknowledges the contributions of the late D. Galeriu (Romania). The IAEA officer responsible for this publication was T. Yankovich of the Division of Radiation, Transport and Waste Safety.

## *EDITORIAL NOTE*

*This publication has been prepared from the original material as submitted by the contributors and has not been edited by the editorial staff of the IAEA. The views expressed remain the responsibility of the contributors and do not necessarily represent the views of the IAEA or its Member States.*

*Neither the IAEA nor its Member States assume any responsibility for consequences which may arise from the use of this publication. This publication does not address questions of responsibility, legal or otherwise, for acts or omissions on the part of any person.*

*The use of particular designations of countries or territories does not imply any judgement by the publisher, the IAEA, as to the legal status of such countries or territories, of their authorities and institutions or of the delimitation of their boundaries.*

*The mention of names of specific companies or products (whether or not indicated as registered) does not imply any intention to infringe proprietary rights, nor should it be construed as an endorsement or recommendation on the part of the IAEA.*

*The authors are responsible for having obtained the necessary permission for the IAEA to reproduce, translate or use material from sources already protected by copyrights.*

*The IAEA has no responsibility for the persistence or accuracy of URLs for external or third party Internet web sites referred to in this publication and does not guarantee that any content on such web sites is, or will remain, accurate or appropriate.*



## CONTENTS

SUMMARY .....	1
1. INTRODUCTION .....	3
1.1. BACKGROUND TO THE MODARIA PROGRAMME .....	3
1.2. BACKGROUND TO MODARIA WORKING GROUP 7: HARMONIZATION AND INTERCOMPARISON OF MODELS FOR ACCIDENTAL TRITIUM RELEASES .....	4
1.3. OBJECTIVES.....	4
1.4. SCOPE.....	5
1.4.1. Task 1: Analysis of the transfer of tritium in terrestrial ecosystems .....	5
1.4.2. Task 2: Intercomparison of models for specific scenarios .....	6
1.5. STRUCTURE OF THIS REPORT.....	6
2. LITERATURE REVIEW .....	7
2.1. EXCHANGE OF TRITIUM FROM THE SOIL ENVIRONMENT: DEPOSITION AND RE-EMISSION OF HT AND HTO .....	7
2.1.1. Overview.....	7
2.1.2. Background from previous IAEA programmes.....	7
2.1.3. Deposition and re-emission of HTO.....	8
2.1.4. Deposition of HT .....	13
2.1.5. Treatment of HTO re-emission in the models used in the intercomparison .....	16
2.1.6. Conclusion and potential future research.....	18
2.2. IN-CANOPY PROCESSES DURING WET DEPOSITION OF HTO ..	18
2.2.1. Overview.....	18
2.2.2. Theoretical considerations .....	19
2.2.3. Modelling approaches.....	20
2.2.4. Conclusions.....	21
2.3. DYNAMICS OF HTO TRANSFER INTO THE PLANT– ATMOSPHERE SYSTEM: FOLIAR UPTAKE AND RE-EMISSION .....	22
2.3.1. Overview.....	22
2.3.2. Exchange mechanism .....	22
2.3.3. Models for short term exposure (dynamic equations) .....	24
2.3.4. Conclusions.....	26
2.4. TURNOVER OF ORGANICALLY BOUND TRITIUM IN LITTER AND SOIL.....	26
2.4.1. Overview.....	26
2.4.2. Sources of OBT in litter and soil .....	27
2.4.3. Experimental and theoretical aspects of turnover of OBT in litter and soil .....	27
2.4.4. Modelling approaches.....	28
2.4.5. Conclusions.....	29

2.5.	FORMATION OF ORGANICALLY BOUND TRITIUM IN DARKNESS .....	30
2.5.1.	Overview .....	30
2.5.2.	Experimental studies .....	30
2.5.3.	Theoretical aspects .....	30
2.5.4.	Existing models of OBT formation by metabolism .....	31
2.5.5.	Conclusions .....	33
3.	DESCRIPTION OF MODEL SCENARIOS .....	34
3.1.	IRSN-EDF SCENARIO .....	34
3.1.1.	Purpose of the study .....	34
3.1.2.	Site description .....	34
3.1.3.	Experimental set-up and instrumentation .....	34
3.1.4.	Environmental sampling .....	34
3.2.	CNL: CHALK RIVER SCENARIO .....	35
3.2.1.	Atmospheric data .....	37
3.2.2.	Atmospheric HTO .....	37
3.3.	CNSC MODEL SCENARIO .....	38
3.3.1.	Purpose of the CNSC 2012 research study .....	38
3.3.2.	Site description .....	38
3.3.3.	Experimental set-up and instrumentation .....	39
3.3.4.	Analytical methods .....	40
4.	MODELS USED IN THE INTERCOMPARISON .....	41
4.1.	SUMMARY OF THE MODELS .....	41
4.2.	KEY DIFFERENCES AND SIMILARITIES BETWEEN MODELS ..	41
5.	ANALYSIS OF MEASURED AND SAMPLED DATA .....	46
5.1.	FORMS OF ATMOSPHERIC TRITIUM SAMPLED .....	46
5.2.	UNCERTAINTIES IN MEASUREMENTS .....	47
5.2.1.	Uncertainties due to sampling methodology .....	47
5.2.2.	Uncertainties due to analytical processes .....	47
5.2.3.	Uncertainties in atmospheric hourly data reconstruction .....	49
5.3.	ANALYSIS OF THE THREE DATASETS .....	50
5.3.1.	Measurements of HTO in air and TFWT and OBT activity concentrations in plants .....	50
5.3.2.	Comparison of averaged concentrations of HTO in air, TFWT and OBT in plants .....	55
5.3.3.	Comparison of moving average of air HTO activity concentrations with OBT activity concentrations measured in plants .....	57
5.4.	QUALITY ASSURANCE OF EXPERIMENTAL DATASETS .....	64
5.4.1.	General considerations and quality assurance requirements .....	64
5.4.2.	Quality assurance of the scenarios used in the intercomparison ..	64
6.	KEY FINDINGS FROM MODEL INTERCOMPARISON AND DIRECTIONS FOR FUTURE WORK .....	66

APPENDIX I. DESCRIPTION OF MODELS USED FOR INTERCOMPARISON EXERCISE .....	69
APPENDIX II. INTERCOMPARISON OF RESULTS AND DETAILED DISCUSSION .....	87
REFERENCES.....	115
LIST OF ABBREVIATIONS .....	131
CONTRIBUTORS TO DRAFTING AND REVIEW .....	133
LIST OF PARTICIPANTS .....	135



## SUMMARY

This report describes the work undertaken by Working Group 7 of the IAEA MODARIA Programme on the harmonization and intercomparison of models for accidental tritium releases. This report is concerned with the pulsed release of tritium into the atmosphere and the subsequent terrestrial processes that determine the post-accident distribution of different chemical forms of tritium in the environment.

The first half of the report is concerned with a literature review carried out by members of the Working Group regarding state-of-the-art modelling of tritium for the following processes:

- Exchange of tritium with the soil environment for deposition and re-emission of tritium gas (HT)<sup>1</sup> and tritiated water (HTO);
- Canopy processes during wet deposition of HTO;
- Dynamics of tritium transfer in the form of HTO in the plant–atmosphere system with the focus on foliar uptake and re-emission of HTO;
- Turnover of organically bound tritium (OBT) in litter and soil;
- Formation of OBT in the absence of light.

The second half of the report summarizes the results of an intercomparison exercise carried out using the following four models:

- TOCATTA- $\chi$  by Institut de Radioprotection et de Sûreté Nucléaire (IRSN, France) and Electricité de France (EDF, France);
- CERES by Commissariat à l'Énergie Atomique et aux Énergies Alternatives (CEA, France);
- SOLVEG-II by Japan Atomic Energy Agency (JAEA, Japan); and
- CTEM-CLASS-TT by Canadian Nuclear Laboratories (CNL)<sup>2</sup> (Chalk River, Canada).

Three scenarios developed by IRSN, the Canadian Nuclear Safety Commission (CNSC) and CNL were the basis for the intercomparison. Scenarios were developed from the best available data collected in three experimental campaigns and analyzed for coherence and completeness of the drivers needed as inputs for modelling. The intercomparison consisted of two parts:

- (1) A comparison of modelled and measured results (model–measurement comparison);
- (2) A comparison of the model performance for each scenario (model–model comparison).

The similarities in the modelling concepts, key differences between models, and model performance are discussed. The results of the intercomparison are used to inform future research directions.

---

<sup>1</sup> Sometimes called 'tritiated hydrogen'.

<sup>2</sup> Previously, 'Chalk River Laboratories'.



## 1. INTRODUCTION

### 1.1. BACKGROUND TO THE MODARIA PROGRAMME

The IAEA organized a programme entitled Modelling and Data for Radiological Impact Assessments (MODARIA) from 2012 to 2015, which had the general aim of improving capabilities in the field of environmental radiation dose assessment by means of acquiring improved data for model testing and comparison, reaching consensus on modelling philosophies, approaches and parameter values, development of improved modelling methods and exchange of information.

The following topics were addressed in ten working groups:

#### **Remediation of Contaminated Areas**

- Working Group 1: Remediation strategies and decision aiding techniques
- Working Group 2: Exposures in contaminated urban environments and effect of remedial measures
- Working Group 3: Application of models for assessing radiological impacts arising from naturally occurring radioactive material and radioactively contaminated legacy sites to support the management of remediation

#### **Uncertainties and Variability**

- Working Group 4: Analysis of radioecological data in IAEA Technical Reports Series publications to identify key radionuclides and associated parameter values for human and wildlife exposure assessment
- Working Group 5: Uncertainty and variability analysis for assessments of radiological impacts arising from routine discharges of radionuclides
- Working Group 6: Common framework for addressing environmental change in long term safety assessments of radioactive waste disposal facilities
- Working Group 7: Harmonization and intercomparison of models for accidental tritium releases

#### **Exposures and Effects on Biota**

- Working Group 8: Biota modelling: Further development of transfer and exposure models and application to scenarios
- Working Group 9: Models for assessing radiation effects on populations of wildlife species

#### **Marine Modelling**

- Working Group 10: Modelling of marine dispersion and transfer of radionuclides accidentally released from land based facilities

The activities and results achieved by the Working Groups are described in individual IAEA Technical Documents (IAEA-TECDOCs) where appropriate (see Refs [1–3]; see also Refs [4–6]). This report describes the work of the Harmonization and intercomparison of models for accidental tritium releases Working Group (Working Group 7).

## 1.2. BACKGROUND TO MODARIA WORKING GROUP 7: HARMONIZATION AND INTERCOMPARISON OF MODELS FOR ACCIDENTAL TRITIUM RELEASES

This section describes previous IAEA programmes during which the environmental transfer of tritium following accidental or long term releases to the atmosphere was investigated. For additional information, readers are directed to the relevant IAEA reports and technical documents (TECDOCs) which were produced at the conclusion of each respective programme (e.g. see Refs. [7, 8]).

The Tritium Working Group under Theme 3 of the IAEA Programme on BIOSphere Modelling and ASSESSment (BIOMASS) was established in order to improve model capabilities with regard to tritium released from continuous primary and secondary sources. The report of the BIOMASS Tritium Working Group provides detailed conclusions and recommendations on how to improve future modelling, data acquisition and field studies [7].

Subsequent IAEA Programmes looked at different models and the dose consequences of the behaviour of tritium in the terrestrial and freshwater environments.

The two phases of the IAEA Programme on Environmental Modelling for Radiation Safety (EMRAS and EMRAS II) were the immediate predecessors of the MODARIA programme. The main focus of Working Group 7 under EMRAS II was the development of a standardized conceptual and mathematical model to simulate the transfer of tritium in the environment following accidental releases to the atmosphere under a wide range of environmental and weather conditions. The results of this work were published in an IAEA TECDOC entitled 'Transfer of Tritium in the Environment after Accidental Releases from Nuclear Facilities' [8].

Tritium is volatile and predictions of environmental tritium transfer are inevitably associated with large uncertainties. The work of MODARIA Working Group 7 (WG7) focussed on the theoretical analysis of processes relevant to environmental transfer in the terrestrial environment in post-accident or pulsed release situations. Specifically, WG7 evaluated the naturally occurring variability of field observations as this variability limits the accuracy of predictions. This natural variability consists of meteorological, hydrological, pedological and biochemical variations existing at the micro- to meso-scale.

In controlled laboratory experiments (which currently provide the bulk of existing observations pertaining to tritium transfer) the majority of processes that occur naturally are 'frozen' (controlled) due to key relevant parameters being held constant. However, under natural conditions these processes are variable, which may affect the environmental transfer of tritium. As a result, field observations pertaining to environmental tritium often deviate from those of controlled experiments.

Controlled experiments are also characterized by the elimination or reduction of well understood field processes, which may contribute to the differences between experimental results and natural outcomes. Tritium transfer in natural environments involves the mutual interaction of multiple participating processes and can only be simulated through modelling. Consequently, in addition to analyzing disparate field observation data, along with the underlying physics, chemistry and biology, WG7 also proceeded with modelling multiple interacting processes in terrestrial environments relevant to tritium transfer, as well as working towards improving existing model parameterization.

## 1.3. OBJECTIVES

The overall goal of WG7 was to investigate previously neglected processes that are relevant to predicting the transfer of tritium within the terrestrial environment and to move toward the



simplification of tritium transfer models. The objectives of WG7 were to further develop state-of-the-art environmental transfer models for the soil–plant–atmosphere system applicable to accidental or pulsed tritium releases, to test and compare those models, and to also develop harmonized approaches to predicting the environmental transfer of tritium. The environmental behaviour of tritium after accidental or pulsed releases is highly relevant to all facilities that have a significant tritium inventory. The dynamics of tritium in the terrestrial environment are the result of complex interactions involving a number of processes that are subject to hourly, daily and annual variations [8]. Due to the uncertainties associated with the environmental conditions at the time of a release and also due to incomplete knowledge about the precise effect of the relevant environmental processes, predictions are inherently associated with considerable uncertainties [8]. The work performed during previous IAEA model testing and comparison programmes has assisted in improving the understanding of many processes related to tritium washout and transfer in freshwater food chains, as well as its transfer within the terrestrial food chain [8]. However, more work is still needed in order to enable reliable assessments of exposures related to accidental or pulsed tritium releases to the atmosphere, taking into account the actual weather, and the environmental and agricultural conditions.

#### 1.4. SCOPE

The work carried out by WG7 under the MODARIA programme focused on the modelling of tritium transfer processes as listed below, along with their integration into an easy-to-use assessment model, as outlined in the following tasks:

##### 1.4.1. Task 1: Analysis of the transfer of tritium in terrestrial ecosystems

The first task was the compilation of state-of-the-art knowledge and the completion of comprehensive parameterization of tritium transfer models, which need to cover a wide range of environmental conditions in terrestrial environments. The discussion of state-of-the-art parameterization, mainly focused on the following high priority processes, which were highlighted as being important at the conclusion of the EMRAS II programme [8]:

- Interception of wet deposited tritium by plant canopies and uptake of tritium by leaves;
- Uptake of tritium by vegetated and non-vegetated soil;
- Transfer of tritiated water (HTO) and the dynamics of HTO in the soil–plant–atmosphere system;
- Re-emission of HTO from soil as a secondary source;
- Formation of organically bound tritium (OBT) in darkness;
- Turnover of OBT in litter and soil.

In recent times, the Institut de Radioprotection et de Sûreté Nucléaire (IRSN) in France launched a large-scale project to study the transfer of tritium in the terrestrial ecosystem (the VATO Project). The main objective of this project was to better understand and quantify the processes of tritium (HTO and tritium gas (HT)) transfer from the atmosphere (air and rainwater) to grass and soil. IRSN identified and targeted five key topics that needed detailed investigation in order to enable the development of improved models:

- Dynamics of OBT formation in grass, depending on the contribution from the various compartments of the environment, i.e. air (water vapour), rainwater, and soil water;
- Dynamics of HTO formation in soil from an atmospheric source of HT;
- Speciation of tritium in air (HT–HTO);

- Quantification of dry deposition of HTO;
- Quantification of wet deposition of HTO.

In order to address the enormous range of factors that affect the transfer of tritium (e.g. humidity in air and soil, temperature, current and recent rainfall, season, stage of growth), IRSN's VATO Project was carried out with high frequency (daily) sampling of air, rainwater and soil in order to reduce the uncertainties of tritium transfer coefficients. This project began in January 2013 and ran for five years. The results of the VATO Project provided invaluable input to the work of MODARIA Working Group 7.

#### **1.4.2. Task 2: Intercomparison of models for specific scenarios**

A key activity of WG7, and the second task, was the analysis and evaluation of recently executed field experiments, the development of realistic scenarios for intercomparison studies, and the conduct of model intercomparison studies. Scenarios were developed to include dry and wet deposition of tritium for prolonged dry or wet weather periods, as well as associated tritium transfer on a fine (hourly) scale during the day and during the night. State-of-the-art models were then tested against observations representing a wide range of environmental conditions in terrestrial environments. Finally, and most importantly, an analysis of model performance was conducted. The model intercomparison exercise provided information on the applicability and limitations of each model. It allowed WG7 to evaluate the efficiency of proposed model parameterization, to define further development work (starting with parameterization improvements), and ultimately, to identify knowledge gaps pertaining to longer term research and development goals.

### **1.5. STRUCTURE OF THIS REPORT**

Section 2 provides a literature review, covering:

- Exchange of tritium from the soil environment: deposition and re-emission of tritium gas (HT) and tritiated water (HTO) (Section 2.1);
- In-canopy processes during wet deposition of HTO (Section 2.2);
- Dynamics of HTO transfer in the plant–atmosphere system: foliar uptake and re-emission of HTO (Section 2.3);
- Turnover of OBT in litter and soil (Section 2.4);
- Formation of OBT in darkness (Section 2.5).

Sections 3 to 5 provide information on the model intercomparison, specifically:

- Section 3 provides a description of the three scenarios studied by MODARIA WG7;
- Section 4 provides information on the four models used for the intercomparison;
- Section 5 gives an analysis of measured and sampled data;
- Section 6 summarizes the key findings from model intercomparison and outlines possible directions for future work.

Finally, the main report is followed by two appendices:

- Appendix I describes the four models used for the intercomparison exercise;
- Appendix II provides detailed discussion of the intercomparison results.

## **2. LITERATURE REVIEW**

### **2.1. EXCHANGE OF TRITIUM FROM THE SOIL ENVIRONMENT: DEPOSITION AND RE-EMISSION OF HT AND HTO**

#### **2.1.1. Overview**

Tritium can be a major contributor to the total effective dose to members of the public living near facilities such as nuclear power plants and tritium processing facilities. Of the three principal forms of tritium (HT, HTO and OBT), HTO and OBT are the primary contributors to effective dose [9, 10]. In order to accurately predict effective dose due to exposure from a release of tritium, either under normal operations or an accident scenario, it is important to know and understand the sources (primary and secondary) of HTO and OBT to the environment. This review focuses on understanding a potential secondary source of HTO to the environment; notably the re-emission of HTO from soil (i.e. evaporation) and plants (i.e. transpiration). This review does not include the dynamics of OBT deposition or formation in soils, although these processes may be coupled with the dynamics of HT and HTO in soil.

Soil and vegetation are the main accumulation sites for tritium and are consequently the most important media for environmental sampling. Therefore, having accurate, temporal predictions of tritium in different environmental media is necessary for determining its radiological impacts [11].

During an accident or a pulsed release during normal operations, a significant amount of HT could be released to the environment, especially from certain facilities, such as fuel reprocessing plants, old generation types of CANDU reactors, and tritium processing facilities such as SRB Technologies (Canada). Once emitted, HT is deposited to the soil surface and can be oxidized to HTO by soil microorganisms [12]. The HTO that is formed can either enter soil water or be re-emitted to the air. The re-emission of tritium in the form of HTO becomes an important process for calculating the dose from tritium since the dose coefficient for HTO is four orders of magnitude higher than that for HT [11, 13–15]. Under certain conditions, the re-emission of tritium as HTO from soil may double the total dose from inhalation and skin absorption [14].

There are many uncertainties regarding deposition and re-emission of tritium with regard to both routine releases and accidental releases. This review summarizes the status of knowledge with respect to the deposition and re-emission of HT and HTO in the environment. Key findings and observations from laboratory experiments and field studies are also presented. Section 2.1.6 concludes with discussion of how the key findings have been applied to improve the mathematical approaches used to model the deposition and re-emission of tritium to the atmosphere.

#### **2.1.2. Background from previous IAEA programmes**

An understanding of tritium deposition and re-emission processes has emerged, based on work conducted in previous IAEA programmes that investigated the environmental transfer of tritium following accidental or long term releases to the atmosphere (see Section 1.2). Readers are directed to Ref. [7], which explains that, following a release of HT, the amount of HTO is completely controlled by the oxidation of HT at the soil surface and the subsequent re-emission to the atmosphere. In order to estimate the HTO concentration in air, the empirical value from the CNL experiments conducted in 1994 in Canada may be used, given the difficulty modelling oxidation and re-emission: the HTO concentration in air ( $\text{Bq/m}^3$ ) due to a release of HT is

approximately equal to 0.04 times the HT concentration in air (Bq/m<sup>3</sup>) (see Ref. [7]), recognizing that uncertainties may exist in this parameter value depending on site-specific conditions.

Additionally, Section 5 of IAEA-TECDOC-1738 [8] provides a more rigorous theoretical approach to model the processes that control HT and HTO dry deposition and re-emission. These processes need to be considered in tritium dynamic models, and models need to be validated with experimental data [8].

### 2.1.3. Deposition and re-emission of HTO

The main chemical forms of tritium released from facilities, such as nuclear power plants and tritium processing facilities, are HT and HTO. Following release, tritium is dispersed throughout the atmosphere, and when in the form of HT and HTO, may subsequently deposit to soil, vegetation and water surfaces. The processes by which these two forms of tritium deposit differ based on their physical and chemical properties. Sections 2.1.3.1–2.1.3.4 and Section 2.1.4 describe the current understanding of the deposition of HTO and HT, respectively, to soil surfaces. The re-emission of HTO is discussed in Section 2.1.3.3 below.

#### 2.1.3.1. Dry deposition of HTO

The exchange of HTO between the air and soil surfaces includes transport through the air to the surface and diffusion in soil. The reversible exchange of HTO between the air and soil can also be described by a flux equation, for example [16]:

$$F_{HTO} = v_{HTO}(\chi_a - \chi_s) \quad (1)$$

where:

$F_{HTO}$  is the exchange flux (Bq m<sup>-2</sup> s<sup>-1</sup>);

$v_{HTO}$  is the exchange velocity (m/s);

$\chi_a$  is the concentration of HTO in the air at a reference height, i.e. the height where the HTO concentration is measured in the air (Bq/m<sup>3</sup>);

$\chi_s$  is the concentration of HTO in the air in the soil (Bq/m<sup>3</sup>).

The magnitudes of  $\chi_a$  and  $\chi_s$  determine whether or not the conditions favour HTO deposition or re-emission. Deposition occurs when  $\chi_a > \chi_s$  and re-emission occurs when  $\chi_s > \chi_a$ . The exchange velocity ( $v_{HTO}$ ) describes the efficiency of exchange of HTO between the atmosphere and the soil and is dependent on the amount of turbulent mixing in the air and the number of absorption sites at the soil surface [13, 17]. One assumption of this process is that tritium is able to freely absorb at the soil surface [17].

The total transfer resistance ( $r_g$ ) for the deposition of HTO to soil is expressed as the sum of the aerodynamic resistance ( $r_a$ ), the boundary layer resistance ( $r_b$ ) and the soil resistance ( $r_s$ ) [18]:

$$r_g = (r_a + r_b + r_s) \quad (2)$$

where:

$r_g$  is the sum of total transfer resistance (s/m);

$r_a$  is the aerodynamic resistance that describes the transfer of HTO from a reference height to the air-soil interface (s/m);

- $r_b$  is the boundary layer resistance that describes the transfer of HTO from the air-soil interface to the air sublayer above the soil surface (s/m);  
 $r_s$  is the soil resistance that describes the transfer to HTO from the surface to water in the soil (s/m).

The HTO exchange velocity ( $v_{HTO}$ ) is, therefore, expressed as the inverse of the total transfer resistance:

$$v_{HTO} = (r_g)^{-1} \quad (3)$$

$$v_{HTO} = (r_a + r_b + r_s)^{-1} \quad (4)$$

where:

$v_{HTO}$  is the exchange velocity (m/s).

Both the aerodynamic resistance and the boundary layer resistance are dependent on the wind speed at a reference height ( $u(z)$ ) and the friction velocity ( $u$ ). These two resistances describe the atmospheric stability and the properties of the soil surface, respectively [14, 18]:

$$r_a = \frac{u(z)}{u^2} \quad (5)$$

$$r_b = \frac{1}{Bu} \quad (6)$$

where:

- $r_a$  is the aerodynamic resistance that describes the transfer of HTO from a reference height to the air-soil interface (s/m);  
 $r_b$  is the boundary layer resistance that describes the transfer of HTO from the air-soil interface to the air sublayer above the soil surface (s/m);  
 $u(z)$  is the wind speed at a given height  $z$  (m/s);  
 $B$  is the Stanton number (dimensionless);  
 $u$  is the friction velocity (m/s).

Transport of HTO in soil occurs by diffusion in either the air or water phases of soil [17]. The soil (or surface) resistance ( $r_s$ ) to soil transport can be calculated from the effective diffusivity ( $D_{eff}$ ) and the thickness of the soil layer ( $z$ ) [14]:

$$r_s = \frac{z}{D_{eff}} \quad (7)$$

where:

- $r_s$  is the soil resistance that describes the transfer to HTO from the surface to water in the soil (s/m);  
 $z$  is the thickness of soil layer (m);  
 $D_{eff}$  is the effective diffusivity of HTO in the soil (m<sup>2</sup>/s).

The effective diffusivity is dependent on temperature, soil water content and the tortuosity factor of the soil [11]:

$$D_{eff} = \frac{\gamma\theta_A D_{HTO}^A + \theta_W D_{HTO}^W}{\tau(\gamma\theta_A + \theta_W)} \quad (8)$$

where:

$D_{eff}$  is the effective diffusivity of HTO in the soil (m<sup>2</sup>/s);

$D_{HTO}^A$  is the diffusion coefficient of HTO in air (m<sup>2</sup>/s);

$D_{HTO}^W$  is the diffusion coefficient of HTO in water (m<sup>2</sup>/s);

$\theta_A$  is the volumetric air content in soil or air volume fraction in soil (m<sup>3</sup>/m<sup>3</sup>);

$\theta_W$  is the volumetric water content in soil or water volume fraction in soil (m<sup>3</sup>/m<sup>3</sup>);

$\tau$  is the tortuosity factor (dimensionless);

$\gamma$  is the ratio of the saturated water vapour density in the soil to the density of water, also called the equilibrium ratio (dimensionless):

$$\gamma = \frac{\rho_v}{\rho_w} \quad (9)$$

where:

$\rho_v$  is the saturated water vapour density in the soil at the prevailing soil temperature (g/m<sup>3</sup>);

$\rho_w$  is the density of water (g/m<sup>3</sup>).

#### 2.1.3.2. Field studies and laboratory experiments on the dry deposition of HTO

The following observations have been made based on field studies and laboratory experiments investigating the deposition of atmospheric HTO to soil:

- HTO deposition occurs within the top several millimeters of soil [11, 14, 19, 20];
- The HTO concentration profile from HTO deposition decreases exponentially with depth assuming constant soil moisture and a constant HT–HTO conversion rate throughout the soil [11, 15].

#### 2.1.3.3. Re-emission of HTO

Once in the soil, HTO can either be transported with soil water or be re-emitted to the atmosphere as a secondary source of tritium. The main similarities and differences between the re-emission of HTO and the evaporation of water from soil have been summarized and are presented in Ref. [11]. The three main similarities between the two processes are:

- The need for energy for the liquid–gas phase transition;
- Diffusion from deeper soil layers to resupply the soil surface;
- Overcoming boundary layer resistances.

The main difference between HTO re-emission and water evaporation is that HTO and water each follow their respective vapour pressure gradients. The differences in the vapour pressure gradients result in differences between the concentrations of HTO and water in the boundary layer, the amounts of HTO and water in the uppermost soil layer, and the distributions of HTO and water in the soil profile.

Re-emission of HTO occurs when  $\chi_s > \chi_a$  (see Eq. (1) above). This process can be characterized by the emission rate ( $k_{re}$ ), which is defined as the tritium content in soil that re-enters the atmosphere per unit time and expressed as percentage per hour [14], which decreases over time:

$$k_{re} \propto \exp\left(-\frac{t}{T}\right) \quad (10)$$

where:

$k_{re}$  is the tritium content in soil that re-enters the atmosphere per unit time (%/h).

The function  $\exp(-\frac{t}{T})$  represents the reduction of the re-emission rate over time.

In general, the re-emission rate consists of two components: the daytime component of the re-emission rate used to account for the fact that HTO and water follow their respective vapour pressure gradients, and the basic re-emission rate ( $k_b$ ), which is assumed to be independent of meteorological conditions.

In order to simulate the movement of the maximum HTO concentration to deeper soil layers as re-emission occurs, the re-emission rate may also be expressed by the following time dependent function [14]:

$$k_{re} = \frac{E_a}{s_w} C_1 \times \exp\left(-\frac{t}{T}\right) + k_b \times \exp\left(-\frac{t}{T}\right) \quad (11)$$

where:

$k_{re}$  is the tritium content in soil that re-enters the atmosphere per unit time (%/h);  
 $E_a$  is the evaporation rate of water from soil ( $\text{kg m}^{-2} \text{h}^{-1}$ );  
 $s_w$  is the actual water content of the top 5 cm layer ( $\text{kg/m}^2$ );  
 $C_1$  is the conversion factor describing the differences between HTO and  $\text{H}_2\text{O}$  behaviour in soil (%), which ranges from 500–1200% (a default value of 500% can be assumed);  
 $k_b$  is the basic re-emission rate (%/h), which ranges from 1–23%/h;  
 $t$  is time (h);  
 $T$  is the effective residence time of tritium in soil (h) and ranges from 5–50 h, where a smaller  $T$  value reflects a larger re-emission fraction rate (a default value of 50 h is assumed) [11].

The re-emission of HTO is dependent on the amount of HTO at the soil surface due to the resupply of HTO by upward diffusion and soil water movement [11, 13]. The concentration gradient between the different soil layers drives the resupply of HTO at the soil surface.

The similarities between HTO re-emission and water evaporation allow re-emission to be modelled with the help of evaporation processes. The UFOTRI computer code, which was developed to assess the dose consequences from accidental tritium releases [7], includes a re-emission module based on the evaporation of water.

The evaporation of water from soil ( $E_a$ ) may be calculated by applying the Monteith equation, which is typically used for plant canopies, but it can also be applied to soils by replacing the canopy resistance with the soil resistance [7, 14]:

$$\lambda E_a = \frac{\Delta R_a + \rho c_p (e_s - e_a) (r_a + r_b)^{-1}}{\Delta + \gamma (1 + r_s) (r_a + r_b)^{-1}} \quad (12)$$

where:

$\lambda$  is the latent heat of evaporation ( $\text{J/kg}$ );  
 $E_a$  is the evaporation rate of water from soil ( $\text{kg m}^{-2} \text{s}^{-1}$ );  
 $\Delta$  is the gradient of the vapour pressure curve at ambient temperature ( $\text{J m}^{-3} \text{K}^{-1}$ );

- $R_a$  is the incoming solar radiation ( $\text{W/m}^2$  or  $\text{kg/s}^3$ );  
 $\rho$  is the air density ( $\text{kg/m}^3$ );  
 $c_p$  is the specific heat of air at constant pressure ( $\text{J kg}^{-1} \text{K}^{-1}$ );  
 $e_s$  is the actual saturation vapour pressure of air ( $\text{N/m}^2$ );  
 $e_a$  is the actual vapour pressure of air ( $\text{N/m}^2$ );  
 $r_a$  is the aerodynamic resistance that describes the transfer of HTO from a reference height to the air-soil interface ( $\text{s/m}$ );  
 $r_b$  is the boundary layer resistance that describes the transfer of HTO from the air-soil interface to the air sublayer above the soil surface ( $\text{s/m}$ );  
 $r_s$  is the soil resistance that describes the transfer to HTO from the surface to water in the soil ( $\text{s/m}$ );  
 $\gamma$  is the psychrometric constant that relates the partial pressure of water in air to air temperature ( $\text{J m}^{-3} \text{K}^{-1}$ ).

The equations for the aerodynamic resistance (Eq. (5)) and boundary resistance (Eq. (6)) provided in Section 2.1.3.1 for the deposition of HTO also apply to the re-emission of HTO [7, 14]. The soil resistance is defined by the expression given in Eq. (7), whereas, in the UFOTRI model, the parameter  $z$  is the thickness of the dry ‘help layer’ of soil. The soil water content in the top 0.5 cm to 1 cm of the upper soil layer (the ‘help layer’) is needed in order to calculate the soil resistance [7, 14].

Two different approaches in the UFOTRI model for calculating soil water content were considered in Ref. [18]. In the simple model, water transport increases when there is precipitation and decreases by evaporation. The equation for soil resistance was modified to include a minimum resistance,  $r_{\min}$ , of 50 s/m for the wet soil surface because zero soil resistance did not seem reasonable, even if the soil were saturated with water:

$$r_s = \frac{z}{D_{eff}} + r_{\min} \quad (13)$$

where:

- $r_s$  is the soil resistance that describes the transfer to HTO from the surface to water in the soil ( $\text{s/m}$ );  
 $z$  is the thickness of soil layer ( $\text{m}$ );  
 $D_{eff}$  is the effective diffusivity of HTO in the soil ( $\text{m}^2/\text{s}$ );  
 $r_{\min}$  is the minimum resistance of soil ( $\text{s/m}$ ).

The second, more complex model, considered the matrix forces between each soil layer. The matrix forces are capillary and absorptive forces that arise due to the interaction between the solid soil phase and the liquid and gaseous phases. In this case, the hydraulic conductivity and suction tension are needed in order to calculate water transport in soil. The transfer of moisture between two soil layers can, therefore, be represented by a simplified version of Darcy’s law [18]:

$$V_{12} = K_{12} \left[ \frac{(S_1 - S_2)}{(\Delta z_1 + \Delta z_2)/2} - 1 \right] \quad (14)$$

where:

- $V_{12}$  is the moisture transfer from layer 2 to layer 1 ( $\text{mm/h}$ );  
 $S_1, S_2$  are suction tensions of soil layers 1 and 2, respectively ( $\text{mm}$ );  
 $\Delta z_1, \Delta z_2$  are diameters of soil layers 1 and 2, respectively ( $\text{mm}$ );  
 $K_{12}$  is the suction-conductivity function ( $\text{mm/h}$ ).



$K_{12}$  can be calculated, as follows:

$$K_{12} = \frac{\alpha_k}{s^{m+\beta}} \quad (15)$$

where:

$\alpha_k, m, \beta$  are soil specific constants (see Ref. [18] for further details).

#### 2.1.3.4. *Field studies and laboratory experiments of the re-emission of HTO*

A review of field and experimental studies investigating the re-emission of HTO from soil resulted in the following observations:

- The re-emission rate is highest immediately after deposition and decreases during the subsequent hours [11, 13–15, 21];
- The decrease in the re-emission rate is believed to be due to a decrease in the amount of HTO in the upper soil layer with time due to HTO evaporation and diffusion of HTO to deeper soil layers;
- Diurnal effects have been observed for the re-emission of HTO from soil. Measurements of soil and air showed that evaporation processes during the day support re-emission and, furthermore, dewfall at night inhibits re-emission and supports deposition [13, 15, 22].

#### 2.1.4. **Deposition of HT**

Similar to HTO, HT released to the environment will disperse and deposit to the soil surface. The HT may then be oxidized to HTO by soil microorganisms near the soil surface [15, 23, 24]. The conversion of HT to HTO in soil is several orders of magnitude greater than conversion rates in air [25–27]. Consequently, very little HT is oxidized in the air. Descriptions of how this pathway (i.e. HT deposition to soil) was accounted for in the models used as part of this intercomparison are provided in Section 4.2. Following conversion, HTO will either be re-emitted to air or enter soil water [27]. The processes described in Section 2.1.3.3 above apply to the HTO formed following the oxidation of HT in soil.

##### 2.1.4.1. *Dry deposition of HT*

The deposition of HT to the soil surface is a two-step process [28]:

- (1) Diffusion of HT to the soil surface and in the soil;
- (2) Oxidation of HT to HTO by soil microorganisms.

The efficiency of the deposition process is described by a deposition velocity [10, 16]. Similar to deposition of HTO, the deposition of HT can be described by a flux equation [16]:

$$F_{HT} = v_{HT} \chi_a \quad (16)$$

where:

$F_{HT}$  is the exchange flux ( $\text{Bq m}^{-2} \text{s}^{-1}$ );

$v_{HT}$  is the deposition velocity ( $\text{m/s}$ );

$\chi_a$  is the concentration of HT in the air at a reference height ( $\text{Bq/m}^3$ ).

The exchange velocity for HT is expressed using a similar equation to the expression for the exchange velocity of HTO:

$$v_{HT} = (r_a + r_b + r_s)^{-1} \quad (17)$$

where:

- $v_{HT}$  is the deposition velocity (m/s);
- $r_a$  is the aerodynamic resistance that describes the transfer of HT from a reference height to the air-soil interface (s/m);
- $r_b$  is the boundary layer resistance that describes the transfer of HT from the air-soil interface to the air sublayer above the soil surface (s/m);
- $r_s$  is the soil resistance that describes the transfer of HT from the air-soil interface to air pores in the soil and depends on rate of HT diffusion into the soil pores and the oxidation rate at which HT is converted to HTO within these pores (s/m).

Equations (5) and (6) above can also be applied to calculate the aerodynamic and boundary layer resistances for HT.

In previous models, the variable for soil resistance included the processes of diffusion and oxidation of HT in soil. However, more recently it has been determined that in order to accurately describe HT deposition, oxidation of HT to HTO needs to be accounted for separately [29]. In the corresponding conceptual model, HT deposition was parameterized based on three processes [10, 29]:

- (1) Vertical transport in the atmosphere ( $r_a$ );
- (2) Transport in soil ( $r_s$ );
- (3) Oxidation in soil ( $r_{ox}$ ).

The three outlined processes are each represented by a resistance that occurs in series. Similar to the case for the deposition of HTO, the deposition velocity for HT ( $v_{HT}$ ) may be written as the inverse of a sum of resistances:

$$v_{HT} = (r_a + r_s + r_{ox})^{-1} \quad (18)$$

where:

- $v_{HT}$  is the deposition velocity (m/s);
- $r_a$  is the aerodynamic resistance that describes the transfer of HT from a reference height to the air-soil interface (s/m);
- $r_s$  is the soil resistance that describes the transfer of HTO from the air-soil interface to air pores in the soil (s/m);
- $r_{ox}$  is the oxidation rate of HT to HTO in soil (s/m).

Following dry deposition of HT and conversion to HTO in soil, the HTO can either be transported with soil water or be re-emitted to the atmosphere as described previously (see Section 2.1.3.3).

#### 2.1.4.2. *Laboratory and field studies of dry deposition and oxidation of HT in soil*

A number of field studies and laboratory studies have been conducted to further investigate the primary factors and processes that influence the deposition and oxidation of HT in the environment [11, 14, 16, 21, 23, 30–33].

With respect to the deposition of HT to the soil surface, research efforts to date have focused on quantifying the deposition velocity and investigating the influence of different soil and meteorological parameters. The main observations are as follows:

- HT deposition occurs mainly in the upper few centimeters of soil and decreases rapidly with soil depth [16, 23, 31];
- Experimental HT deposition velocities range from  $10^{-5}$  to  $10^{-3}$  m/s [16, 21, 34, 35]. A range of published deposition velocities is provided in Ref. [36];
- A seasonal dependence has been observed for HT deposition velocities. Deposition velocities are higher in the summer and autumn than in the winter and spring. This dependence may be due to the effect of soil moisture on the deposition velocity rather than temperature [16, 31];
- Deposition velocities are mainly dependant on the water content of the soil [16, 18, 31] and high soil water content can inhibit the diffusion of HT in soil [31].

HT deposited to the soil surface may be oxidized to HTO. Studies investigating the parameters that govern the oxidation of HT to HTO in soil have noted the following:

- HT oxidation is highest in the top section (0–5 cm) of soil and decreases with depth [23, 37];
- HT oxidation rates were determined for 14 different types of soil. The oxidation rate ranged from  $12 \pm 2\% \text{ hr}^{-1}$  to  $66 \pm 6\% \text{ hr}^{-1}$ . The reaction rates were independent of soil type and soil chemical properties (e.g. pH, organic matter content) [12];
- HT oxidation rates are dependent on soil temperature and soil water content [12, 24, 29]. Microbial activity in soil is dependent on temperature and water content and therefore these parameters may affect the efficiency of the microorganisms responsible for converting HT to HTO;
- Concentrations of HTO and oxidation rates were higher in undisturbed soil compared to disturbed soil [22, 38]. The lower concentrations and oxidation rates in disturbed soil may be due to a reduction in the microbial activity in the soil [22].

#### *2.1.4.3. Comparison of oxidation of HT in air and on plant surfaces*

Sections 2.1.4.1 and 2.1.4.2 outlined the theoretical background and provided a summary of the results of field studies and laboratory experiments, respectively, on the oxidation of HT in soil. The subsections that follow aim to summarize the existing literature regarding the oxidation of HT in air and by vegetation to provide rationale for why this pathway is often neglected in models as a secondary source.

##### ***HT oxidation in air***

The atmospheric oxidation of HT is very slow [25–27] and the main mechanism is believed to be through the reaction with the hydroxyl radical. Current input parameters based on data retrieved from Canadian experiments suggest a conversion rate of 2.4% from the oxidation of HT both in air and soil. Of this total, approximately 0.4% is likely due to the conversion of HT to HTO in air. Field experiments were conducted around the Darlington nuclear generating station (in Canada) to investigate the uncertainty in the conversion rate [36]. The results of this work indicate that the conversion rate for air and soil might be closer to 0.5% (0.1% from HT oxidation in air and 0.4% from HT oxidation in soil).

### ***HT oxidation on plant surfaces***

Experimental studies investigating the uptake and oxidation of HT in vegetation foliage have been conducted in the past [39], where three vegetation species (i.e. tomato, corn and white poplar) were exposed to tritium in a plant growth chamber. Over the course of the experiment, the specific activities of the tissue free water tritium (TFWT) (HTO specific activity in plants) decreased. The TFWT was expected to increase if the plants were converting HT to HTO. Further evidence that the conversion of HT to HTO in plants was negligible was provided by the extremely small values for the TFWT:HT ratios (ranging from  $6.0 \times 10^{-9}$  to  $9.2 \times 10^{-9}$ ) compared to the values obtained for the TFWT:HTO ratios (0.57 to 0.80).

Deposition of HT and HTO to pine needles was investigated [40] where plant needles were exposed to either HT and HTO, or HTO only. The TFWT concentration in pine needles that had been exposed to both HT and HTO was the same or lower than pine needles that had only been exposed to HTO. Based on the results, it was concluded that HT deposition to pine needles was negligible compared to HTO deposition.

Another study was carried out aiming to quantify the oxidation rate of HT in soil and vegetation using samples from forests and fields in Japan [41]. In this work, the highest oxidation rate was observed in soil, followed by mosses and lichen, and finally pine needles. The oxidation rate in woody plant leaves (such as pine needles) was  $10^3$  to  $10^5$  times less than that in surface soil.

The results of these selected studies demonstrate that the rate of oxidation in plant foliage is extremely slow and is not the main contributor of TFWT concentrations in plant and thus is a negligible secondary source of tritium to the atmosphere.

#### **2.1.5. Treatment of HTO re-emission in the models used in the intercomparison**

Sections 2.1.3 and 2.1.4 describe the transfer of HTO and HT, respectively, in the terrestrial environment following release to the atmosphere. Sections 2.1.5.1 and 2.1.5.2 that follow describe how the models used in the intercomparison considered the processes that might lead to the re-emission of HTO to the atmosphere. The four models used in the intercomparison are described in detail in Section 4.

##### ***2.1.5.1. Model treatment of HT deposition and oxidation in soil***

The TOCATTA- $\chi$  model does not consider the deposition or oxidation of HT in soil. Each of the three remaining models used during in the intercomparison comprised a different approach to how HT deposition and oxidation were treated. Firstly, the CTEM-CLASS-TT model assumes that a constant 5% of the total HT emitted is deposited to soil and eventually oxidized to HTO. Next, deposition of HT in CERES deploys a predefined HT dry deposition velocity of  $3 \times 10^{-4}$  m/s with an assumption that 50% of deposited HT is re-emitted back to the atmosphere and the rest is oxidized to HTO. Finally, SOLVEG-II includes parameterization of the transport of HT by considering both diffusion and oxidation in soil [42]:

$$\frac{\partial\{(\eta_{sat}-\eta_w)\chi_s\}}{\partial t} = \frac{\partial}{\partial z}\left(D_{eff}\frac{\partial\chi_s}{\partial z}\right) - e_o \quad (19)$$

where:

- $\eta_{sat}$  is the porosity (fractional);
- $\eta_w$  is the volumetric soil water content ( $m^3/m^3$ );
- $\chi_s$  is the concentration of HT in the air in the soil ( $Bq/m^3$ );
- $t$  is the time (s);

$z$  is the thickness of soil layer (m);  
 $D_{eff}$  is the effective diffusivity of HT in the soil ( $m^2/s$ );  
 $e_o$  is the degree of HT oxidation defined as a volumetric sink ( $Bq\ m^{-3}\ s^{-1}$ ).

The amount of HT oxidation in soil is modelled as:

$$e_o = \rho_b v_{ox} \quad (20)$$

where:

$e_o$  is the degree of HT oxidation ( $Bq\ m^{-3}\ s^{-1}$ );  
 $\rho_b$  is the dry bulk density ( $kg\ dry\ mass/m^3$ );  
 $v_{ox}$  is the HT oxidation rate ( $Bq\ kg^{-1}\ s^{-1}$ ).

#### 2.1.5.2. Model treatment of HTO re-emission from soil

The models used in the intercomparison did not treat the re-emission of HTO explicitly. Evapotranspiration was used in CTEM-CLASS-TT to model the emission of tritium from the soil compartment. TOCATTA- $\chi$  and SOLVEG-II both consider the net exchange of tritium between soil and the atmospheric compartment [43, 44]. Moreover, the SOLVEG-II model can be used to calculate the vertical flux of HTO from the difference of gaseous HTO concentrations between the soil air and the atmosphere [43]:

$$F_{HTO} = c_E u_1 (\chi_{air} - \chi_{sa}) \quad (21)$$

where:

$F_{HTO}$  is the exchange flux ( $Bq\ m^{-2}\ s^{-1}$ );  
 $c_E$  is the exchange coefficient at the ground surface (dimensionless);  
 $u_1$  is the wind velocity at the bottom atmospheric layer (m/s);  
 $\chi_{air}$  is the HTO concentration in the bottom atmospheric layer ( $Bq/m^3$ );  
 $\chi_{sa}$  is the HTO concentration in soil air ( $Bq/m^3$ ).

The TOCATTA- $\chi$  model uses the following equation to describe the net HTO flux between the air and soil compartments [44]:

$$THTO_{Air,S}^{SExc} = v^{exc} \{p_{HTO} [^3H]_{Air} - \varepsilon^{-1} \rho_s [HTO]_s\} \quad (22)$$

where:

$THTO_{Air,S}^{SExc}$  is the surface exchange of HTO between the plant canopy, atmosphere and soil surface ( $mol\ m^{-2}\ d^{-1}$ );  
 $v^{exc}$  is the rate of exchange of HTO vapour between the soil surface and the atmosphere (m/d);  
 $p_{HTO}$  is the proportion of tritium releases as HTO (dimensionless);  
 $[^3H]_{Air}$  is the HTO concentration in the plant canopy atmosphere ( $mol/m^3$ );  
 $\varepsilon$  is the isotope separation factor between HTO vapour and light water vapour (dimensionless);  
 $\rho_s$  is the absolute humidity of soil air ( $m^3/m^3$ );  
 $[HTO]_s$  is the HTO concentration in soil pore water ( $mol/m^3$  of soil pore water).

The approaches used in Refs [43, 44] are simpler than the methods used in previous models to simulate the emission of HTO from soil. In previous models, mathematical approaches were based on the Penman-Monteith relationship [14, 44].

As part of efforts undertaken to improve the TOCATTA- $\chi$  model, IRSN (particularly under the VATO Project) has been investigating the exchange of tritium between different environmental compartments (e.g. air, soil and plants). To this effect, research was aimed [45] at quantifying tritium evaporation using both experimental methods and modelling based on Penman-Monteith theory. The experimental methods for calculating tritium flux included gradient and eddy covariance methods. The results from the two experimental methods were consistent with each other and with the results produced from the Penman-Monteith model. The advantages and disadvantages of each method are described in Ref. [45]. The results will be used to improve parameters used in tritium transfer models, such as TOCATTA- $\chi$  [46].

### **2.1.6. Conclusion and potential future research**

Models for tritium releases under normal and accident scenarios are needed in order to calculate tritium concentrations in the atmosphere and to estimate the dose consequences of tritium releases under diverse conditions. This review has focused on summarizing the primary and secondary sources of HTO to soil and subsequent re-emission of HTO to the atmosphere.

Even simplified models need an accurate estimate of parameters describing tritium deposition and HTO re-emission. However, the reversible nature of the exchange processes makes it difficult to quantify the effect on dose [16]. Further research focused on understanding the mechanistic details of the processes underlying re-emission is needed before meaningful results can be obtained from models [22]. This review has summarized some of the research that has been conducted in order to better understand the parameters and meteorological conditions that influence tritium deposition and re-emission. However, there are still some uncertainties which remain, and future research could, therefore, focus on the following areas:

- Conducting experiments with different types of soil;
- Investigating the meteorological, seasonal and diurnal effects on tritium deposition and re-emission;
- Understanding the relative importance of re-emitted HTO compared to HTO which is released directly from facilities;
- Quantifying the relative importance of the re-emission of HTO which first deposits onto the soil from the decomposition of OBT in leaf litter and is then incorporated in soil.

## **2.2. IN-CANOPY PROCESSES DURING WET DEPOSITION OF HTO**

### **2.2.1. Overview**

HTO that is released to the atmosphere from a facility is incorporated into the regional water cycle and part of the HTO in the atmosphere is deposited to land surfaces through scavenging by rain (wet deposition) [47–49]. When HTO is deposited to the vegetated land by rain, HTO deposits to the aboveground part of vegetation and the remainder is deposited to soil. HTO that is deposited to the plant canopy or soil is re-emitted to the air, which in turn elevates the concentration of HTO in the atmosphere near the ground [14, 15]. The re-emission mechanism is identical to dry deposition and follows a reverse HTO gradient. As a result of the release of HTO from the vegetation canopy and soil, production of OBT by vegetation is enhanced during and after the wet deposition of HTO [43]. Therefore, it is necessary to precisely predict the dynamics of HTO deposited to the land surface by rain in order to assess the dose consequence of HTO releases [50].

Re-emission of HTO from the soil has been ranked as an important process influencing the dose consequences of tritium releases [50, 51]. Therefore, behaviour of HTO re-emission from the soil after wet deposition of HTO has been widely studied in field experiments [14, 15] and the process has been incorporated into most tritium models [18, 43, 44, 52, 53].

In contrast, studies on the canopy related processes during HTO deposition by rain have rarely been investigated, and therefore, few tritium models include this process [43, 44]. It is expected that interception of HTO in rain by the plant canopy and re-emission of the intercepted HTO from the canopy can be a critical process that regulates land surface tritium transfer during and after the wet deposition of HTO. This is especially the case if the large surface area of leaves is considered, particularly for a dense canopy. Section 2.2, therefore, provides an overview of the current understanding of canopy processes during wet deposition of HTO by rain, and it introduces a possible modelling approach for this process.

### **2.2.2. Theoretical considerations**

Deposition of HTO by rain onto the land surface around a facility is influenced by the atmospheric dispersion of HTO and scavenging by rain [47, 54]. In general, most deposition of airborne pollutants by rain occurs near the release point. This is because the released pollutants have not been diluted, and a greater fraction remains in the air column and experiences the scavenging by rain [55–58]. Indeed, during the passage of an HTO plume, the concentration of HTO in the rain at the ground surface near the release point exceeds the concentration of HTO in the air by several orders of magnitude when the HTO is released at a high altitude [57, 58]. It can, therefore, be expected that the re-emission of HTO (and thus the related canopy process) will be more important for the land surface tritium transfer near the release point.

In the vegetation canopy, HTO added onto the land by wet deposition undergoes the following processes: interception by the leaves, drip from the leaf surface water, and release from the leaf surface water to the atmosphere [43]. Plant leaves can retain a certain amount of liquid water on their surface, and therefore, during rainfall a fraction of the precipitating water is trapped by the leaves (and perhaps other aboveground parts, such as stems) [59, 60]. This means that interception becomes particularly important for weak rain events. In fact, in a tropical forest, as much as 80% of the gross rainfall is intercepted by the forest canopy, without it reaching the ground surface during weak rain events of several millimeters of precipitation [59, 61]. Clearly, rain interception by the canopy will play an important role in controlling the dynamics of HTO deposition during weak rain events.

Once HTO is intercepted by the canopy, the efficiency of re-emission of HTO from the wet canopy is characterized by the exchange coefficient of HTO (or water) between the leaf surface water and the surrounding air. For instance, a reported exchange coefficient of water vapour between the leaf surface water and air is 3 cm/s for a wind speed of 1 m/s [62]. For the exchange of HTO between the soil and atmosphere, some tritium models use exchange coefficients of 0.01–0.1 cm/s [15, 19, 51, 63]. This comparison shows that HTO emission from the leaf surface water can be more significant than that from the soil, in the case that the same amount of HTO is deposited on these sites. Alternatively, one can expect that the emission of HTO from the wet canopy becomes greater than that from the soil because HTO added to the soil is diluted by the pre-existing soil water.

It has previously been reported that the canopy process influences the concentration of HTO in the air during and after rainfall. Earlier numerical studies demonstrated that concentrations of HTO in the surface atmosphere are elevated during a weak rain event (precipitation of ~1 mm)

due to HTO release from the wet canopy [43]. As a result of the elevated concentration of HTO in the canopy air, production of OBT by the vegetation after the rain was significantly increased [43].

Overall, the canopy process during wet deposition of HTO is important in the land surface tritium transfer, particularly for a weak rain event near a tritium release. Inclusion of this process in tritium models is, therefore, encouraged in order to accurately predict the concentration of HTO in the air and the resulting OBT production by vegetation, and thus, the dose consequences of tritium releases.

### 2.2.3. Modelling approaches

This section presents the modelling approaches for tritium transfer related to the canopy processes during wet deposition of HTO by rain.

During rain, HTO contained in the rainwater deposits on the leaf surfaces and the HTO content in the leaf surface water can be calculated by considering the interception of rain HTO, the dripping of HTO from the leaf surface water, and the exchange of HTO between the leaf surface water and the surrounding air [43]:

$$\frac{\partial \eta_v \partial \chi}{\partial t} = F_i - F_d - F_e, \quad (23)$$

where:

- $\eta_v$  is the amount of leaf cellular water per unit leaf area ( $\text{m}^3/\text{m}^2$ );
- $\chi$  is the HTO concentration in the leaf surface water ( $\text{Bq}/\text{m}^3$ );
- $t$  is the time (s);
- $F_i$  is the flux of HTO by the rain interception ( $\text{Bq m}^{-2} \text{s}^{-1}$ );
- $F_d$  is the flux of HTO from the drip from the leaf surface ( $\text{Bq m}^{-2} \text{s}^{-1}$ );
- $F_e$  is the flux of HTO from the exchange from the leaf surface to air ( $\text{Bq m}^{-2} \text{s}^{-1}$ ).

The interception of HTO contained in the rainwater by the leaf surface is calculated from the efficiency of interception and the vertical HTO flux by rainfall:

$$F_i = f F_p \chi_r, \quad (24)$$

where:

- $F_i$  is the flux of HTO by the rain interception ( $\text{Bq m}^{-2} \text{s}^{-1}$ );
- $f$  is the efficiency of the interception (dimensionless);
- $F_p$  is the precipitation intensity above the canopy ( $\text{m}^3 \text{m}^{-2} \text{s}^{-1}$ );
- $\chi_r$  is the concentration of HTO in the precipitating rainwater ( $\text{Bq}/\text{m}^3$ ).

The efficiency of interception by the plant canopy depends on the physical characteristics of the canopy, such as leaf area and the angles of the leaves [60, 64, 65]. Several empirical models have been proposed to calculate the interception fraction. For example, Ref. [64] proposed a model that uses a single sided leaf area index  $A$  ( $\text{m}^2/\text{m}^2$ ):

$$f = 1 - \exp(-\mu_A A), \quad (25)$$

where:

- $f$  is the efficiency of the interception (dimensionless);
- $\mu_A$  is an empirically determined constant ( $\text{m}^2/\text{m}^2$ );
- $A$  is the leaf area index ( $\text{m}^2/\text{m}^2$ ).



The following biomass-based model was proposed in Ref. [66]:

$$f = 1 - \exp(-\mu_B B), \quad (26)$$

where:

- $f$  is the efficiency of the interception (dimensionless);
- $B$  is the standing biomass of the plant ( $\text{kg/m}^2$ );
- $\mu_B$  is an empirically determined constant ( $\text{m}^2/\text{kg}$ ).

If the amount of leaf surface water exceeds the maximum holding capacity, which is parameterized by the plant types [67] and typically has the value of 0.1–0.2 mm [59, 60], dripping of the retained water from the leaf surface occurs. The flux of HTO due to this water dripping is calculated by:

$$F_d = F_{d,water} \chi, \quad (27)$$

where:

- $F_d$  is the flux of HTO due to dripping of water ( $\text{Bq m}^{-2} \text{s}^{-1}$ );
- $F_{d,water}$  is the vertical flux of the dripping water ( $\text{m}^3 \text{m}^{-2} \text{s}^{-1}$ );
- $\chi$  is the HTO concentration in the leaf surface water ( $\text{Bq/m}^3$ ).

The amount of the leaf surface water and the flux of dripping water are calculated by using existing leaf surface water models [59, 60, 62, 68, 69].

Finally, exchange of HTO between the leaf surface water and atmosphere is calculated by:

$$F_e = A \frac{1}{r_a + r_b} (\chi - \chi_a), \quad (28)$$

where:

- $F_e$  is the flux of HTO from the exchange from the leaf surface to air ( $\text{Bq m}^{-2} \text{s}^{-1}$ );
- $A$  is the single sided leaf area index ( $\text{m}^2/\text{m}^2$ );
- $\chi$  is the HTO concentration in the leaf surface water ( $\text{Bq/m}^3$ );
- $\chi_a$  is the concentration of HTO in the atmosphere ( $\text{Bq/m}^3$ );
- $r_a$  is the aerodynamic resistance characterized by the turbulence in the surface boundary layer ( $\text{s/m}$ );
- $r_b$  is the boundary layer resistance, which describes mass transfer in the quasi-laminar flow layer adjacent to the leaf surface ( $\text{s/m}$ ).

Derivation of these resistances can be found in various literature sources (e.g. Refs [14, 18, 52]).

#### 2.2.4. Conclusions

The role of canopy related processes during rain in controlling the dynamics of HTO deposited by the rain was reviewed. Studies suggest that emission of HTO from the wet canopy would be important in enhancing concentrations of HTO in the air and, therefore, production of OBT by the vegetation, particularly for weak rain events at locations near facilities that release tritium. A simple modelling approach to calculate the re-emission of HTO from the wet canopy was presented, which considered the interception of rain HTO, the dripping of HTO from the wet leaves and the exchange of HTO between the leaf surface water and atmosphere.

The transfer of HTO from the wet canopy to the land surface depends on many environmental factors, for example, rain intensity, duration of the rain, timing of the rainfall (i.e. day or night) and density of leaves in the plant canopy. More experimental work and modelling studies on this process are needed in order to better understand the importance of this process relative to the other processes such as re-emission of HTO from the soil.

## 2.3. DYNAMICS OF HTO TRANSFER INTO THE PLANT-ATMOSPHERE SYSTEM: FOLIAR UPTAKE AND RE-EMISSION

### 2.3.1. Overview

The current standard approach to the modelling of the dynamics of HTO transfer into the plant-atmosphere system is based on the assumption that the aerodynamic resistance and the boundary layer resistance are of minor significance for HTO uptake and re-emission and can, therefore, be neglected in a first approximation. Under this simplification, the dynamics of HTO in the plant-atmosphere system can be limited to, and broken down into, two processes:

- Foliar uptake (or absorption) of HTO vapour by leaves when the plume of HTO passes above the plants;
- Re-emission (or transpiration) of HTO through the leaves into the atmosphere, after the plume passage, and the subsequent slowing of re-emission.

Moreover, these exchange processes can be reasonably simplified, primarily using the resistance analogy.

### 2.3.2. Exchange mechanism

The absorption of HTO vapour by the aerial parts of the plants (mainly the leaves, hence this absorption phenomenon is usually called ‘foliar uptake’) is a diffusion phenomenon through small pores (stomata) and is controlled mostly by climatic conditions (i.e. daylight, temperature, rainfall, humidity as water vapour concentration in leaf air spaces and in external air) and plant physiology (i.e. stomatal density, stomatal gating, hormonal factors, age of the plant) [12]. A small percentage of water exchange, typically comprising less than 10%, may also involve direct passive diffusion across the cuticle (i.e. the external layer, which covers the aerial organs of a plant). Under adequate conditions of moisture for C3 plants (accounting for more than 95% of the Earth’s plant species, and thus, most edible plants), stomata are open during the day with a low resistance to the transfer of water vapour and are more or less closed at night with a high resistance. As a result, atmospheric uptake of HTO occurs easily in daylight (even when there is strong transpiration by plants) and occurs more slowly in the dark for various types of plants [12, 70–78]. More precisely, the opening/closure of stomata controls the flux of transpiration, i.e. they are open when there is light and sufficient water coming from soil and can be moderated by some internal regulation (abscisic acid, ABA, for water stress, e.g. see Ref. [79]).

#### 2.3.2.1. *Consideration of kinetics*

HTO exchange between leaves and the atmosphere is a rapid phenomenon. As a result, increases and decreases in HTO activity concentrations occur hourly during the day. The atmospheric exchange of tritium, and consequent fluctuation in plant tissue, is much slower under conditions of darkness than in daylight, where loss of HTO is primarily dependent on transpiration. The nighttime period can last many hours and the exact time of HTO release is important, as the greatest decline in concentration will occur the following morning under

daylight conditions. Therefore, the HTO activity concentration of leaves increases from zero at the start of the period to a maximum value at the end of the release, returning to ‘standard’ activity concentration (i.e. the level of soil water activity) some hours later.

Consequently, foliar uptake and re-emission of HTO need to be modelled with fast dynamics<sup>3</sup>, using climatic data and the appropriate dynamics of plant parameters.

### 2.3.2.2. *The resistance approach*

It is well established [80] that the transfer of HTO vapour by diffusive exchange from air vapour to free water of the leaves is dependent on the difference in the concentration of tritiated water vapour between leaf air spaces and the external air, as well as on the resistance of the plant to water loss (i.e. to maintain adequate water in the tissue). It is necessary to consider the transfer of HTO from a reference height to the canopy air (aerodynamic resistance), together with HTO transfer from canopy air to the leaves (boundary layer resistance) and transfer from the leaf surface through the stomata and cuticle (canopy stomatal resistance)<sup>4</sup>. This transfer is dependent on the leaf area index (m<sup>2</sup> of leaves per m<sup>2</sup> of soil) and the stomatal resistance, which characterizes stomata opening. Analogous to the resistance of a flow of electrons in an electric circuit, the exchange velocity of water vapour between air and leaves,  $V_{exc}$  (m/s) is defined as:

$$V_{exc} = \frac{1}{R_a + R_b + R_c} \quad (29)$$

where:

$V_{exc}$  is the exchange velocity of water vapour between air and leaves (m/s);

$R_a$  is the aerodynamic resistance (s/m);

$R_b$  is the boundary layer resistance (s/m);

$R_c$  is the canopy stomatal resistance (s/m).

$R_a$  and  $R_b$  depend on the aerodynamic characteristics of the crop (height) and/or the leaves (size, surface properties) and on the wind speed in the canopy. Both resistances decrease with the increase of wind speed and crop height.  $R_c$  depends on surface properties, temperature, photosynthetically active radiation, humidity and soil water content. In Eq. (29) above, the canopy stomatal resistance  $R_c$  is the predominant factor [8].

Many studies emphasize the need to consider the variability of the exchange velocity rate since there is a large variability between plants and based on environmental conditions [81–84]. From a mathematical point of view, it is thus important to propose a model that reflects the dynamics of the evolution of stomatal resistance (see below) because this resistance has very significant variations within a 24 hour cycle (i.e. from a daytime average of 300 s/m during the daytime when the stomata are completely open, to a nighttime average of 10 000 s/m when stomata are closed).

---

<sup>3</sup> In the case of ‘fast dynamics’, the time step for input parameters of the model are short: for meteorological parameters, the time step is of the order of 10 mins and for plant physiological parameters, it is between 10 mins and 1 hour. The term ‘fast dynamics’ is frequently used by tritium modellers for physiologically based submodels for plants.

<sup>4</sup> This process occurs when HTO vapour in air is deposited on the leaf surface and then transferred, by diffusion, through stomata and cuticle into the inner cavities of the leaf, where because of photosynthesis (during the day) or biochemical reactions (at night), OBT is produced. Therefore, this represents the transfer of HTO vapour from the leaf surface to the leaf interior.

### 2.3.3. Models for short term exposure (dynamic equations)

As previously mentioned, it has been established in Refs. [71, 80] that the flow of tritium ( $J$ ) through leaf surfaces (stomata and cuticle) is proportional to the differences in volumetric concentrations of tritiated water vapour between the atmosphere and the leaf surface itself:

$$J = V_{exc}(\rho_a C_a - \beta \rho_v C_f) \quad (30)$$

where:

- $J$  is the flow of tritium through leaf surfaces (stomata and cuticle) ( $\text{Bq m}^{-2} \text{ s}^{-1}$ );
- $V_{exc}$  is the water exchange velocity ( $\text{m/s}$ );
- $C_a$  is the HTO concentration in the atmospheric water vapours surrounding the plants ( $\text{Bq/kg}$ );
- $C_f$  is the HTO concentration in the leaf tissue water or TFWT ( $\text{Bq/kg}$ );
- $\rho_a$  is the absolute air humidity at the reference height ( $\text{kg/m}^3$ );
- $\rho_v$  is the saturated air humidity at the vegetation temperature ( $\text{kg/m}^3$ );
- $\beta$  is the inverse of the isotopic discrimination factor ( $\beta = 0.91$  at ambient temperature) (dimensionless).

#### 2.3.3.1. Modelling approaches for the kinetics of HTO exchange between air and plants

Various models and equations have been proposed to express the uptake kinetics of HTO. Among them, a classical approach to describe the dynamic transfer of HTO from the atmosphere to aerial parts is based on mass balance. Equation (31) comes from the balance between inflow (see Eq. (30)) and outflow of the foliar compartment [80, 85] and includes the transpiration flux of tritiated water through the stomata. It has been applied in models such as RODOS [86] and TOCATTA- $\chi$  [46].

$$\frac{dC_f}{dt} = \frac{V_{exc}}{M_w}(\rho_a C_a - \beta \rho_v C_f) + \underbrace{\frac{V_{exc}}{M_w}(\rho_v - \rho_a)C_{sr}}_{\text{Transpiration}} \quad (31)$$

where:

- $C_f$  is the HTO concentration in the leaf tissue water or TFWT ( $\text{Bq/kg}$ );
- $t$  is time ( $\text{s}$ );
- $V_{exc}$  is the water exchange velocity ( $\text{m/s}$ );
- $M_w$  is the free water mass in plant leaves over a unit of soil surface ( $\text{kg/m}^2$ );
- $\rho_a$  is the absolute air humidity at the reference height ( $\text{kg/m}^3$ );
- $C_a$  is the HTO concentration in the atmospheric water vapours surrounding the plants ( $\text{Bq/kg}$ );
- $\beta$  is the inverse of the isotopic discrimination factor ( $\beta = 0.91$  at ambient temperature) (dimensionless);
- $\rho_v$  is the saturated air humidity at the vegetation temperature ( $\text{kg/m}^3$ );
- $C_{sr}$  is the HTO concentration in the water in the root layer of the soil ( $\text{Bq/kg}$ ).

The vegetation model of SOLVEG-II [43] computes TFWT per unit leaf area by considering HTO exchanges as:

$$\frac{\partial \eta_f C_f}{\partial t} = E_{stom} + E_{root} - E_{phot} + E_{res} \quad (32)$$

where:

- $\eta_f$  is the volume of the leaf cellular water per unit leaf area ( $\text{m}^3/\text{m}^2$ );
- $C_f$  is the TFWT concentration in the leaf cellular water ( $\text{Bq/m}^3$ );

$t$  is the time (s);  
 $E_{stom}$  is the HTO flux through stomatal exchange between the canopy air and the leaf cellular water ( $\text{Bq m}^{-2} \text{ s}^{-1}$ );  
 $E_{root}$  is the HTO flux through HTO loading by the root uptake ( $\text{Bq m}^{-2} \text{ s}^{-1}$ );  
 $E_{phot}$  is the flux through TFWT assimilation into OBT via photosynthesis ( $\text{Bq m}^{-2} \text{ s}^{-1}$ );  
 $E_{res}$  is the flux through TFWT production from OBT via respiration ( $\text{Bq m}^{-2} \text{ s}^{-1}$ ).

In SOLVEG-II, the HTO exchange between the canopy air and the leaf cellular water is also expressed by a resistance approach (see below). Both CTEM-CLASS-TT and CERES use an exchange velocity based on stomatal resistance.

### 2.3.3.2. *Modelling approaches for canopy stomatal conductance*

There are many approaches that can be used to model leaf stomatal resistance (see reviews published in Refs [8, 87]). A mechanistic approach [88] can be used to estimate minimal canopy resistance based on four uncorrelated environmental factors (light, temperature, vapour pressure deficit). The Ball-Woodrow-Berry (BWB) model [89] uses semiempirical coefficients in addition to environmental factors. An improved version of the BWB model [90] (herein referred as the ‘Leuning model’) takes into account the compensation point for  $\text{CO}_2$  (i.e. the concentration of  $\text{CO}_2$  at which  $\text{CO}_2$  uptake is equal to  $\text{CO}_2$  production) and replaces the relative humidity at the leaf surface with a function that is dependent on vapour pressure deficit. The Jacobs-Calvet model proposes a physiological approach for stomatal conductance, i.e. it assumes that leaf conductance is determined by the ratio between the photosynthetic rate and the concentration difference of  $\text{CO}_2$  for leaf surface and leaf interior [91, 92]. A simplified empirical formulation of the Jacobs-Calvet approach was proposed [93] that allows for the effect of soil moisture stress on the canopy conductance to be taken into account. However, because these stomatal conductance models are empirical, their parameters — although readily estimated from data — have no meaning attached. This empirical basis is, therefore, unsatisfactory because it means that confidence is low when applying the model in novel situations. In addition, it indicates that there is no theoretical basis for the prediction or interpretation of differences in the parameter values among species and vegetation types [94]. Moreover, most of these models do not capture the responses to soil water status. There is, however, experimental evidence in many species of a mechanistic link between stomatal closure and soil drying [94], and that is governed by a chemical signal, with abscisic acid (ABA) being a central component of the signal [95]. By combining the ABA signaling and the photosynthetic flux, the model proposed in Ref. [95] has the advantage of being dependent on only four variables, i.e. net assimilation, water flux, atmospheric  $\text{CO}_2$  concentration and soil moisture content. This framework has been recently implemented in the TOCATTA- $\chi$  model for grassland ecosystems [46], providing a more mechanistic description of soil–plant interactions than existed previously.

To scale up stomatal conductance from leaf to canopy level, several approaches are usually adopted:

- The ‘big leaf’ approach: integrates the stomatal resistances of the plant leaves, by considering the canopy as one single leaf (e.g. TOCATTA- $\chi$ ). Recent advances have used more sophisticated in canopy models (e.g. Refs [96, 97]);
- The ‘physiological approach: integrates the photosynthetic rate over the canopy height (i.e. leaf area index (LAI)). The most complex model (SOLVEG-II) considers the HTO uptake and the re-emission from leaves based on the Ball-Berry formalism [89] for canopy resistance, together with the biogeochemical photosynthesis model of Farquhar [98].

There are many models describing photosynthesis, from simple, empirical models to very complex models. Some of these models are reported in Ref. [8].

#### **2.3.4. Conclusions**

Models vary from simple (e.g. use of constant exchange velocities for daytime and nighttime) to complex (e.g. with a multilayered canopy, extensive dynamics of HTO in leaves, and coupling of the BWB model with a generic Farquhar model for photosynthesis).

In choosing a model, accurate representation of predominant processes is a primary consideration. With regard to minor processes, more simplified models could be applied in order to not add more complexity than is absolutely necessary. It is thus important to understand which processes are predominant and which parameters are most affecting the results.

Foliar uptake and re-emission of HTO are predominant processes controlling the short term dynamics of tritium transfer to plants before it is photosynthesized to OBT. Foliar uptake and re-emission of HTO thus need to be modelled with fast dynamics (i.e. from 1 hour during the day to less than 10 hours at night), using climatic data and appropriate dynamics for plant parameters such as stomatal resistance. It is particularly important to use a model that reflects the dynamics of the evolution of stomatal resistance because this resistance has very significant variations within a 24-hour cycle. In addition, the model needs to achieve a balance between mechanistic detail and mathematical simplicity.

### **2.4. TURNOVER OF ORGANICALLY BOUND TRITIUM IN LITTER AND SOIL**

#### **2.4.1. Overview**

Even though the litter layer<sup>5</sup> and the mineralized soil layer<sup>6</sup> beneath are considered as important ecological compartments for transfer of tritium in a terrestrial ecosystem, little is known about the behaviour of OBT once it is added to the litter layer and the soil [9, 99, 100]. Thus far, several observations on the turnover of OBT in the litter layer and the soil have been conducted. However, there is no agreed modelling approach for the turnover of OBT in these horizons [50] and the dose consequence of OBT accumulation in litter and soil remains uninvestigated.

Overall, Section 2.4 aims to provide an overview of the current understanding of OBT turnovers in the litter and the soil. Firstly, possible sources of OBT in the litter and the soil are identified, after which the experimental and theoretical aspects of the turnover of OBT in the litter and the soil are reviewed. Finally, a possible modelling approach for OBT turnover in soil is introduced, based on existing models of turnover of organic matter in soils.

In this context, the focus is placed on the dynamics of non-exchangeable OBT (hereinafter, referred to simply as OBT). Basically, two types of OBT, i.e. non-exchangeable and exchangeable OBT, can occur in the natural environment. However, the exchangeable OBT is essentially in equilibrium with the tritium in natural water sources [101]. Therefore, the exchangeable OBT is not expected to participate in the long-term accumulation of OBT in litter and soil.

---

<sup>5</sup> The litter layer is the aboveground layer consisting of decomposing and decomposed plant debris, namely the O-horizon [102].

<sup>6</sup> The mineralized soil layer is the layer below the O-horizon, namely the A-horizon [102].

### **2.4.2. Sources of OBT in litter and soil**

Past experiments and observations have shown that OBT can occur in the litter or the soil due to direct input of plant synthesized organic material as litter fall [103], conversion of HT to OBT by microorganisms contained in dead leaves existing in litter and humus layers [104] and soil [28, 31], and conversion of HTO to OBT in soil microorganisms [13, 105]. However, studies have shown that conversions of HT and HTO to OBT in the organic layer and soil are slow and much smaller compared with the direct inputs of plant synthesized OBT by the litter fall [30, 105–107]. Therefore, the remainder of Section 2.4 focuses on the input of OBT by the litter fall as the main source of OBT in the natural soil environment.

### **2.4.3. Experimental and theoretical aspects of turnover of OBT in litter and soil**

Only a limited number of experiments have been conducted on the turnover and accumulation of OBT in the litter layer and soil horizons. This may be due to the challenging nature of OBT analysis in soil, or to the fact that soil monitoring is not part of the usual monitoring of facilities [108]. However, several observations provide important insights regarding accumulation and turnover of OBT in soils.

At a historical HT release site in Canada (i.e. Chalk River Laboratories), the concentrations of OBT in the soil remained considerably higher than the concentrations of HTO in the same soil sample, even 15 years after the expected pulsed input of OBT to the soil (i.e. after past HT release experiments at the site) [99, 108]. In France, elevated OBT activities in soil were observed around a nuclear power plant 15 years after it was shut down [103, 109]. Accumulation of OBT in soils has also been observed near an operating facility in Canada [110]. Furthermore, OBT concentrations in litters and soils that are higher than the background tritium level have been observed in the general environment, i.e. areas not specifically impacted by tritium releases from facilities [76, 101, 104, 110]. These observations suggest that OBT accumulates and remains in soils over an extended period, e.g. decades [103, 107].

There are no direct measurements of OBT decomposition in soils. However, it is expected that OBT in soil follows organic matter turnover in the soils because OBT represents the hydrogen that is bound to organic molecules [9, 103, 109]. For example, temporal decreases of fallout derived OBT were tracked in soil in Oklahoma, USA, over an extended period between 1963 and 1970 [101]. A mean residence time of OBT in soil was estimated to be approximately 5 years (corresponding to a half-life of 3.5 years). The estimated half-life of OBT in the soil is less than that of the radioactive decay of tritium (half-life of 12.3 years). This shorter residence time of OBT in soil, compared with the radioactive decay of tritium, possibly reflects a fast turnover of soil organic matter at the site.

In contrast, certain types of plant organic matter reside in soils for longer periods. Soil organic matter consists of many types of organic compounds which have different physicochemical natures, and therefore, different responses to microbial decomposition in the soil [111, 112]. As a result, there is a turnover rate of about 1–2 years during the first phase of decomposition of natural organic matter in soils, while the second phase involves slow decomposition, which can last decades and accounts for about 90% of the loss of organic matter in soils [113, 114]. Turnover of these rapid and slow cycles of organic matter can vary with environmental factors, such as climate, vegetation, and soil quality [112, 115–117]. These two types of organic matter turnover in soil indicate that a certain fraction of OBT added to the soil can remain for longer time periods. This may account for the previously mentioned high OBT concentrations in natural soil samples found in some studies, which is likely attributable to the slow

decomposition of OBT in soils and historically higher environmental tritium levels due to nuclear facility releases [99, 103, 108–110] or weapons testing [76, 101, 104, 110].

Overall, decomposition of organic matter in soils by microbial activity seems to be a key process that controls the turnover of OBT in soil. Therefore, modellers need to consider the long-term turnover of organic matter that is caused by microbial decomposition processes in soil in order to precisely predict the belowground accumulation of OBT and the resulting impact on environmental tritium transfer [99].

#### **2.4.4. Modelling approaches**

This section presents an overview of the current understanding and modelling of dynamics of organic matter (or organic carbon) in litter and soil. It then proposes a possible modelling approach for the OBT turnover in soils, based on existing models of organic matter turnover.

In a vegetated ecosystem, organic matter synthesized by photosynthesis is transferred to the litter layer through litterfall of dead leaves and plant debris (aboveground litter) or transferred to soil by death of the roots (belowground litter) [112, 117]. In the aboveground litter layer, the added organic matter is decomposed to  $\text{CO}_2$  and  $\text{H}_2\text{O}$  by microorganisms, leached to the underlying soil by rain [118, 119], or transferred to the soil by sedimentation of the degraded litter materials [120].

In the soil, organic matter transferred from the overlying litter layer, or directly added by the belowground litter input, is microbially decomposed and mineralized to  $\text{CO}_2$  and  $\text{H}_2\text{O}$ . In general, well accepted soil organic carbon (SOC) models define multiple carbon pools that have different timescales of turnover by the microbial decomposition [111, 112, 114, 121–125], as shown in Fig. 1(a) below. In these models, SOC contained in each pool is decomposed to  $\text{CO}_2$  at a defined rate of turnover, and a fraction of the decomposing organic carbon is, in turn, transferred to the more resistant carbon pool. For example, the CENTURY model [121, 122] defines active, slow and passive carbon pools, that reveal timescales of turnover of years, decades and centuries, respectively (see Fig. 1(a)). Conceptually, the active carbon pool represents rapidly degradable plant materials and soil microbes. The slow pool represents the resistant plant materials, such as lipids and lignin, as well as organic carbon weakly stabilized by physical and chemical processes in the soil. The most resistant passive pool represents the organic carbon that is stabilized by the interactions with mineral surfaces and metal ions of soil constituents [112, 115, 116].

Acknowledging these models of SOC turnover, a conceptual model of OBT turnover in soil is proposed. Particular focus is given to the soil compartment rather than the litter layer, because organic matter accumulates in the soil over long periods of time due to slower turnover of soil organic matter, compared with rapider turnover of fresh organic matter in the litter layer [114, 125]. Assuming that microbial decomposition of OBT in soil fully follows that of organic matter (i.e. organic carbon) in the soil, turnover of OBT can be modelled in a similar manner to that of organic carbon shown in Fig. 1(a), with an additional loss of OBT by radioactive decay (Fig. 1 (b)). In this proposed model, a fraction of OBT is converted to HTO during the course of microbial decomposition, and the remainder forms more resistant OBT. The HTO produced by the microbial decomposition will follow the transport of HTO in soil.



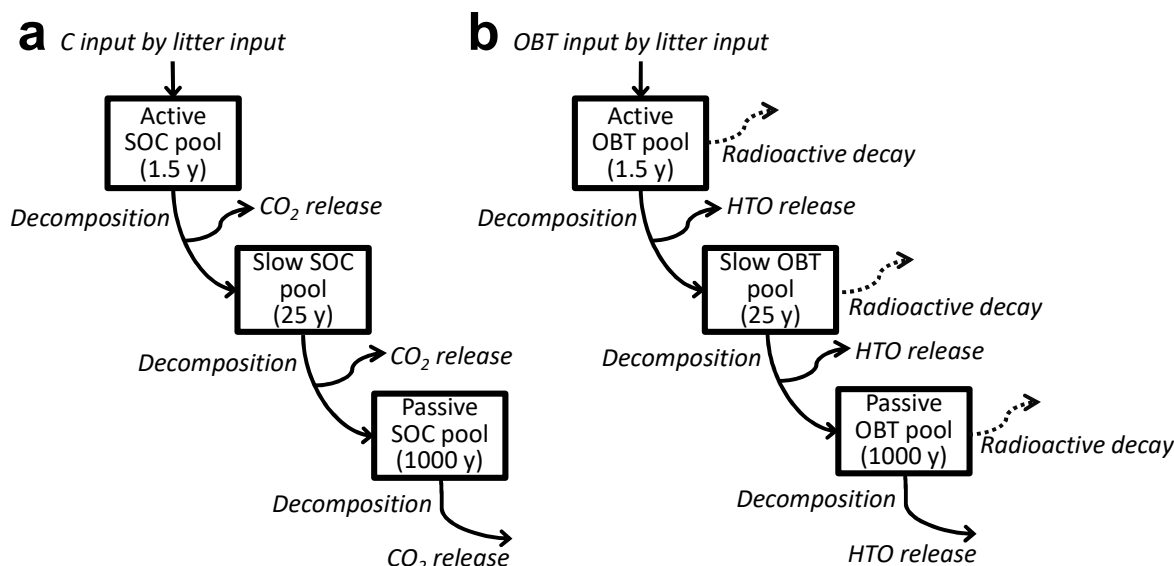


FIG. 1. Conceptual models of turnover of soil organic carbon (SOC) (a) and OBT (b).

Although the proposed soil OBT model assumes three OBT pools, like existing SOC models, the most recalcitrant (passive) pool may not be needed to predict the turnover of OBT in soils because of loss of OBT in the slow pool by radioactive decay; i.e. a large fraction of OBT in the slow pool will decay and does not enter the passive pool. This assumption may be supported by observations showing that decrease of OBT concentration in soils with increasing soil depth is more pronounced, compared with the decrease of the organic matter content in the same soil [30, 99], indicating that OBT is lost in the soil more rapidly than the organic matter and is not transported to deeper parts of the soil.

The concept shown in Fig. 1(a) is based on the three pool models, such as the CENTURY model [121], but is much simplified. Active, slow and passive SOC pools, respectively, have turnover times of 1.5, 25 and 1000 years for the microbial decomposition. Figure 1(b) shows that OBT in each pool is also lost by the radioactive decay of tritium.

#### 2.4.5. Conclusions

This review of experimental and theoretical aspects of soil OBT has found evidence that OBT accumulates in soil and the OBT concentration in soil will remain elevated over decades, which may reflect past environmental tritium levels. Turnover of OBT in soil is probably controlled by the inputs of plant synthesized OBT via litter falls and microbial decomposition of organic matter (OBT) in soil. Based on existing models of turnover of organic matter in soils, a possible modelling approach for the turnover of OBT in soil is proposed.

Theoretical and experimental studies on dynamics of OBT in the litter layer and soil are limited and this process is not well understood. Turnover of organic matter in soil is affected by many environmental factors such as the temperature [126, 127] and the water regime at the site [121, 122], indicating that the impact of OBT accumulation on environmental tritium transfer may differ by ecosystem. More studies are, therefore, needed in order to better understand OBT turnover in the litter layer and soil, and to assess impacts of belowground accumulation of OBT on doses from tritium releases.

## 2.5. FORMATION OF ORGANICALLY BOUND TRITIUM IN DARKNESS

### 2.5.1. Overview

For existing tritium models, nighttime or darkness is a special case of the formation of OBT, as certain physiological reactions are involved in the formation of OBT in plants during darkness [99, 128–130]. However, there is no harmonized modelling approach for this process [100, 131, 132] and as a result, large differences exist between tritium models for OBT formation in darkness [131, 133]. Most models do not include the formation of plant OBT at night [43, 44, 46, 134, 135]; however, there is a model that includes this process [130], and there is evidence for OBT production at night [133, 136–139].

The different approaches among existing tritium models are mainly attributable to the lack of understanding of the processes involved in nighttime OBT formation, and partly due to the reported slower rate of formation of OBT during darkness than during daylight hours [132]. Section 2.5 provides an overview of the current understanding of OBT formation by plants during darkness. Initially, available experimental results of OBT formation during darkness are outlined, and theoretical aspects of this process are then discussed. Finally, some modelling approaches for this process are presented.

### 2.5.2. Experimental studies

Several studies have observed OBT formation at nighttime as part of HTO plant exposure experiments. OBT formation by the plant in dark conditions was first observed as part of a study on HTO exposure to *Chlorella* algae [140], where it was found that TFWT is incorporated into the non-exchangeable sites of organic compounds during the dark phase at a rate of one third of that during the daylight phase.

Formation of OBT in darkness has also been observed for many types of crops, and laboratory experiments showed that nighttime OBT formation occurs in wheat plants after a short term HTO exposure [78, 136]. Results showed that OBT formation at night in wheat leaves amounted to about 50% of that produced under daytime HTO exposures. For rice plants, the formation rate of OBT during night exposure was about one third of that during daytime exposure [138]. For soybean plants, it was observed that nighttime OBT formation rates are several orders of magnitude smaller than in the daytime [83, 141]. Assimilation of OBT at nighttime has also been observed for leaves of tangerine trees [84]. Buildup of OBT concentrations after nighttime HTO exposure has been observed not only in leaves but also in storage organs, such as beans and grains of wheat and rice plants [83, 84, 138, 141].

Overall, formation of OBT during darkness occurs regardless of plant type and is not negligible compared with the daytime formation of OBT by photosynthesis [130, 133]. Tritium models would, therefore, benefit from the inclusion of nighttime OBT formation to accurately predict OBT concentrations in plants impacted by tritium releases.

### 2.5.3. Theoretical aspects

Recently, it has been recognized that OBT is formed in plant tissue by two major pathways, i.e. photosynthesis under daylight conditions and non-photosynthetic process independent of light [100, 128–130]. Therefore, daytime OBT formation by photosynthesis is only partly correlated with the total OBT formation, i.e. photosynthetic plus non-photosynthetic formation [78].

Photosynthetic formation includes carbon reduction in the Calvin cycle. In this process, photolysis of water (and thus HTO) produces reduction equivalents, nicotinamide adenine dinucleotide phosphate and  $H^+$  ( $T^+$ ), and energy equivalents, adenosine triphosphate. These compounds are used in the Calvin cycle and organic substrates are newly synthesized [76, 128].

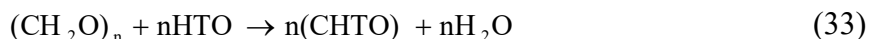
Non-photosynthetic formation is a metabolic process which includes anabolic and catabolic reactions that occur independently of light [130, 132, 136, 137]. Processes related to the tricarboxylic acid cycle, one of the respiratory chemical processes, are thought to be responsible for the incorporation of TFWT into non-exchangeable OBT during this metabolism [130, 133, 142]. Experimental results on the assimilation of HTO and radiocarbon dioxide by *Chlorella* [140] demonstrated that, in dark conditions, tritium is preferentially incorporated into substances associated with the tricarboxylic acid cycle. Similar results were obtained by experiments that used soybean leaves [141], supporting the role of metabolic process in assimilating TFWT.

Plant tissue is dynamic, breaking down and rebuilding organic compounds continuously through metabolism for energy supply, growth and maintenance of structure [9, 100, 143]. During daytime, photosynthetic products are temporally stored as intermediate materials such as starch [136, 143], and these materials are, in turn, used for metabolism. In the course of metabolism, a new synthesis of organic material does not occur, but conversion of one type of organic compound to another does occur [78, 99, 100, 128, 144]. Through this conversion, tritium atoms contained in the tissue free water behave as a substrate of chemical reactions, being incorporated to the non-exchangeable sites of the rebuilt organic compounds [99, 100, 142].

Another important aspect of this OBT assimilation process is that metabolism occurs continuously and, therefore, incorporation of TFWT to OBT is expected to occur during both daytime and nighttime [78, 130, 139]. Therefore, only considering OBT assimilation by daytime photosynthesis in a model may result in underestimation of OBT concentrations, even for daytime exposures [78, 131]. Overall, OBT formation at night (or more precisely, OBT formation independent of light) is probably caused by metabolic processes and always occurs in plant tissues.

#### 2.5.4. Existing models of OBT formation by metabolism

In this section, an existing model of OBT formation by metabolic process is introduced. Currently, only a few tritium models consider incorporation of OBT due to the plant metabolism. Theoretically, a reaction equation has been proposed [99] for the incorporation of TFWT to OBT due to the hydrolysis of organic compounds during plant metabolism, as follows:



where:

$(CH_2O)_n$  is the starch (a polymer of glucose) synthesized by plant metabolism;  
 $CHTO$  is the tritiated glucose synthesized by plant metabolism;  
 $n$  is the number of water molecules.

In this reaction, HTO in the free water behaves as a substrate for the reaction. Therefore, one can expect that OBT incorporation through metabolism will be expressed using metabolic activity (i.e. conversion rate of organic compounds) in plants and the concentration of HTO in free water.

The easiest way to calculate OBT incorporation during metabolic processes may be the use of a constant transfer rate from the TFWT pool to the OBT pool in the plant, as assumed by the TRILOCOMO model [131] and an earlier version of the UFOTRI model [18].

A more sophisticated modelling approach is proposed by the Plant-OBT model [136, 137], which is used in an enhanced version of UFOTRI [139]. This model assumes that the rate of OBT incorporation  $F_m$  (Bq/s) in each compartment by metabolism depends on metabolic activity and TFWT concentration:

$$F_m = \chi_{TFWT} B \quad (34)$$

where:

$F_m$  is the rate of OBT incorporation (Bq/s);

$\chi_{TFWT}$  is the TFWT concentration in the target tissue (e.g. leaves) defined per unit weight of the organic matter (Bq/kg);

$B$  is the metabolism rate of the target tissue (kg/s).

The model assumes that 0.4% of the organic compounds of each compartment turns over during a day [136]. Therefore, the rate of metabolism,  $B$ , is calculated by:

$$B = rM \quad (35)$$

where:

$B$  is the rate of metabolism (kg/d);

$M$  is the weight of the target compartment (kg);

$r$  is the metabolic turnover rate ( $d^{-1}$ ) ( $r = 0.004 d^{-1}$ ).

A more complex physiologic model for OBT production (hereinafter, referred to as CROPTRIT) during the day [129, 145] and night [130, 146] was proposed and tested with experimental data for wheat [78]. For OBT production during day and night, the CROPTRIT model considers the photosynthetic reactions and stoichiometric relationships and links the OBT production to the HTO concentration in leaves and the photosynthesis rate. In order to use a gross photosynthesis rate, a transition between gross and net photosynthesis rate is assumed, considering maintenance and growth respiration [147]. The isotopic fractionation ratio differs between photosynthesis and respiration, but a single value of 0.5 is assumed. Integrating the temporal interval considered in the model (one hour), the following relationship for OBT production during day and night is obtained [147]:

$$P_{OBT} = \int 0.6 \gamma C_{HTO} (P_{assim,g} - R_{m,OBTg} - R_{g,OBTg}) dt \quad (36)$$

where:

$P_{OBT}$  is the OBT production at day and night ( $Bq L^{-1} h^{-1}$ );

$C_{HTO}$  is concentration of HTO in plant (leaf) water (Bq/L);

0.6 is a stoichiometric factor that links the assimilation of water in organic molecules with dry matter production ( $m^2 h^{-1} kg^{-1} (CO_2)$ );

$\gamma$  is the isotopic fractionation ratio, which is the ratio between OBT formation and OBH formation, with an average of 0.5 and a range between 0.45 and 0.55 (dimensionless);

$t$  is the integration time (h);

$P_{assim,g}$  is the assimilate production by metabolic process during the day and night ( $kg CO_2 h^{-1} m^{-2}$ );

$R_{m,OBTg}$  is the maintenance respiration participating to OBT formation ( $kg CO_2 h^{-1} m^{-2}$ );

$R_{g,OBTg}$  is the growth respiration participating to OBT formation ( $kg CO_2 h^{-1} m^{-2}$ ).

In the nighttime, the starch/sucrose reserves in leaves, which have been accumulated in the light, drive plant maintenance and growth. Also, during the nighttime, the starch is gradually hydrolysed to form soluble sugars (sucrose). This sucrose is used for night metabolism. During starch hydrolysis and subsequent processes, HTO can enter into various biochemical reactions and OBT can then be produced. The following processes were taken into account:

- (1) The role of starch and the circadian clock in plant metabolism;
- (2) The contribution of the nighttime processes to overall plant maintenance and growth and to edible plant parts during their development;
- (3) Nighttime and daytime canopy respiration and its correlation with canopy transpiration and nighttime growth;
- (4) The role of protein turnover in plant maintenance respiration;
- (5) The meaning of nighttime biochemical reactions that produce OBT and the dependence of these reactions on plant type and genotype.

More detailed information on these processes is available elsewhere (e.g. Ref. [130]).

### **2.5.5. Conclusions**

From the review of literature on experiments of nighttime OBT formation, it was found that non-photosynthetic metabolic reactions are responsible for the incorporation of OBT by the plant during darkness hours, and this reaction is independent of light and occurs continuously. The rate of OBT formation in darkness is relatively small, but not negligible, compared with that in daylight hours.

OBT formation during darkness is not well understood, although some progress has been made [130], and further experimental and theoretical studies are needed to improve this understanding [130, 133] to clarify the relevant mechanisms and processes, and to develop modelling tools to describe them [128, 130, 132].

### 3. DESCRIPTION OF MODEL SCENARIOS

#### 3.1. IRSN-EDF SCENARIO

##### 3.1.1. Purpose of the study

Section 3.1 provides a brief description of the VATO experiments, which were conducted by the Institut de Radioprotection et de Sûreté Nucléaire (IRSN) and Electricité de France (EDF) to reduce uncertainties relating to tritium transfer from atmospheric emissions (currently releasing HTO and HT) to a soil–grass ecosystem (see Section 3.1.4). A technical platform was established, with specifically designed instruments, including lysimeters, downwind of the AREVA (now Orano) NC La Hague reprocessing plant in the Northwest of France (now Orano La Hague).

The first phase of this study commenced in 2013 and mainly focused on the quantification of tritium transfer kinetics to grass from various compartments of the environment, such as air water vapour, rainwater and soil water. In the second phase of the project, which began in 2016, measurements related to dry and wet deposition processes, HT oxidation in soil, and isotopic fractionation in plants were collected. The main objective of the VATO project was to obtain a complete, high frequency dataset to allow robust validation of tritium transfer models, in particular the French TOCATTA model.

##### 3.1.2. Site description

An experimental field was set up by IRSN at 2 km downwind from the nuclear fuel reprocessing plant of La Hague (AREVA (now Orano) NC). The facility is located in the North Cotentin Peninsula (Normandie), close to the La Manche seashore, about 20 miles from Cherbourg-Octeville. Tritium is emitted during the work week (i.e. Monday to Friday) in pulses from four adjacent stacks as tritiated water (HTO) and from two stacks as tritium gas (HT).

##### 3.1.3. Experimental set-up and instrumentation

Data from the first phase of the VATO project was used in the current model intercomparison. This dataset was utilized for the evaluation of the kinetics of TFWT and OBT formation (both exchangeable, as E-OBT, and non-exchangeable, as NE-OBT) in grass leaves, as well as HTO in soil.

More detailed information about the methodology used for sample collection and measurements, as well as one year of data acquisition, are given in Ref. [148].

##### 3.1.4. Environmental sampling

Different physicochemical forms of tritium (i.e. aerosols, HT, HTO, tritiated organic compounds<sup>7</sup>) in the atmosphere at the level of the technical platform were monitored and evaluated (when detected). During the campaign, the only physicochemical forms detected were HTO and HT, with HT being predominant (83%) over HTO.

A specifically designed methodology and experimental set-up were developed to measure concentrations of HT and HTO in the atmospheric compartment (air, water vapour and

---

<sup>7</sup> Tritiated organic compounds include different types of organic tritium, such as tritiated methane, tritiated amino acids, tritiated pump oil, radiochemicals and others and can be released in any chemical or physical form from nuclear facilities and activities.

rainwater) and concentrations of TFWT and OBT in grass. The data were recorded over the following time steps:

- HT activity concentrations in air measured once per month<sup>8</sup>;
- Averaged concentrations of atmospheric HTO measured over 48 hours;
- <sup>85</sup>Kr activity concentrations measured hourly;
- Meteorological data at various time steps.

A reconstruction of hourly activity concentrations of HT and HTO in air and rain was achieved using <sup>85</sup>Kr hourly activity concentrations, monthly emissions (of HTO and <sup>85</sup>Kr) and hourly wind directions.

### 3.2. CNL: CHALK RIVER SCENARIO

The Canadian Nuclear Laboratories (CNL) Chalk River Scenario provides data for modelling of tritium activity concentration in vegetation (i.e. plant HTO and total (exchangeable and non-exchangeable) OBT) and soil and dynamical inputs for model runs (forcings).

The Chalk River Scenario data refers to an experimental garden plot in the vicinity of the Acid Rain Site (ARS) of CNL (see Fig. 2). The Chalk River Scenario data were collected in parallel with tritium in air samples and form a comprehensive dataset sufficient for unambiguous reconstruction of environmental tritium behaviour. It includes site pedological data, half hourly meteorological data and half hourly concentrations of HTO in the atmospheric water vapour.

The Chalk River research reactor ('NRU') is heavy water moderated and emits HTO: approximately 50% from the reactor building roof vents, and 50% from the reactor stack located 1 km to the west of the reactor. During the experiment, the released airborne tritium averaged 7 TBq/week. The resulting concentration of HTO in the atmospheric water vapour at the experimental garden plot ranged from 90 to 2500 Bq/L (depending on wind direction) and showed strong correlation with ambient gamma radiation from <sup>41</sup>Ar stack emissions recorded by the monitoring station located 150 m east from the plot. A custom-built bubbler [149] with a detection limit of 0.04 Bq/kg (0.06 Bq/m<sup>3</sup>) for tritium in air was deployed at the garden plot and concentrations of HTO in air were measured at half hour time intervals on nine occasions. Experiments also used the weekly data obtained from a similar bubbler serving the CNL Environmental Monitoring Programme, which was installed beside the gamma monitoring station 150 m away from the garden plot. The meteorological data were recorded at the Perch Lake tower located approximately 4.5 km southeast of the garden plot (approximately along prevailing winds).

Scenario data starts at 00:00 local time on 15 April 2008 (i.e. the 105<sup>th</sup> day of the year). The Chalk River Scenario documents atmospheric data from day 105 to day 342 of 2008. Days in the Chalk River Scenario are enumerated sequentially so that scenario day 1 corresponds to day 105 of the year and so on. Local time at Chalk River is (UTC-05:00) Eastern Time (US and Canada). The period covered by the CNL Scenario is 15 April 2008 to 8 December 2008 and observations for blind comparison with model predictions were collected during the period 30 June 2008 to 20 October 2008.

---

<sup>8</sup> HT was emitted concomitantly with <sup>85</sup>Kr, the latter of which was measured at hourly intervals. The hourly <sup>85</sup>Kr measurements were then used to downscale monthly HT activity concentrations to an hourly time step (see Ref. [148]).

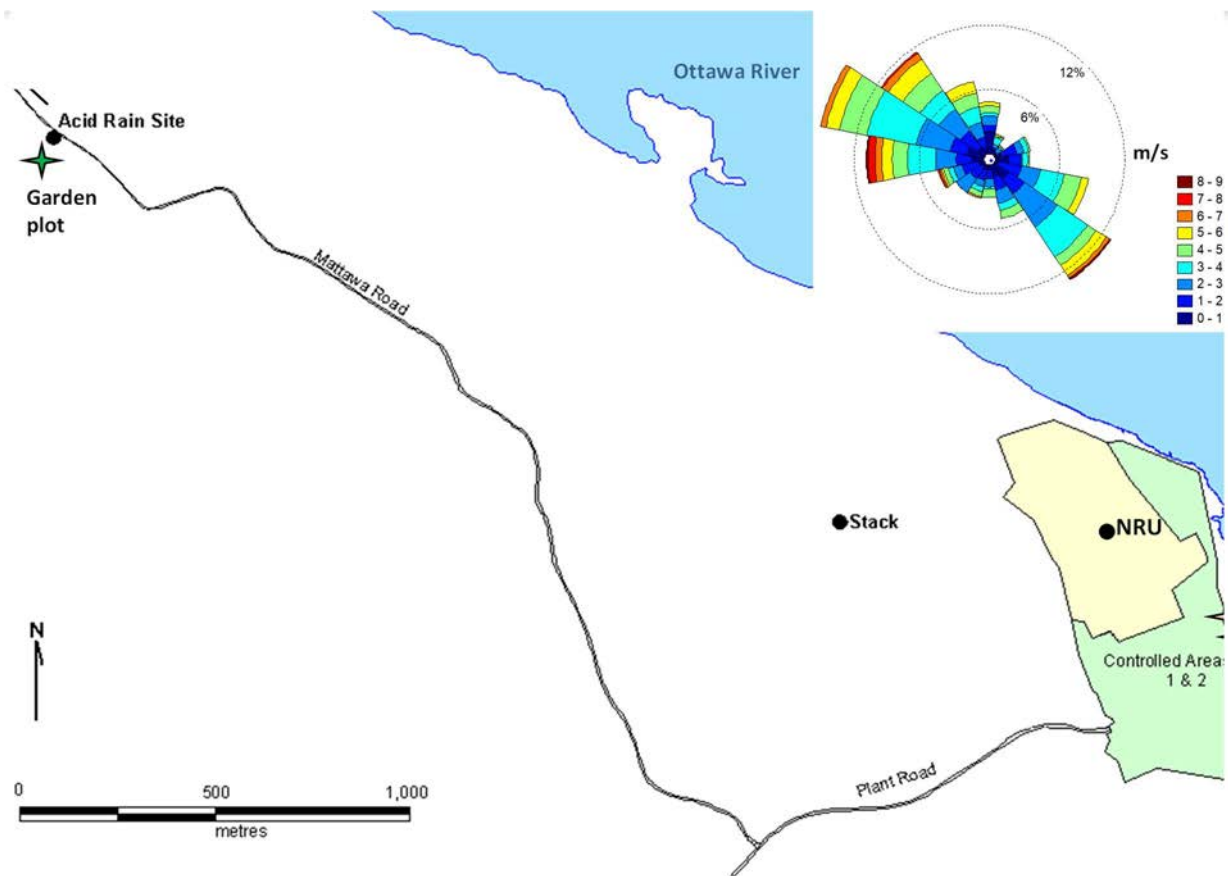


FIG. 2. Location of the CNL experimental garden plot.

Fully developed tomato seedlings and sprout potato seedlings were planted mid-June 2008. However, the date of the initial planting of tomato and potato (start of growth) is needed for modelling; this is, therefore, approximately 15 April 2008.

Site specific data needed for the site initialization input file and the plant initialization input file include fractional coverage of the surface by foliage, log of roughness length, visible albedo, near infrared albedo, aboveground canopy mass, rooting depth and the maximum and minimum LAI. Initialization variables for model simulation time duration, soil moisture and temperatures in all layers are also included. The layers were presented in accordance with CLASS-CTEM-TT requirements with three layers of soil thicknesses, i.e. 0.10 m, 0.25 m, and 3.75 m and thus, of bottom depths of 0.10 m, 0.35 m and 4.10 m, respectively providing a basis for further extrapolation for more refined model setting in TOCATTA- $\chi$  and SOLVEG-II.

Many variables are expected to be evaluated within a model, like the LAI corresponding to a reference crop and climate, or the energy associated with phase change of water in soil layers (gaseous condensation to liquid). The LAI of tomato and potato can also be taken from literature (e.g. tomato from Ref. [99] and potato from Ref. [150]) as the discrepancy introduced by different methods of LAI evaluation are assumed to be small.

Some data are to be specified within the model code by a set of default parameters. For example, the pre-defined soil data correspond to a user defined water table depth and three layers of the vadose zone. Also, only vertical fluxes of energy and moisture are modelled so that all



horizontal fluxes, overland flow from top of soil column, and lateral soil water flow, are accommodated in user defined parameterization of surface runoff and drainage at the bottom of the soil column.

### **3.2.1. Atmospheric data**

#### *3.2.1.1. Observations*

The atmospheric data for the Chalk River Scenario are comprised of actual CNL observations and include half hourly data for:

- Temperature;
- Wind speed and direction;
- Precipitation.

Observations were taken from the CNL meteorological tower at Perch Lake at the level of 30 m above ground level and from the CNL automated rain gauge.

#### *3.2.1.2. Synthesized (modelled) data*

Synthesized (modelled) data were produced based on remote observations at other meteorological stations within a 200 km radius, which were collected at timescales different from the half hourly/hourly intervals. Time series synthesis, therefore, involved spatial interpolation and dynamical downscaling to half hourly intervals. Variables included:

- Short wave solar radiation;
- Long wave solar radiation;
- Pressure;
- Specific humidity.

Short wave solar radiation data were reconstructed using solar radiation data from Ottawa, Canada, visibility data from North Bay and Petawawa, as well as historical (1985–1990) solar radiation data from Ottawa, Petawawa Research Forest Station and North Bay, following information provided in Ref. [151]. Long wave solar radiation was modelled on the basis of the theoretical optical thickness of the atmosphere, hourly solar declination and observed temperature [151]. Pressure was interpolated between that observed at Ottawa and North Bay, and specific humidity was extrapolated from that observed at Petawawa.

### **3.2.2. Atmospheric HTO**

#### *3.2.2.1. Observations*

The main observations provided as part of the scenario were as follows:

- Bi-weekly monitoring of air HTO;
- Data from half hourly measurements of HTO in air by an active sampler in a series of short experiments undertaken in 2008, 2010 and 2011 (which includes the local HTO in air background recorded at the time of the experiments).

In addition, the following auxiliary observations were provided:

- Fine scale (0.1 Hz)  $^{41}\text{Ar}$  data from an automated monitoring station, with the minimum detection limit of the monitor at  $0.1\ \mu\text{Gy/h}$ , i.e. above the local background;
- Local background data for gamma radiation collected by an EXPLORANIUM instrument;
- Monthly rain HTO measurements obtained at Balmer Bay gate located approximately 7 km northwest of the stack, i.e. along prevailing winds and in the same direction as the experimental garden plot, but 3.5 km further downwind.

#### 3.2.2.2. *Modelled data*

The concentration of HTO in atmospheric water vapour fluctuated significantly as a function of whether or not the plume from the reactor stack and other tritium sources (such as in controlled areas on site; see Fig. 2) were in the direction of the ARS. The HTO activity concentration in atmospheric water vapour (HTO in air) data were synthesized using the methodology described in Refs [149, 152].

The local background HTO concentration in atmospheric water vapour when the plume was absent, was estimated both from the low end of the distribution of HTO measurements and the established correlation with gamma radiation using the local gamma background. The background value was estimated at  $68 \pm 19\ \text{Bq/L}$ .

The HTO concentration in rain at half hourly time steps was needed and a simplified modelling approach (traditionally used for snow scavenging of HTO) was used for reconstruction of HTO in rainwater in this CNL Scenario, where the HTO concentration in rainwater was calculated using a washout ratio approach, i.e. made proportional to the atmospheric HTO concentration during the given half hourly interval. The washout coefficient was empirically fitted to monthly rain HTO data collected at Balmer Bay gate to be equal to 0.2 (i.e. rain HTO concentration in  $\text{Bq/L} = 0.2 \times \text{HTO concentration in the atmospheric moisture in Bq/L}$ ). This approach provided a reasonable fit to monthly observations of the HTO concentration in rainwater collected at the Balmer Bay monitoring site.

### 3.3. CNSC MODEL SCENARIO

#### 3.3.1. **Purpose of the CNSC 2012 research study**

The objective of the research study described in Ref. [153] was to obtain carefully matched sets of short term measurements of tritium in air, soil and vegetation, with accompanying data for stack emissions, as well as on-site meteorology in order to understand the circumstances under which high OBT/HTO ratios may evolve, as observed in previous Canadian Nuclear Safety Commission (CNSC) studies [110, 154, 155].

The study was carried out from June to September 2012 near a Canadian tritium processing facility in Pembroke, Ontario (SRB Technologies). During experiments, the facility released 575 GBq per week of total (HT plus HTO) tritium, with an HT:HTO ratio of 2.6.

#### 3.3.2. **Site description**

The gaseous tritium light source manufacturing facility, SRB Technologies, began operations in 1990. The facility is located in Pembroke, Ontario, in a semi-industrial location, however,

there are residential neighbourhoods nearby. Tritium is emitted during the work week (i.e. Monday to Friday) in pulses from two adjacent stacks as both HT and HTO.

### **3.3.3. Experimental set-up and instrumentation**

#### *3.3.3.1. Experimental garden*

The experimental garden consisted of vegetation grown in 200 L barrels with local commercial topsoil. The plants were grown in barrels in order to isolate the vegetation from the native soil near the facility. Samples were obtained weekly to match the stack emissions monitoring programme of the facility. The experimental garden was set up 48 m from the facility<sup>9</sup> and was in full sun with no shade throughout the day. The meteorological tower, adjacent to the garden, provided on-site data. Information from the tower was sufficient for interpretation, except for the exact timing of precipitation, which was obtained from an Environment and Climate Change Canada weather station based in Petawawa, Ontario, approximately 16 km from Pembroke.

There were three irrigation treatments with different levels of HTO concentration:

- Natural rainfall (weighted mean: 55.5 Bq/L; range: 2–321 Bq/L);
- Low activity concentration tritium tap water (mean: 5 Bq/L; range: 3–8 Bq/L);
- High activity concentration tritium well water (mean: 10 013 Bq/L; range: 9011–10 775 Bq/L).

Reference [156] provides additional information regarding the tritium concentrations of the different irrigation treatments and the initial tritium concentration for soil.

All vegetation was exposed to natural rain (i.e. irrigated plants were not protected from rain). The facility stops processing tritium as soon as any precipitation starts. However, fugitive releases of tritium from the maintenance and handling of devices and storage of tritium may occur at any time.

#### *3.3.3.2. Environmental sampling*

##### ***Vegetation***

Native grass, commercially obtained grass (sod), potatoes, Swiss chard and pole beans were grown as part of this study. Grass grown from sod was included in this work to provide a comparison with native grass. A general overview of what was sampled for each irrigation treatment is provide in Ref. [156].

##### ***Soils***

Composite soil samples from the native grass plot were obtained. The thatch and grass layers were manually removed and 3 or 4 cores were taken to a depth of 20 cm. Pooled soil cores of 2 or 3 samples were obtained for the soil in the plant barrels. For the pooled soil cores, samples were collected to a depth of 12 cm.

---

<sup>9</sup> The experimental garden was located at a compass bearing of 238°9'4".

The soils were sandy loams. The organic matter content of the soil was 7% (loss on ignition) and the clay content was 13% (particle size < 4 µm).

### ***Air monitoring***

The concentration of tritium in air was monitored with a custom-built bubbler. The bubbler had two stages in order to differentiate between HTO and HT. The HT was measured through catalytic conversion after the HTO had been removed by the first stage of the bubbler.

The bubbler system was not deployed for the entire length of the study. The mean ambient HTO and HT concentrations at the garden were  $1.9 \pm 5.8$  Bq/m<sup>3</sup> and  $1.4 \pm 3.9$  Bq/m<sup>3</sup>, respectively.

### **3.3.4. Analytical methods**

The methods for determining the HTO and OBT concentrations in environmental samples have previously been described [110] and are explained in more detail in Ref. [156].

Vegetation and soil were analyzed for TFWT and OBT. The OBT concentrations reported in this work represent an estimate of the ‘total’ amount of OBT present in the environmental samples (i.e. both exchangeable and non-exchangeable OBT) [108].

## 4. MODELS USED IN THE INTERCOMPARISON

### 4.1. SUMMARY OF THE MODELS

The following four models were used in the model intercomparisons:

- TOCATTA- $\chi$  by Institut de Radioprotection et de Sûreté Nucléaire (IRSN, France) and Electricité de France (EDF, France);
- CERES by, Commissariat à l'Énergie Atomique et aux Énergies Alternatives (CEA, France);
- SOLVEG-II by Japan Atomic Energy Agency (JAEA, Japan);
- CTEM-CLASS-TT by Canadian Nuclear Laboratories (CNL, Canada).

Further details regarding the assumptions used in the models along with the key equations are provided in Appendix I.

A detailed summary of the key features of each model and processes considered can be found in Table 1.

### 4.2. KEY DIFFERENCES AND SIMILARITIES BETWEEN MODELS

Key differences were noted for the uptake of HTO both by plant and soil, as well as the integration/assimilation of OBT in the plant, among the four models used in the intercomparison (see Table 1). For example, when calculating the exchange of HTO (deposition or re-emission) at the soil–atmosphere interface, CTEM-CLASS and CERES used a fixed exchange velocity (in m/s), while variable, time dependent exchange velocities are assumed in SOLVEG-II and TOCATTA- $\chi$ . The time dependent exchange velocity considers aerodynamic resistance that depends on wind speed, while CTEM-CLASS and CERES do not include this effect for the atmosphere–soil HTO exchange. For the deposition of HT, CTEM-CLASS and CERES use a fixed rate of conversion of HT to HTO in the soil. SOLVEG-II considers diffusive transport of HT throughout the soil profile and uses a depth dependent rate of oxidation of HT in each layer of the soil. The current version of TOCATTA- $\chi$  does not include the deposition of HT from the atmosphere to soil.

Another key difference between models is the consideration of HTO transport in soil. CTEM-CLASS only considers transport of HTO in three fixed relatively thick soil layers of approximately 10 cm, 30 cm and a few meters thick. The upward movement of HTO in the soil due to diffusion was not included in CTEM-CLASS. TOCATTA- $\chi$  and CERES assume a thick (20 cm) soil compartment and deposited HTO is lost from this layer due to downward infiltration of water. In contrast, SOLVEG-II considers a more sophisticated two-phase transport of HTO and interphase changes between HTO in the gaseous and aqueous forms within many soil layers which are freely defined in number and thickness. This approach allows vertical migration of the deposited HTO from the surface to deeper layers to be simulated. In all models, root uptake of HTO in soil is driven by transpiration. In TOCATTA- $\chi$  and CERES, HTO uptake by roots occurs at a single soil layer. CTEM-CLASS and SOLVEG-II apportion the root water uptake to the defined multiple soil layers, which can simulate the effect of non-uniform distribution of plant roots in the soil.

In calculating air–leaf HTO exchange, all four models use the same ‘net exchange approach’ that uses an exchange velocity and the difference in the concentrations of HTO between the air and leaves. However, derivation of the exchange velocity differs between the models. CERES assumes a fixed stomatal resistance (inverse of the conductance) for the HTO exchange between air and leaves in daytime hours. The other three models, CTEM-CLASS, SOLVEG-II and TOCATTA- $\chi$ , use stomatal resistance that is calculated from a relationship with photosynthesis. For nighttime uptake, all four models assume smaller cuticle resistances. The air–leaf HTO exchange depends only on stomatal or cuticle resistance in the calculation by CERES and CTEM-CLASS, while for TOCATTA- $\chi$  and SOLVEG-II it depends on the stomatal plus atmospheric (leaf boundary layer) resistance.

For the processes related to the formation of organic matter, CTEM-CLASS, SOLVEG-II and TOCATTA- $\chi$  rely on a photosynthesis rate (i.e. dry matter production rate) which is calculated from Farquhar’s photosynthesis model. CERES calculates an averaged dry matter production rate estimated from plant yield during each sectioned duration of plant growth. Time integration of the accumulation of OBT also differs between the models. CERES, SOLVEG-II and CTEM-CLASS integrate the calculated OBT assimilation by photosynthesis at each time step, while TOCATTA- $\chi$  progressively integrates the instantaneous OBT assimilation at each time step over the previous 15 day period. Plant growth is dynamically calculated in CTEM-CLASS and TOCATTA- $\chi$ . In the SOLVEG-II model, plant growth needs to be specified to account for leaf growth over time (which is represented as a ‘leaf area index’ input parameter); the model assumes that carbohydrates (i.e. dry matter) in mature leaves are transported to other plant parts and the newly formed leaves use synthesized carbohydrates for their own growth, as well. Translocation and integration/assimilation of the synthesized organic matter and OBT is considered in CTEM-CLASS for leaves, stem and root compartments. SOLVEG-II has no standard translocation model and accumulation of the synthesized organic matter to parts other than leaves needs to be specified. CERES calculates integration/assimilation of organic matter in leaves and roots, and TOCATTA- $\chi$  calculates integration/assimilation of the organic matter in leaves only.

As for the respiration in leaves, CTEM-CLASS, TOCATTA- $\chi$  and SOLVEG-II calculate the loss of non-exchangeable OBT due to decomposition of tritium containing organic matter by respiration. CERES does not consider the loss of OBT due to the respiration. In all four models, formation of non-exchangeable OBT independent of light (namely, dark reactions) is not considered. The exchangeable OBT pool in plants is not defined by any of the four models.

TABLE 1. FEATURES AND KEY PROCESSES OF THE FOUR MODELS USED FOR THE INTERCOMPARISON EXERCISES

Model name	CTEM-CLASS	TOCATTA- $\chi$	CERES@NRBCE	SOLVEG-II
Affiliation	CNL, Canada	IRSN, France	CEA, France	JAEA, Japan
Users	V. Korolevych	S. Le Dizès	L. Patryl	M. Ota
Purpose of model	Research	Research	Operational and research	Research
Model structure	One dimensional model: single canopy compartment, layered root layer; up to 5 cm post-storm ponding at the surface is allowed.	Compartment model.	One dimensional model: atmosphere-vegetation and atmosphere-soil-vegetation transfer.	One dimensional multi layered atmosphere-vegetation-soil model.
Number of soil layers	Three soil layers. The first layer has a thickness of 10 cm, the second layer has a thickness of 30 cm, and the third layer is of variable thickness, extending to a soil depth of up to 0.5–2.0 m.	One soil layer, with variable layer thickness. Layer thickness is User defined.	One soil layer. Variable in thickness.	User defined, variable in thickness and depth.
Structure of plant canopy	Not layered.	Not layered.	Not layered.	Vertically multi layered, with user specified number and thickness of canopy layers.
Deposition of HTO to soil	Variable, calculated using HTO concentration gradient between atmosphere and soil, and constant user defined exchange velocity	Variable, using exchange velocity based on aerodynamic and soil resistances and HTO concentration gradient between soil surface and canopy atmosphere	User defined dry deposition velocity (usually $3 \times 10^{-3}$ m/s for HTO). Wet deposition calculated from HTO rain drop concentration (Chamberlain equation) and rain intensity.	Variable, calculated using HTO concentration gradient between the bottom atmosphere layer and topsoil layer, and exchange velocity based on atmospheric resistances. Soil resistance is not explicitly included but transport of HTO in soil is explicitly calculated.
Re-emission of HTO from soil	Same as 'Deposition of HTO to soil', direction of flux depends on gradient of HTO concentration.	Same as 'Deposition of HTO to soil', direction of flux depends on gradient of HTO concentration.	50% of dry deposition is re-emitted in atmosphere. In case of rain, there is no re-emission.	Same as 'Deposition of HTO to soil', direction of flux depends on gradient of HTO concentration.
Transport of HTO in soil	HTO in aqueous form follows the soil water movement using explicit (numerical) and Green-Ampt solutions.	Migration process for aqueous HTO based on a first order differential equation with a soil hydraulic conductivity varying as a function of soil water content.	There is no HTO transport in soil, but the HTO soil concentration is corrected by a rate of leakage and rate of lixiviation.	Explicitly solves transport equation for gaseous and aqueous HTO in layered soil. Phase change of aqueous and gaseous HTO in soil is also considered. Aqueous transport of HTO is driven by the water transport, calculated with the water movement of classical Richard's type, parameterized by soil texture [157].

TABLE 1. (Cont.)

Model name	CTEM-CLASS	TOCATTA- $\alpha$	CERES® NRBCE	SOLVEG-II
Deposition of HT to soil	Calculated assuming 5% of atmospheric HT activity converted to soil HTO.	No HT in the current version.	HT dry deposition velocity is $3 \times 10^{-4}$ m/s and 50% is re-emitted in atmosphere. HT is converted to HTO.	Same as 'Deposition of HTO to soil', but uses HT concentration gradient. In soil, diffusion and oxidation of HT are explicitly calculated [42].
Root uptake of HTO from soil	Equals to leaf transpiration. Root apportioning to three soil layers is explicitly considered.	Based on surface exchange velocity (inverse of sum of leaf boundary layer and stomatal resistances) and differences in humidity. Uniform root density is considered.	Based on the HTO soil concentration and the ratio of exchange velocities HTO/H <sub>2</sub> O. The ratio is 0.95.	Equals to leaf transpiration. Root distribution in soil is explicitly considered.
Wet deposition of rain HTO	Rain moves directly into soil. Interaction with canopy is not modelled.	Rainfall that is not intercepted by vegetation (interception factor based on LAI) is deposited to soil.	Wet deposition on soil is considered.	Interactions with leaf surface in layered canopy and infiltration to soil are considered [43].
Irrigation of HTO	Not defined.	Not defined.	Not defined.	Not defined.
Deposition of HTO to plant	Variable, using HTO concentration gradient at canopy air–leaf interior and exchange velocity based exclusively on stomatal resistance. Maximum exchange velocity is user defined.	Variable, using HTO concentration gradient at canopy air–leaf and exchange velocity based on leaf boundary layer and stomatal resistances	HTO concentration in the leaf is based on exchange velocity which depends on stomatal resistance.	Variable, calculated using HTO concentration gradient at canopy air–leaf interior and exchange velocity based on leaf boundary layer and stomatal resistances. Stomatal resistance is dependent on photosynthesis and has maximum values around $4000 \text{ s m}^{-1}$ (cuticle resistance) at night [98].
Re-emission from plant	Same as 'Deposition of HTO to plant' plus leaf and root respiration.	Same as 'Deposition of HTO to plant'.	Plant re-emission is considered during the transpiration step.	Same as 'Deposition of HTO to plant'.
Stomatal resistance	Minimal resistance of 300 s/m is divided by a factor (degree) of stomata opening, which is held at 0.1 at nighttime.	Calculated based on the relationship between stomatal resistance and photosynthesis [95]	300 s/m during day, 3000 s/m during night.	Calculated by relationship between stomatal resistance and photosynthesis [158, 159].
Non-exchangeable OBT formation	Variable, depending on HTO concentration in leaves, isotopic discrimination factor, photosynthesis and plant development stage.	Variable, net formation depending on HTO concentration in leaves and rate of photosynthesis, corrected by a discrimination factor.	All organic matter is considered as OBT. Average tritium incorporation rate in OBT is calculated by taking into account plant yield, dry matter rate and time of growth.	Variable, depending on HTO concentration in leaves, isotopic discrimination factor and photosynthesis.



TABLE 1. (Cont.)

Model name	CTEM-CLASS	TOCATTA- $\chi$	CERES® NRBCE	SOLVEG-II
Non-exchangeable OBT loss	Variable, depending on OBT concentration and respiration occurring in leaves and roots.	Variable, depending on OBT concentration and growth and respiration in leaves.	Not defined	Variable, depending on OBT concentration and respiration in leaves.
Non-exchangeable OBT formation at night	Not defined.	Not defined.	Not defined, but at night HTO incorporation decreases according to the exchange velocity, subsequently, also OBT production decreases.	Not defined.
Exchangeable OBT pool	Not defined.	Not defined.	Not defined.	Not defined.
Leaf photosynthesis	Calculated by Farquhar model, mainly depends on solar radiation and temperature.	Calculated by Farquhar model, mainly depends on solar radiation and temperature.	Not defined.	Calculated by Farquhar model [160], mainly depends on solar radiation and temperature.
Plant growth	Modelled by CTEM as per carbon assimilation and allocation [161].	Time dependent and variable, dependent on environmental conditions, according to the PASIM model [162].	User defined, according to plant.	Given as input data (time series of leaf area density, or leaf area index and canopy thickness).
Organic matter accumulation	Accumulation in leaves, stem and roots. Fruits/tubers are not modelled.	Time dependent and variable, dependent on environmental conditions.	OBT concentration is integrated until the harvest.	Accumulation in leaves is considered. Accumulation in the other compartment needs to be specified for each crop type.
Required input data	Meteorological data, concentrations of HTO in air and rainwater.	Meteorological data, (reconstructed) concentrations of HTO in air and rainwater	Meteorological data, concentrations of HTO in air and rainwater.	Meteorological data, concentrations of HTO in air and rainwater, and concentration of HT in air (if HT calculation is applied).
Interval of input data	Half hourly.	Hourly	User defined in the research model	Hourly, or shorter.
Time step of calculation	Predefined in CLASS (seconds).	User defined (time step is generally on the order of seconds).	User defined.	User defined (generally seconds).

## 5. ANALYSIS OF MEASURED AND SAMPLED DATA

### 5.1. FORMS OF ATMOSPHERIC TRITIUM SAMPLED

The three scenarios described in Section 3 were developed for different reasons and with different objectives in mind. The IRSN-EDF scenario was developed to validate processes (both independently and together) considered in tritium transfer models for HTO, HT and OBT and for aerosols that may be present above the experimental site for intermittent routine discharges or accidental release. The objective of the CNL scenario was to investigate the short term processes occurring in the few hours after the passage of the plume above the site for accidental releases. The CNSC scenario was developed to measure tritium activity concentrations in soil and vegetation samples, in a rigorous statistical manner, for characterization of transfer from soil to leaf. The experimental design of the CNSC scenario was centered on the soil–leaf pathway as it was suspected to be a principal contributing factor to formation of high OBT/HTO ratios.

With very different goals in mind, the three datasets do not cover similar periods in time, nor do they have similar sampling frequencies. Furthermore, they do not focus on monitoring the same tritium species or follow the same experimental protocol for collecting samples and measuring tritium (TFWT, OBT) in samples of grass or crops.

Table 2 summarizes the atmospheric tritium species measured as part of the experimental campaigns that were used to support the scenario development. Information regarding the presence or absence of tritium as HTO is available for all three datasets. However, it is important to note that information is lacking regarding tritiated organics and tritiated aerosols above the experimental sites for two out of three datasets.

The models described in this document do not currently consider the transfer pathways related to tritiated organics or tritiated aerosols. If tritiated aerosols were to be released and predominantly transferred to plant (over HTO), gaps may be observed between measurements and models results for OBT activity concentration.

#### 5.1.1.1. *Guidance for future experimental campaigns*

Consideration of tritium speciation in atmospheric releases or above the experimental site for their subsequent transfer in the environment is a prerequisite to the use of data for model validation. As a consequence, it is advised to ensure that all the existing physicochemical forms of tritium are assessed in the plume either at the source or (preferably) directly above the plot.

TABLE 2. TRITIUM IN AIR SPECIATION FOR THE DATASET USED TO INFORM THE THREE SCENARIOS FOR THE INTERCOMPARISON

Datasets	HTO	HT	T <sub>org</sub> (tritiated organic compounds)	T <sub>aerosols</sub> (tritiated aerosols)
CNL	Yes Above DL	Yes Below DL	n/a	n/a
IRSN-EDF	Yes Above DL	Yes Above DL	Yes Below DL	Yes Below DL
CNSC	Yes Above DL	Yes Above DL	n/a	n/a <sup>a</sup>

<sup>a</sup> Identified and measured (above DL) above the experimental site during a previous IRSN/CNSC sampling campaign, but tritiated aerosols were not measured during this sampling campaign.

## 5.2. UNCERTAINTIES IN MEASUREMENTS

### 5.2.1. Uncertainties due to sampling methodology

For both the IRSN-EDF and CNSC experiments, monthly or weekly samples were collected from the same plots of grass and from the same plots of vegetables. In contrast, for the CNL scenario, for practical reasons, hourly samples from potato and tomato leaves, fruits and tubers were collected from different plants using a composite for each plant across the plot. The sampling approach used by CNL may reflect the natural variability between different plants at different growing stages. Interplant variability was further exacerbated by temporal variability on an hourly scale because for the CNL dataset, hourly variations of TFWT and OBT activity concentrations were not integrated/averaged with time and as such, reflected tritium dynamics in plants as per variations in the atmospheric HTO activity concentration. Spatial variability (e.g. due to differences of soil moisture availability across the garden plot) also contributed to measurement uncertainties in composites. Combined, these factors led to additional challenges in interpreting the variability of measurements of TFWT and OBT activity concentrations in the CNL dataset.

#### 5.2.1.1. *Guidance for future experimental campaigns*

A record of the fine scale time evolution of composite samples needs to be accompanied by detailed measurements of soil moisture availability and plant variability across the sampled plot in order to account for the spatial variability. Given the large volume of fresh sample needed for OBT measurements, sampling a single plant over time may be challenging. If possible, collecting samples from the same plant will make data interpretation easier, particularly for model–measurement comparisons.

### 5.2.2. Uncertainties due to analytical processes

There are different analytical methods for analyzing the two main forms of tritium (HTO and OBT) in environmental samples [163, 164]. However, there is no standard methodology for laboratory analysis starting with fresh samples, especially for OBT analysis. Therefore, interlaboratory OBT comparisons are important for estimating uncertainties related to analytical methods. Indeed, differences in analytical methods [165, 166] might be the cause of discrepancies in OBT analysis results between analytical laboratories. In particular, uncertainties may be introduced through the following conditions:

- If the fresh sample is not rapidly sealed and placed in an icebox, as it keeps exchanging HTO with the ambient air. The TFWT concentration might thus be diluted (concentrated) in the case of low background (intermittent high activity of ambient air water vapour) in the laboratory;
- If the water residue in the fresh sample is not completely extracted, since some HTO may then be included in the measurement of OBT;
- If the freeze-dried samples rehydrate with the laboratory ambient air water vapour, known as ‘cross-contamination’ [165, 166];
- If the combustion water is not completely extracted from the dry matter;
- If the collected volume of combustion water is not large enough to yield a large enough quantity for reliable analysis by liquid scintillation counting;
- If the combustion water is not distilled and is, therefore, not neutralized and purified, as is the case when a coloured water affects the counting efficiency.

Procedures for measuring HTO are well established and common to many laboratories [167, 168]. Following these procedures, uncertainty in HTO activity concentrations measured in environmental samples is estimated to be below 10–20% [169, 170]. This estimate is supported by recent results of an experimental intercomparison campaign between IRSN and CNSC [171] on the same experimental plot as the one considered for the CNSC scenario for this intercomparison.

There is no standard procedure for measuring OBT in environmental samples. Measurement of OBT activity concentrations in environmental samples is a long procedure, with many steps. Consequently, it has higher associated uncertainties than those associated with measurements of HTO activity concentrations. As a result of previous interlaboratory comparison exercises using environmental OBT samples [164], uncertainty in OBT activity concentrations measured in environmental samples is about a factor of 2 [170, 172]. This estimate is supported by the recent results of the experimental intercomparison campaign between IRSN and CNSC [171] on the same experimental plot as the one considered for the CNSC scenario. A recent Canadian interlaboratory OBT analysis exercise on freeze-dried samples [173] found an associated error below 20%, but this exercise only focused on analytical steps from freeze-dried samples prepared in the same laboratory. Starting from fresh samples may, therefore, generate more uncertainty in analytical results between analytical laboratories [165, 166, 173]. Real progress was made within the framework of The OBT International Workshop (2012–ongoing), established to validate analytical laboratory skills for OBT analysis. Within the framework of the international workshop, three OBT intercomparison exercises were organized. For the third exercise, the chosen matrix was wheat and the results were based on a large international participation allowing a reliable estimate of the dispersion of results for a very low activity concentration sample. Ultimately, there was a 2-fold decrease in the relative standard deviation for activity concentration in combustion water, compared to a 4-fold decrease in the activity concentration itself relative to the first exercise [174]. In the case of the dehydrated wheat, the dispersion of results was higher as a result of the use of different analytical tools by several laboratories to determine the detection limit. Regardless, the relative standard deviation is of the same order of magnitude as in the first exercise with a 4 times lower activity concentration [174]. This result represents an important advancement in the preparation and validation of the use of environmental matrices, such as Certified Reference Material or Reference Material for determination of tritium fractions.

Special efforts were invested to ensure consistency of measurements among the datasets for all three scenarios. Nevertheless, it is evident that extra caution will be necessary for future sampling campaigns.

#### *5.2.2.1. Guidance for future experimental campaigns*

Analytical errors can be minimized by ensuring:

- An adequate sample volume;
- Sample exposure to ambient air is avoided to prevent cross-contamination [8, 165, 166];
- Background tritium levels in the laboratory are far below the sample concentration, are continuously monitored, and if necessary, OBT concentration is corrected accordingly in order to account for sample rehydration;
- The sample is counted by liquid scintillation counting for a sufficiently long time.

### 5.2.3. Uncertainties in atmospheric hourly data reconstruction

Measurements of HTO (and HT) activity concentrations in air are either instantaneous (half hourly measurements in the CNL dataset) or integrated over a period of time, ranging from a few hours (e.g. 6 or 12 hours in the CNSC dataset) to 48 hours (IRSN-EDF dataset). The integration period is mainly due to limitation in the size of the sampling system for water vapour in air collection. For example, in the case of the tritium in air sampler used for the IRSN-EDF dataset, the air water vapour which has been collected through a cold trap for an hour is added to what was collected the hour before, over a so-called integration period, delimited by the automated sampling system size for individual sample collection. The sampling system size does not allow for the collection of stand-alone samples of air water vapour for every hour individually.

In contrast with the relatively sparse availability of measurements, atmospheric HTO activity concentrations are needed on at least an hourly time step as input data for the models. This is because of the fast dynamics of exchange between HTO in air and TFWT in plants (which is then progressively incorporated into organic matter as OBT through metabolic processes, such as photosynthesis). This warrants development of reconstruction methods in order to have HTO (and HT) activity concentrations downscaled to an hourly time step, based on the following:

- Source monitoring (weekly or submonthly) of releases from the facility;
- If released concomitantly, high frequency monitoring (subhourly) of radioactive tracers, such as  $^{41}\text{Ar}$  in the CNL scenario or  $^{85}\text{Kr}$  in the IRSN-EDF scenario;
- If necessary, wind direction (used in the IRSN-EDF scenario for one chimney, and in the CNSC scenario).

The reconstruction method was validated by comparing the results against HTO monitoring results for both the IRSN-EDF and CNL scenarios. Tritium monitoring at CNL is conducted bi-weekly and on a monthly basis at IRSN. The IRSN scenario reconstruction was further validated against a second HTO sampler, which was located in the immediate vicinity of the plot. Validation of the CNL dataset was more limited as the HTO sampler at the plot was only deployed sporadically and therefore only a limited number of half hourly measurements were available for reconstruction.

Regarding the CNSC scenario, verification of the air concentration data was not an intended purpose, therefore, this type of validation was not carried out.

Uncertainties in the reconstructed hourly atmospheric HTO activity concentration might result from the following:

- A limited amount of instantaneous half hourly measurements of HTO in air instead of a continuous record, as in the CNL scenario. Some of this uncertainty was overcome due to the bi-weekly atmospheric HTO monitoring results routinely measured at the same location at the experimental site, plus a continuous record of  $^{41}\text{Ar}$ ;
- Gaps between intervals of integration for measurements of HTO activity concentrations, as in the CNSC scenario. The tritium bubbler system was deployed from 9 July to 26 September 2012, but there was no sample collection for 23.5% of the time hence no monitoring data is available for this time gap. Consequently, assumptions were made regarding the tritium concentrations during these periods;

- The use of hourly wind direction along with weekly/monthly releases from the facility, as there is no atmospheric tracer released concomitantly with HTO and HT for validation.

#### *5.2.3.1. Guidance for future experimental campaigns*

As atmospheric HTO concentrations are the most important model inputs due to their dose consequences, it is necessary that their measurement be obtained in a continuous manner to the extent possible. Continuity in the atmospheric HTO measurements translates into more reliable model outputs, while gaps in the atmospheric HTO activity concentrations induce biases in model results, and thus datasets with gaps pose additional challenges for model validation and interpretation.

These limitations about measurements and subsequent modelling need to be kept in mind when designing future sampling campaigns.

### 5.3. ANALYSIS OF THE THREE DATASETS

This section discusses observations from the three experimental datasets and their further use in scenarios. Both TFWT and OBT results are plotted for each scenario. It is important to note that only total (exchangeable plus non-exchangeable) OBT was measured.

#### **5.3.1. Measurements of HTO in air and TFWT and OBT activity concentrations in plants**

##### *5.3.1.1. The IRSN-EDF dataset*

The TFWT and OBT activity concentrations in grass vary over the experimental campaign with an average activity concentration of 10 Bq/L. As expected, the TFWT activity concentrations show larger variations than the OBT activity concentrations (see Fig. 3), because of rapid exchanges between the TFWT and HTO activity concentrations in the environment (i.e. in air and groundwater).

The role of groundwater is thought to be minor in the IRSN-EDF scenario since the grass TFWT activity concentration evolves in accordance with spikes in atmospheric HTO activity concentration over the previous 24 hours (see Fig. 4). A minimum TFWT activity concentration of approximately 3 Bq/L was measured in grass; this corresponded to background activity concentrations that were measured 2 km north of the facility. The background samples are obtained when there is no spike in the atmosphere over the previous 24 hours. The maximum TFWT activity concentration measured in grass was 60 Bq/L (on 3 December 2013 at noon).

In this field campaign, the relatively low frequency of measurements allows effective integration of short term dynamical variability in the soil–plant–atmosphere system and fully represents long term average tritium levels in the system.

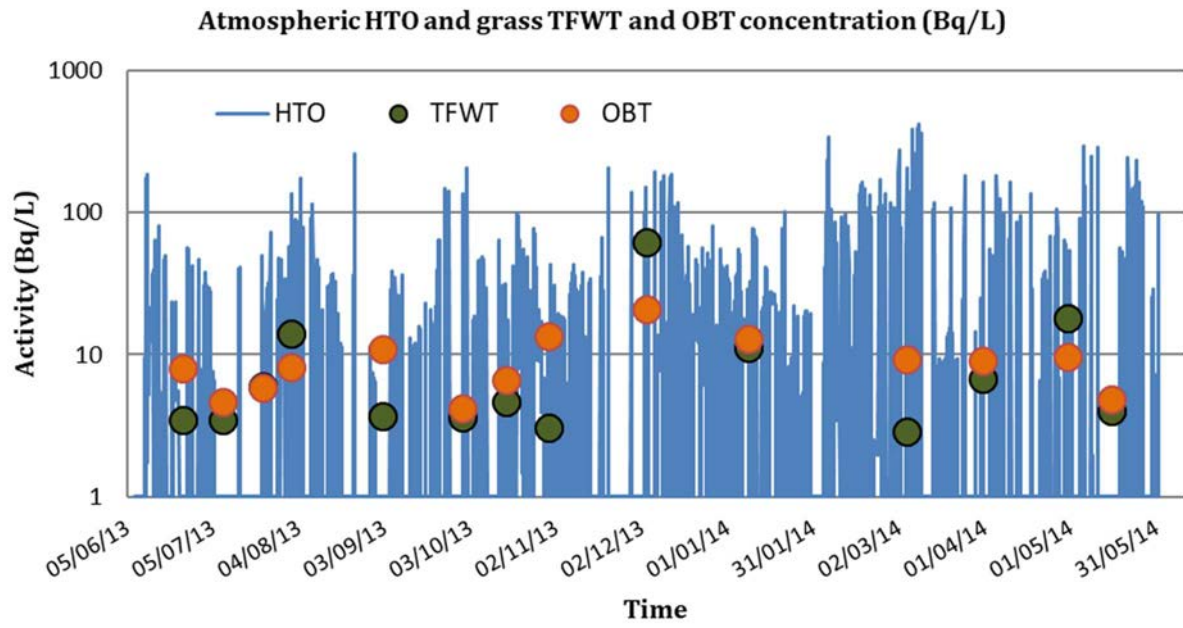


FIG. 3. The IRSN-EDF dataset on the whole period considered for the MODARIA modelling exercise.

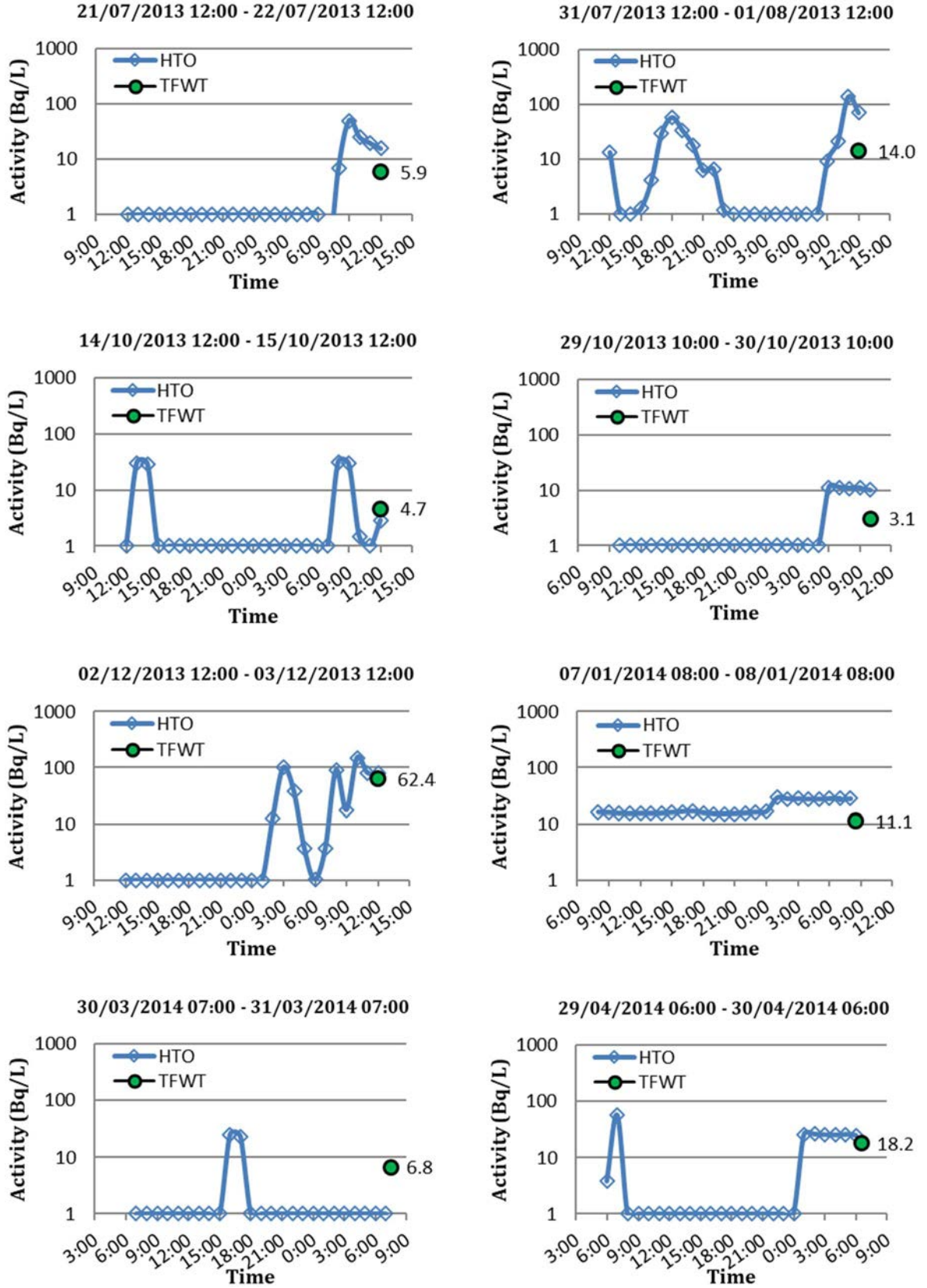


FIG. 4. Examples from the IRSN-EDF dataset over the 24 hours prior to grass sampling for TFWT measurements.



### 5.3.1.2. The CNL dataset

The TFWT activity concentration in leaves varies around an average value of 200–300 Bq/L whereas the OBT activity concentration in leaves varies around an average of 1000 Bq/L (see Fig. 5). Both the TFWT and OBT activity concentrations vary substantially around the average values. This variability reflects the fast kinetics of transfer from atmospheric HTO to TFWT (and presumably to exchangeable OBT) in leaves and is further exacerbated by the natural spatial variability between the different plants which were sampled. The spatial variability was assessed to be of a factor of 2.

It is worth noting again that the objective of the CNL experimental design specifically targeted fast exchange processes occurring in the immediate wake of the plume. Therefore, the results do not reflect long term average levels of tritium in the soil–plant–atmosphere system. For comparison, the spikes in TFWT activity concentration closely corresponded to spikes in atmospheric HTO activity concentration over previous hours, and the highest TFWT spikes (i.e. the maximum TFWT activity concentration measured in various plants) approached 2260 Bq/L (obtained on 30 July 2008) which far exceeded the minimum TFWT activity concentration of 35 Bq/L measured in the absence of a plume under the background atmospheric level of 45 Bq/L.

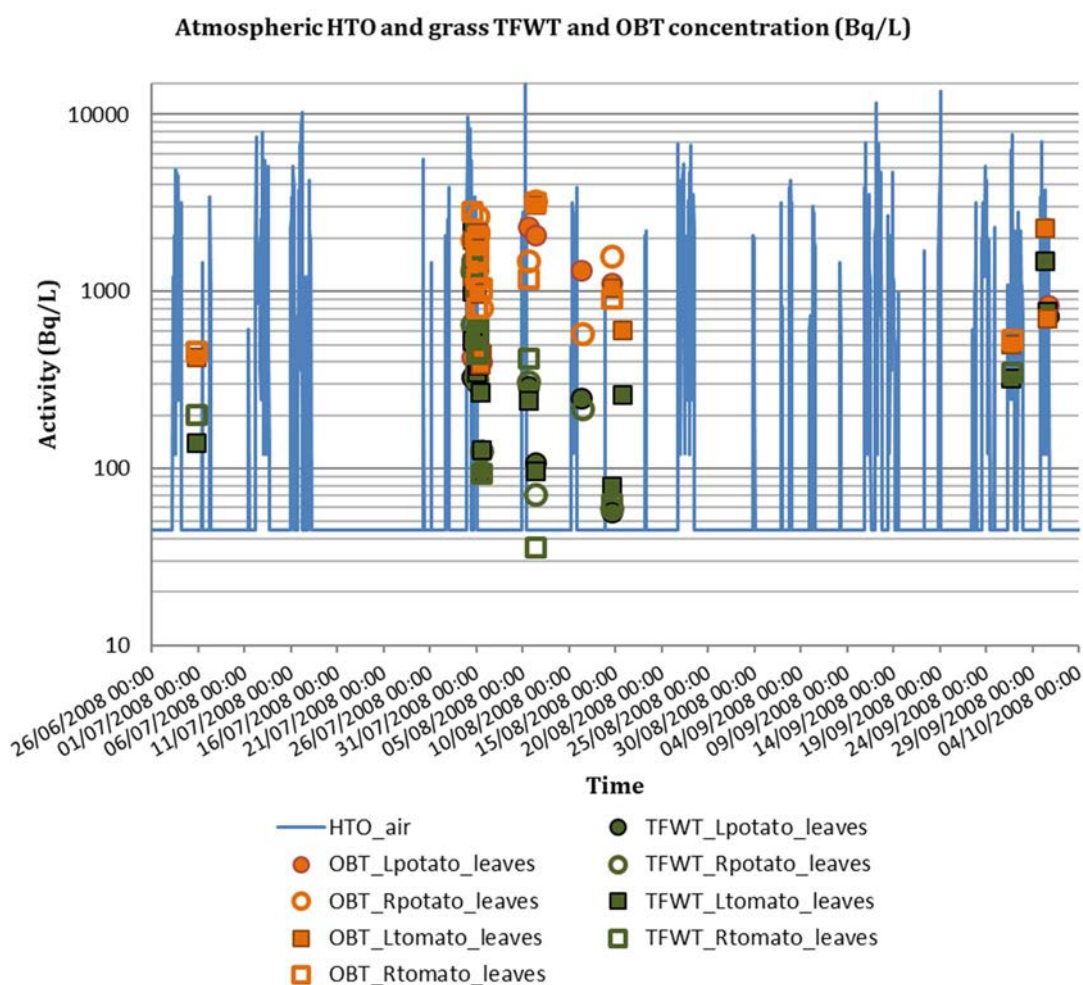


FIG. 5. The CNL dataset on the whole period considered for the MODARIA modelling exercise.

It was also noted that instances of elevated atmospheric HTO could be missing in the CNL dataset because there were only a limited number of instantaneous half hourly measurements of HTO in air and estimates were based on the assumption that atmospheric HTO exactly follows  $^{41}\text{Ar}$  emissions all the time. For example, some HTO at detectable levels could be re-emitted locally (e.g. from the swamp which is 500 m away and separated by a patch of dense forest), while the wind blows away from the stack and so there is no  $^{41}\text{Ar}$  at the plot. The probability of a locally re-emitted plume is relatively high. Moreover, with much lesser probability, as shown by the HTO -  $^{41}\text{Ar}$  scatterplot, there might have been a particular instance in the CNL scenario dataset when  $^{41}\text{Ar}$  was released (and used as an atmospheric HTO proxy) and HTO was not released simultaneously. In both situations the reconstructed/downscaled air HTO activity concentration used as input data in the model would be not realistic. Therefore, the utility of the CNL dataset for blind validation is somewhat limited.

#### 5.3.1.3. *The CNSC dataset*

The TFWT activity concentration in grass (with rainwater irrigation treatment) is variable during the experimental campaign with an average activity concentration of 300 Bq/L. The OBT activity concentration in grass is also variable with an average of 1000 Bq/L. The TFWT activity concentration shows larger variations than the OBT activity concentration. The measured OBT activity concentration is always higher than the TFWT activity concentration.

The analysis and interpretation are made difficult due to missing HTO activity concentration data (see Fig. 6). HTO activity concentrations were missing in the CNSC dataset for 23.5% of the time (i.e. there was no record of air HTO). Measured values of TFWT and OBT activity concentrations in grass preceded by missing data in atmospheric HTO activity concentrations over the previous 24 hours are not to be considered, since TFWT (and presumably exchangeable OBT) evolves in accordance with spikes in atmospheric HTO activity concentrations within a few hours. It is necessary to exercise caution in the interpretation of the OBT activity concentrations, since OBT formation results mainly from a progressive integration of TFWT (hence HTO) into plant organic matter over a period of a week to a month. Any missing data during this period introduces uncertainty to the results.

The role of rain and groundwater is thought to be minor in this particular case since TFWT and OBT activity concentrations in samples with (low tritium) tap water irrigation treatment (instead of rain water irrigation treatment) are similar (not shown in Fig. 6) to those observed with rain water irrigation treatment. When irrigated with high tritium well water (10 000 Bq/L), the role of soil (and root uptake) becomes the predominant transfer pathway compared to air to leaf transfer [156, 175].

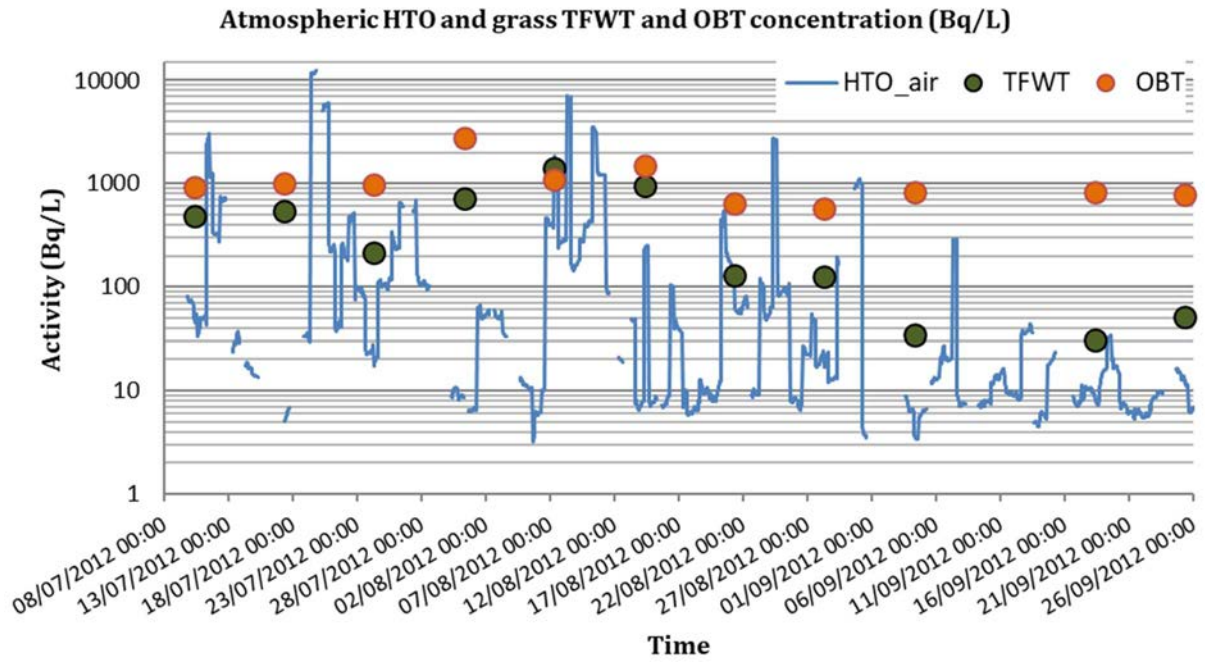


FIG. 6. The CNSC dataset for the experimental campaign from July to September 2012.

### 5.3.2. Comparison of averaged concentrations of HTO in air, TFWT and OBT in plants

Table 3 summarizes the mean and standard deviation of tritium concentrations measured in environmental samples obtained during the respective experimental campaigns. In general, for all three datasets, the following observations were made (see Table 3):

- The standard deviation of HTO atmospheric concentrations was about three times the average concentration;
- The standard deviation of TFWT concentrations in grass was similar to the average TFWT concentration;
- The standard deviation of OBT concentrations in grass was about half the average OBT concentration.

In all other cases, the three datasets show different trends and different relationships between HTO, TFWT and OBT.

In the IRSN-EDF dataset, the average concentrations of TFWT and OBT in grass were equal to the average HTO atmospheric activity concentration; thus, the average OBT/HTO ratio was close to 1. This is consistent with other randomly sampled datasets around the world, including two nuclear power plants and one nuclear fuel cycle facility in Canada [110], where average OBT/HTO ratios in garden products are close to unity (between 1 and 2).

TABLE 3. MEAN AND STANDARD DEVIATION OF TRITIUM CONCENTRATIONS IN ENVIRONMENTAL SAMPLES

Dataset	HTO Activity concentration in atmosphere (Bq/L)		TFWT Activity concentration in grass (Bq/L)		OBT Activity concentration in grass (Bq/L)	
	Mean	Standard deviation	Mean	Standard deviation	Mean	Standard deviation
IRSN-EDF	11.3	27.2	10.5	15.7	9.2	4.5
CNSC	181	676	343	397	1081	513
CNL	L-potato		318	169	1290	685
	R-potato		409	324	1823	705
	L-tomato	337	521	543	1274	754
	R-tomato		441	347	1456	826

The CNSC dataset (collected around a tritium processing facility in Canada) was different from the IRSN-EDF dataset, and also from datasets collected around three facilities in Canada [110]. This was because the randomly sampled OBT activity concentration in the CNSC dataset was consistently higher than the concentration of TFWT and not sporadically higher. The average activity concentration of OBT in grass was equal to six times the average HTO atmospheric activity concentration; however, there are some missing data in the HTO atmospheric concentrations and the results may not be representative. It is interesting to note [156] that when irrigated with high activity concentration tritium well water (10 000 Bq/L), the average OBT activity concentration in grass samples tended towards the average HTO activity concentration in the irrigation water (thus the average OBT/HTO ratio was close to 1).

The CNL dataset is comprised of TFWT and OBT activity concentrations measured a few hours after the passage of the plume above the site. As they are not randomly sampled, the results (e.g. consistently very high OBT/HTO ratios) are expected to be biased in comparison to purely random sampling (containing only a small fraction of post-plume episodes) and even more so in comparison to samples systematically collected under quasi-steady state conditions (i.e. not having post-plume episodes at all).

A compilation of literature data on tritium in terrestrial plants and foods was updated [176], reporting a mean value of 1.92 for OBT/HTO ratios, based on 457 samples. It was found that in the absence of isotope fractionation, the distribution of OBT/HTO ratios in terrestrial samples could be explained by the seasonal cycles of atmospheric tritium which exhibits an annual spring maximum precisely during the growing season. Another possible explanation for OBT/HTO ratios greater than 1 is the existence of a bias in some measurements due to rehydration of freeze-dried samples with tritiated ambient air water vapour in the laboratory where samples are prepared, as demonstrated in Ref. [177], which pertains to a previous case for the AREVA (now Orano)-NC laboratory.

Most of the reported results of the OBT/HTO ratio in environmental products were bulked together for all types of environmental samples taken from various sites. It would be useful if the experimental data for HTO and OBT concentrations in various environmental samples were to be analysed for the same sample type and site because OBT/HTO ratios largely depend on receptor location, plant type and history of the dynamics of HTO in air [178].

### 5.3.3. Comparison of moving average of air HTO activity concentrations with OBT activity concentrations measured in plants

In this section, moving averages of atmospheric HTO activity concentrations are plotted with a moving average period of 10 or 20 days (depending on field management practices: i.e. the period of time between two cut plant samples). The resulting curves may not represent the full variability of OBT activity concentration in leaves or grass, but the moving average of atmospheric HTO can be used to highlight inconsistencies in sampling since the plant cannot accumulate, i.e. assimilate, more tritium than is present in the surrounding environment of the atmosphere and soil (as documented in the scenario). The average of tritium integrated as OBT in leaves or grass (in Bq/L) is assumed to be similar to the average tritium concentrations released into the environment (in Bq/L).

The purpose of this effort was to reliably predict the OBT concentration in plants, based on atmospheric emissions of HTO, taking into account type of plant and other relevant factors and processes. In cases where the average tritium in plants and atmospheric HTO are especially inconsistent, it would be necessary to investigate possible missing tritium sources, or other forms of tritium, and/or to consider the impact of other processes.

#### 5.3.3.1. The VATO (IRSN-EDF) dataset

The OBT activity concentration in grass is measured as total OBT with no distinction between exchangeable (E-OBT) and non-exchangeable (NE-OBT). NE-OBT is known to be progressively integrated into organic matter (similar to  $^{14}\text{C}$ ). A moving average period of 15 to 20 days for  $^{14}\text{C}$  integration into organic matter was inferred from observations on the same experimental site for grass [179]. Similarly, the hourly HTO atmospheric concentration was averaged over the past 20 days for each hour (see the dark line in Fig. 7). This averaging period is similar to the average time between grass cuts, i.e. those forcing the complete renewal of organic matter. Secondly, E-OBT is thought to be rapidly exchanging with either TFWT or atmospheric HTO and to constitute approximately one fifth of the total OBT [180]. On the basis of these hypotheses, the E-OBT activity concentration in grass was assumed to be roughly equal to the measured TFWT activity concentration (as a first approximation). Testing of this approach was performed using various proportions of TFWT added to the modelled NE-OBT activity, and the proportion which minimized the Root Mean Square Error (RMSE) was assumed to be the correct one. It appears that the RMSE between calculated total OBT and measured total OBT is minimized with 30% of TFWT (added to 70% of NE-OBT), but fractions such as 25% or 75% did not change the residual RMSE substantially.

The modelled total OBT activity fits quite well with measurement results, with a correlation coefficient  $R^2=0.7$  (see Fig. 8). It is worth noting that the modelled total OBT, with inclusion of different fractions of E-OBT along with NE-OBT (e.g. 25% and 75%, respectively), does fit better with measurements than any of the modelled NE-OBT activity taken in isolation, and this is observed for various averaging periods. This implies some value of future investigation of the dynamics of E-OBT fraction.

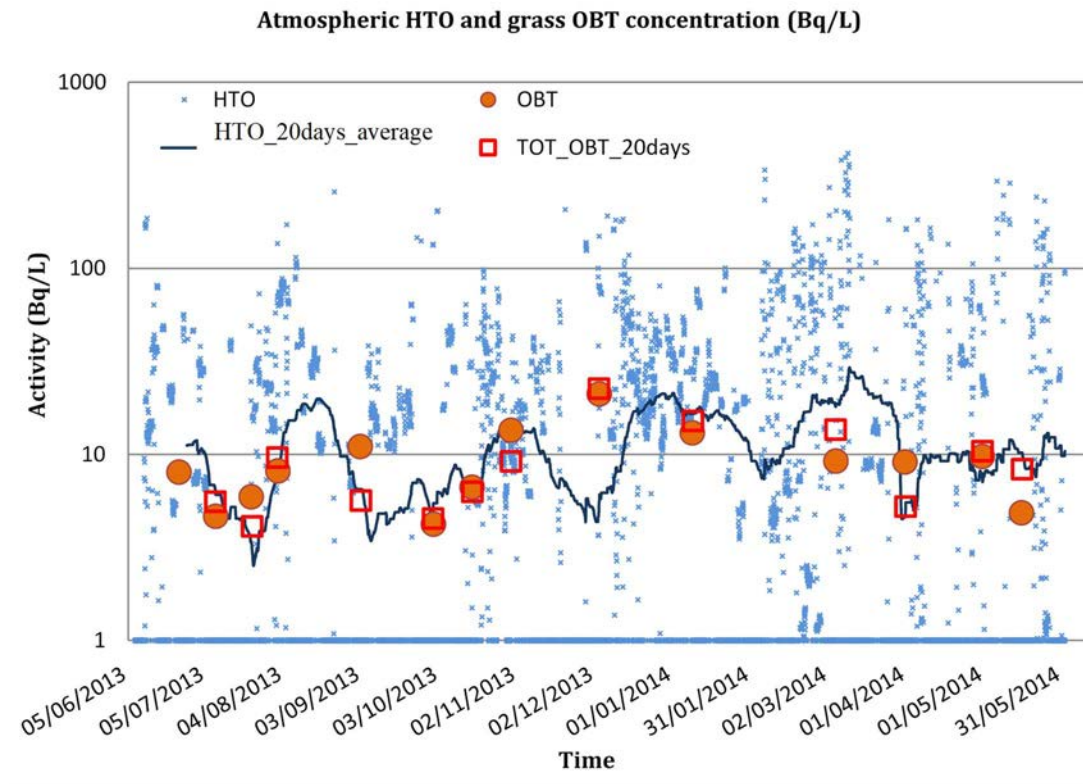


FIG. 7. Atmospheric HTO concentrations (blue data points) as a 20 day moving average (dark blue line) and OBT concentration measured in grass (orange dots) and calculated as a 20 day moving average (red squares) as 70% of NE-OBT (assumed to be equal to 20 days averaged atmospheric HTO) and 30% of E OBT (assumed to be equal to TFWT) – IRSN-EDF dataset.

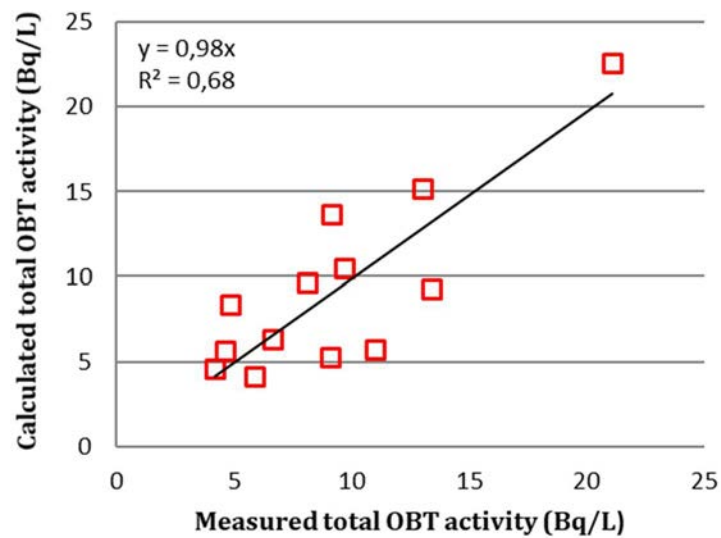


FIG. 8. Modelled and measured total OBT activity in grass – IRSN-EDF dataset.

The maximum OBT concentration measured in grass a few hours after the passage of the plume is difficult to explain solely with a progressive integration of TFWT into organic matter (as total OBT, i.e. E-OBT plus NE-OBT), since HTO concentrations above the plot are decreasing during the previous 15 days (see Fig. 7, evolution of atmospheric HTO moving average). This might be an indication of a more rapid kinetic of exchange (either with atmospheric HTO or with TFWT) since the plume was above the plot a few hours before sample collection (therefore, also inducing a maximum in TFWT concentrations).

The goal of the previous calculation is not to propose a model for OBT but to test the consistency of the IRSN-EDF dataset as a whole, in particular, between measurements of:

- (1) Atmospheric HTO activity concentrations;
- (2) OBT activity concentrations in grass.

The dataset is consistent after a calculation of the mass balance; in particular the averaged OBT activity concentration measured in grass is consistent with the average of atmospheric HTO concentrations. This makes this dataset well suited for model validation.

#### 5.3.3.2. *The CNL dataset*

Measurements of TFWT and (total) OBT activity in potato and tomato leaves, as well as the reconstructed atmospheric HTO hourly activity inferred from measurements of  $^{41}\text{Ar}$  and HTO as part of the CNL campaign, are shown in Figs 9–11. The 10 and 20 day moving averages of the reconstructed hourly atmospheric HTO activity concentrations are represented by dotted and thick dark blue lines, respectively.

Measured OBT activity concentrations are similar to values predicted by the moving averages of atmospheric HTO activity concentrations, which is consistent with the knowledge of the slow integration rate of OBT (as NE-OBT) into organic matter, as presented in Figs 9 and 11. This assumption is reinforced, in Fig. 9, by the absence of a spike in atmospheric HTO activity concentrations over the previous 36 hours.

Figure 10 shows that the 10 and 20 day moving averages of atmospheric HTO activity concentrations are much lower than OBT activity concentrations measured in leaves, for all averaging periods considered. The difference between averaged HTO activity concentration and measured OBT activity concentration may be due to a rapid exchange rate between E-OBT and either the plant TFWT or atmospheric HTO. The fraction of E-OBT equals 20–30% of the total OBT [180]; therefore, the E-OBT activity concentrations are expected to be very high. For example, in Fig. 10 on 31 July 2008, the OBT activity concentration measured in leaves at night is about 2000 Bq/L, which reflects the HTO air concentration in the immediately preceding plume but not the 20-day moving average of atmospheric HTO activity concentrations which is about 400 Bq/L. With E-OBT comprising 30% of total OBT, the calculated E-OBT activity concentration is estimated to be 6000 Bq/L to explain the difference.



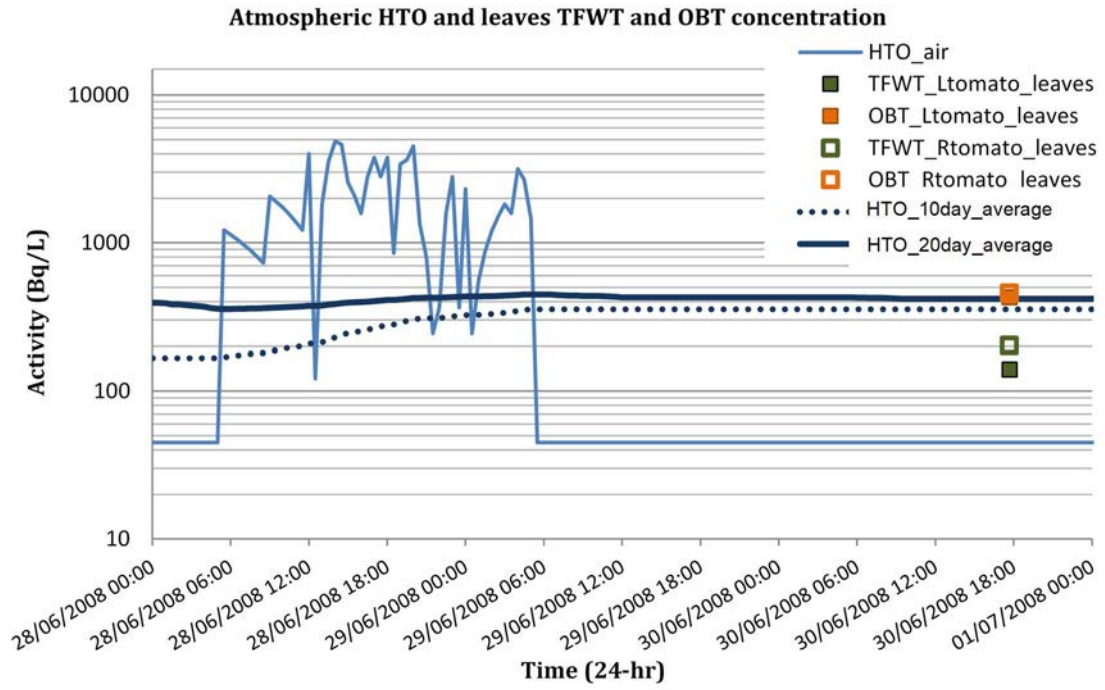


FIG. 9. The CNL dataset between 28 June and 1 July 2008.

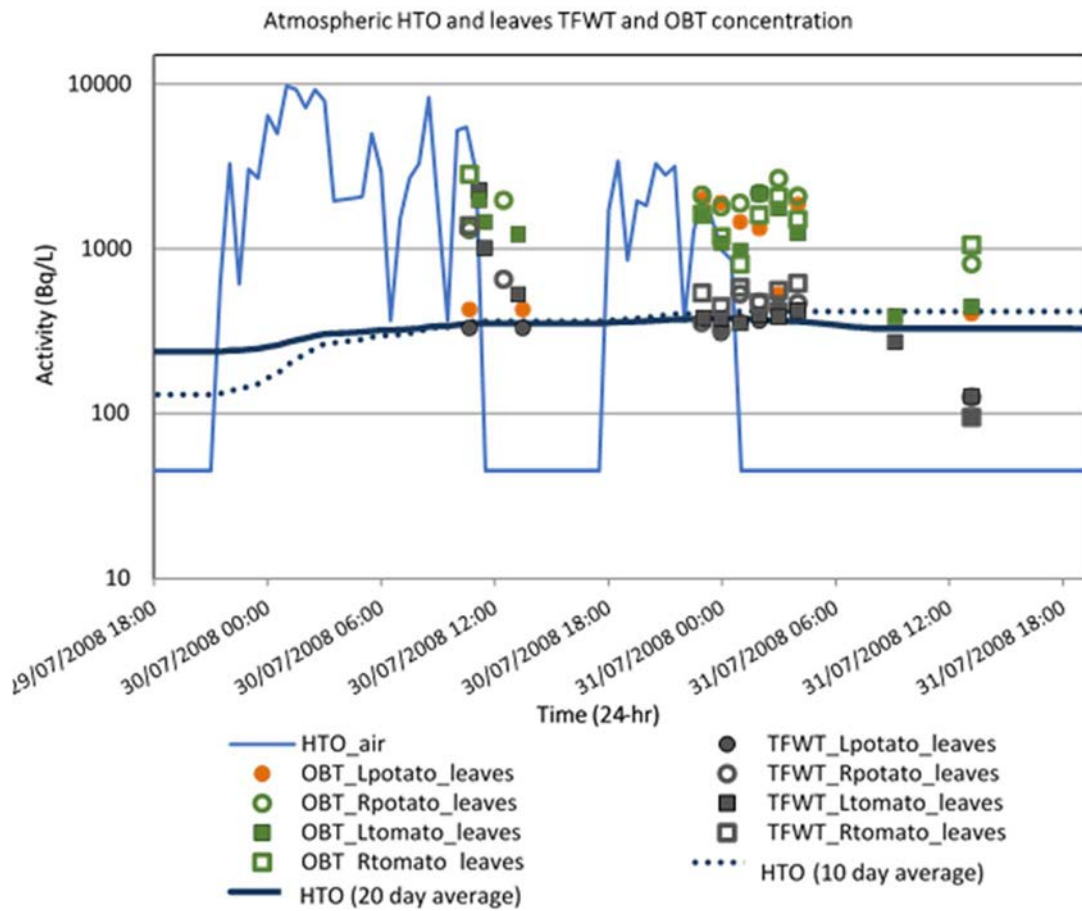


FIG. 10. The CNL dataset between 29 and 31 July 2008.



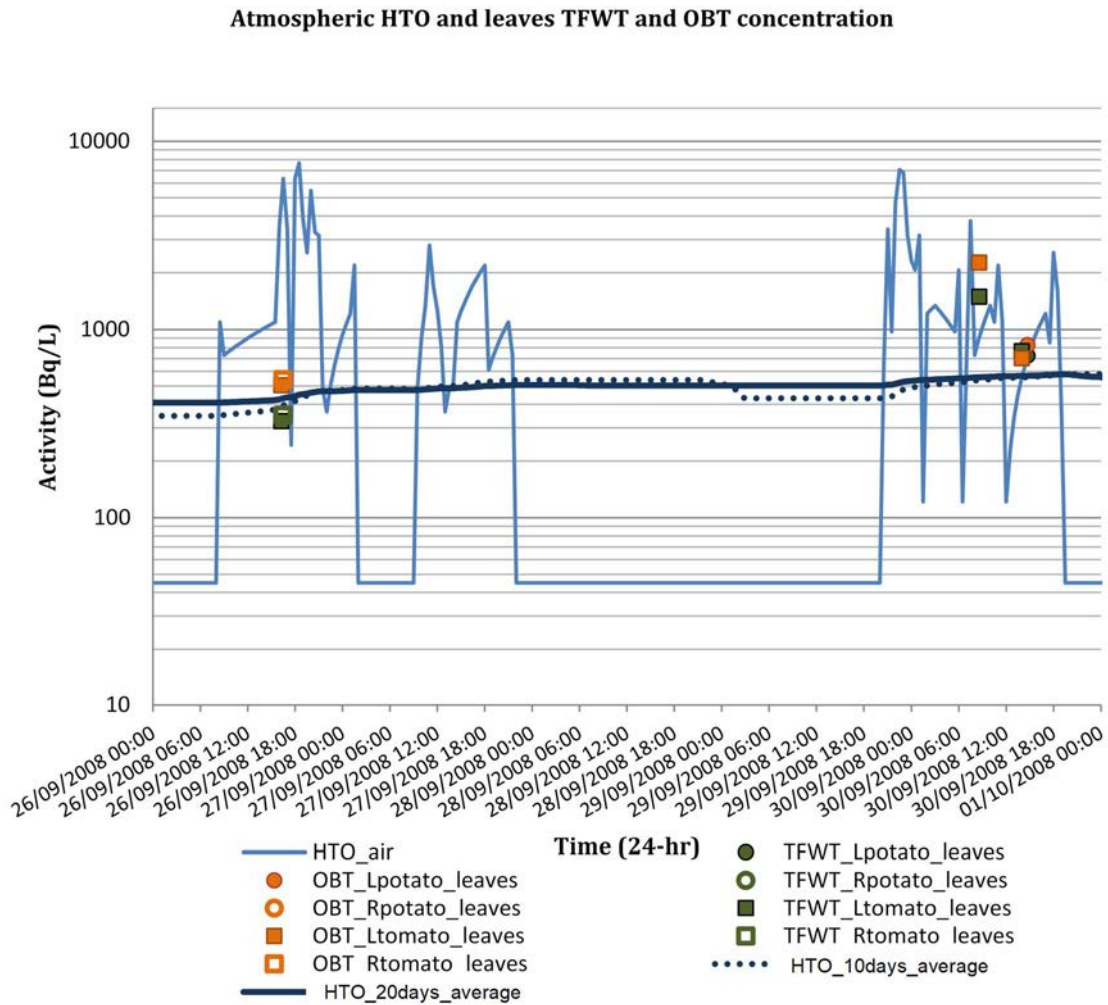


FIG. 11. The CNL dataset between 26 September and 1 October 2008.

The samples taken on 31 July 2008 at 12:00 (Fig. 10) are more than 12 hours after the spike shown in the reconstructed atmospheric HTO activity concentrations. Despite this, the OBT activity concentrations in leaves are higher than the reconstructed atmospheric HTO activity concentration. With uncertainties inherent to measurements in mind (see Section 5.2), this episode still implies a fast rate of exchange between E-OBT and the plant TFWT or atmospheric HTO, along with a certain delay in OBT being accumulated or retained within plant leaves within a day. This apparent delay, which results in elevated OBT activity concentrations, may, however, also be due to the intrusion of air carrying locally re-emitted HTO as discussed in Section 5.3.1.2. In this case, the sampling was carried out shortly after the plume passage, which results in high TFWT and high new OBT production being added to the OBT stored before the plume arrival, and that could also explain why the OBT activity concentration in leaves is higher than the reconstructed atmospheric HTO activity concentration.

Future experiments might be run to try to minimize unidentified sources of atmospheric HTO, and to include OBT aerosols and above background concentrations in other compartments, such as soil (HTO, OBT), as locally re-emitted HTO can be substantial (e.g. at CNL, there is a swamp separated from the garden plot by a patch of dense forest, but is only 500 m away) (see Section 5.3.1.2).

TABLE 4. RECORDS ELIMINATED FROM CNL SCENARIO AS PER QA CHECK

Sample number	Sampling time	Sample type
15	2008/08/05, 15:00, 15:50	all
17–20	2008/08/06, 8:15, 9:00	all
22–26	2008/08/14, 8:10, 14:00, 14:30, 14:50 and 2008/08/15, 16:00	all
31, 32	2008/09/30, 14:15, 16:00	potato OBT
33	2008/10/09, 8:00	potato OBT

In order to avoid differences between some measurements and model results for OBT due to these possible additional sources, in the analyzed CNL scenario, 15 data points collected on 7 days were eliminated, when  $^{41}\text{Ar}$  appears to be uncorrelated with actual atmospheric HTO, and therefore, is not a reliable proxy for local tritium source reconstruction (see Table 4).

#### 5.3.3.3. *The CNSC dataset*

The CNSC dataset contains missing data which therefore limits the ability to draw definite conclusions. Measured TFWT activity concentrations are difficult to explain solely based on the reconstructed atmospheric HTO concentrations available (i.e. from observed values on 24 July, and 7 and 21 August 2012). In particular, TFWT concentrations on 31 July and 14 August 2012 are 20–50 times higher than any of the reconstructed HTO concentrations in the atmosphere over the previous 24 hours (see Fig. 12). Moreover, on 31 July 2012, a high soil HTO activity concentration of 367 Bq/L was observed, above the initial background level (not shown in Fig. 12), whereas input HTO activity concentrations in the atmosphere (shown in Fig. 12) remain low. This is likely the result of missing atmospheric HTO activity concentration data (probably high, previous to 30 July 2012). This could also be due to uncertainties in the reconstructed air HTO or to other possible sources (e.g. HTO in rainwater, due to passive diffusion from a building) and these possible sources were not necessarily measured as part of the field campaign.

Similarly, measured OBT activity concentrations are difficult to explain solely based on the available atmospheric HTO activity concentrations. Ten and 20 day moving averages of the atmospheric HTO concentrations are compared with OBT activity concentrations measured in grass (since grass is cut approximately every 10 days, NE-OBT half-life might be shortened to this time period). NE-OBT half-life involves a NE-OBT turnover rate which represents the balance between anabolism and catabolism. Anabolism is the initial formation in photosynthesis and the subsequent dark reactions, while catabolism is due to respiration, senescence and perhaps root processes. As a result, there are still high OBT concentrations measured in samples (e.g. on 31 July and 18 September 2012), which cannot be explained by moving averages of atmospheric HTO activity concentrations or by supposedly exchangeable OBT dynamics, but appear to be due to the complex processes involved in OBT formation.

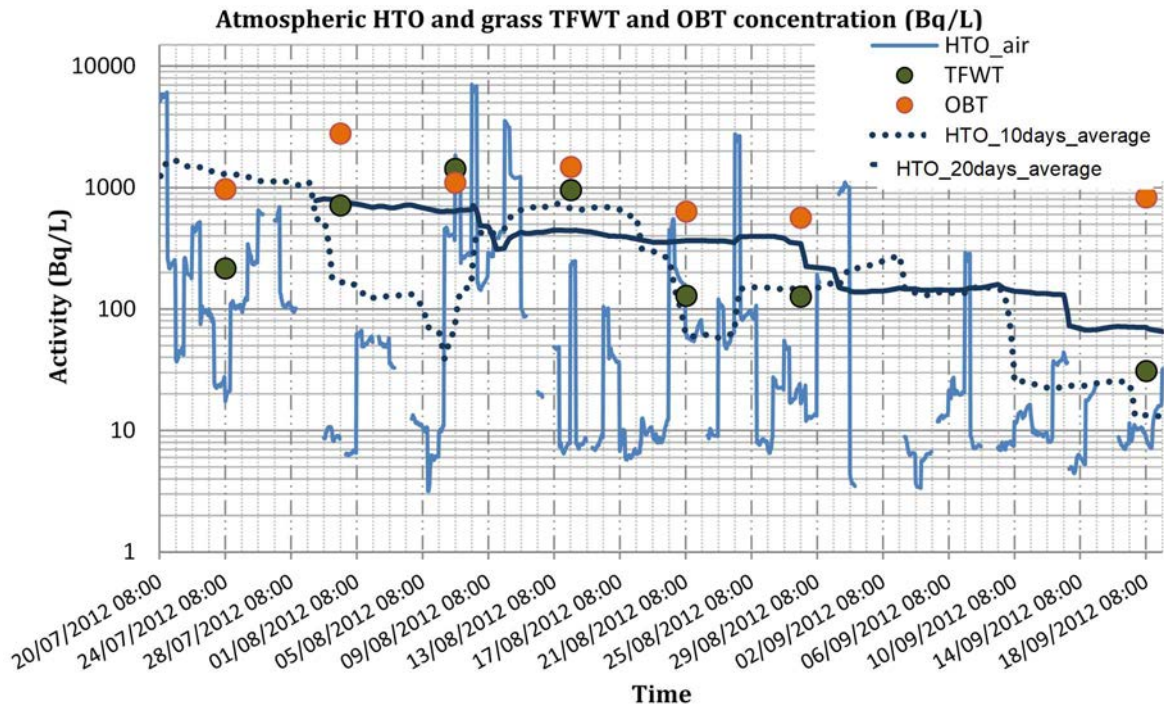


FIG. 12. The CNSC dataset considering only TFWT and OBT values when there is no missing data in HTO over the previous 24 hours.

The following points can be concluded from the CNSC dataset:

- Reconstructed atmospheric HTO activity concentration data are missing over 23.5% of the experiment timescale;
- Some tritiated aerosols were detected above the detection limit during a previous campaign on the same experimental site, but not measured in this campaign, and although the variability of the tritiated aerosols is unknown, this might be substantial, and this might, therefore, affect OBT measurements to an unknown degree;
- The methodology for reconstruction of HTO atmospheric concentrations was not QA checked as it was not the objective of this experiment. Moreover, the HTO atmospheric concentration used as input data for the model is likely to be missing some spikes, which is indicated by TFWT and soil HTO activity concentrations on 31 July 2012;
- Effects of the horizontal diffusion of HTO emitted from barrels irrigated with well water (water with high HTO activity concentrations of 10 000 Bq/L) are not quantified, but might be substantial. If the barrels are closely located to the other test plots of natural meadow and barrels irrigated with tap water, then HTO emitted from the highly contaminated barrel irrigated with the well water may influence the HTO concentration in the atmosphere above the other two plots. The available data for HTO atmospheric activity concentrations appears to be insufficient for any model to reproduce the high concentrations of OBT (and, on certain occasions, also the TFWT activity concentrations) measured in grass exposed to rain and low tritium tap water irrigation treatment.

## 5.4. QUALITY ASSURANCE OF EXPERIMENTAL DATASETS

### 5.4.1. General considerations and quality assurance requirements

As a prerequisite to model–measurement comparisons, it is important to review the quality of the data used. Based on the discussion above, it is important to ensure the following:

- Measurements of tritium speciation in the plume and/or above the plot are needed such that all possible tritium inputs are accounted for;
- To the extent possible, continuous (hourly) measurements of atmospheric HTO activity concentrations are needed as input data for models.

As a first step, the measurements collected could be screened prior to analysis and interpretation to ensure consistency, whenever possible.

The quality of input data is essential to the quality of model results. If some input data are missing or the quality assurance of the datasets is not adequate, the model results may not be adequately robust and could substantially deviate from observations. This is why, for model validation purposes, it is necessary to use datasets that are as complete as possible and quality assured datasets for air, plants and soil are needed.

It is important to note that the main purpose of the three datasets was to validate the processes considered in advanced tritium models and this is further expanded upon later in this report. However, a secondary purpose of the experimental campaigns and the supporting datasets was to further explain the elevated HTO and OBT concentrations observed in each of the scenarios.

### 5.4.2. Quality assurance of the scenarios used in the intercomparison

#### 5.4.2.1. IRSN-EDF scenario

The main objectives of the IRSN-EDF scenario were to:

- Describe the naturally occurring dynamics of TFWT and OBT in grass for a whole year;
- Test the accuracy of TOCATTA- $\chi$  in predicting TFWT and OBT activity concentrations with time over a whole year driven by airborne HTO.

Quality assurance checks confirm that the dataset was good and fit for purpose. The dataset described yearlong variations in concentrations of HTO, TFWT and OBT. Elevated total OBT activity concentrations associated with short episodes of plume departure were not captured in this dataset. It was therefore assumed that the frequency of occurrence of episodes of elevated total OBT is low and that the role of exchangeable OBT is generally minor.

#### 5.4.2.2. CNL scenario

The objectives of the CNL scenario were to test the CTEM-CLASS-TT model with respect to the following:

- The accuracy of the model in predicting the fine scale timeline of TFWT, OBT and soil HTO driven by the high frequency record of airborne HTO;
- The ability of the model to predict fast dynamical exchange processes associated with short episodes of plume departure, and subsequently elevated OBT, as well as elevated OBT/HTO ratios.

In general, the scenario was found to be fit for purpose; however, some episodes of plume departure provide a sufficient basis for model testing and intercomparison, whereas some other episodes need to be discarded a priori (as shown in Table 4 above) and investigated in the future, because the properly measured or reconstructed air HTO is either completely missing, or reconstructed with insufficient resolution to accurately correspond with the other measured results.

#### 5.4.2.3. *CNSC scenario*

The CNSC scenario provides a unique dataset addressing the currently not well understood importance of soil to leaf HTO transfer pathways in controlling leaf tritium dynamics. In general, the dataset was fit for this purpose. However, as acknowledged in previous sections, there were many data gaps in the atmospheric tritium record. The measurement of tritium in air was not a primary objective of this experimental campaign and consequently there are some limitations in the application of this scenario for the model intercomparison. Nonetheless, the results of this work provide insights into the impact of soil to leaf HTO transfer on the leaf tritium dynamics.

## 6. KEY FINDINGS FROM MODEL INTERCOMPARISON AND DIRECTIONS FOR FUTURE WORK

Calculations of land surface tritium transfers were conducted for four tritium transfer models (i.e. CTEM-CLASS, SOLVEG-II, CERES and TOCATTA- $\chi$ ) using three prepared scenarios (i.e. the IRSN-EDF, CNL and CNSC scenarios). The model results were compared with measurements obtained during the experimental campaigns used for each scenario. In addition, the outputs of the four models were compared and the processes important for predicting foliar uptake of atmospheric HTO and soil to plant tritium transfer were discussed. This section briefly summarizes the key findings of this work, based on more detailed discussions of the results of the intercomparisons provided in Appendix II below.

Comparison of the model predictions of TFWT activity concentrations in leaves affected by plume arrivals (i.e. for the IRSN-EDF and CNL scenarios) indicate that the exchange of HTO at the air–leaf interface is extensively regulated by the opening or closure of stomata (stomatal resistance). The model outputs also indicate that aerodynamic leaf boundary layer transport has an impact on the exchange of HTO at the air–leaf interface. The effect of stomata opening and stomatal resistance, therefore, needs to be represented in any tritium model dealing with air–leaf transport. For the CNL scenario, outputs from all four models showed a high retention of TFWT activity concentrations within plant leaves during the dusk period following the arrival of the HTO plume. This implies that tritium models have to precisely calculate (or parameterize) not only the daytime stomatal resistance, but also nighttime cuticle resistance. Comparisons of long-term trends (over seasons) of OBT concentrations, predicted for the IRSN-EDF scenario, demonstrated that variability of OBT concentration in leaves is mainly caused by that of TFWT concentration, and that short term (daily) variability of dry matter production in plants is less important. Furthermore, the similarity in OBT concentrations predicted by simple (CERES) and complex (SOLVEG-II and TOCATTA- $\chi$ ) models implies that plant respiration has a minor impact on the dynamics of OBT in leaves and, therefore, can be neglected in model predictions. Nevertheless, respiration is a very important process, contributing to OBT formation during day and night, and cannot be neglected [130]. About 50% of fixed carbon is lost by respiration, but about 50% remains in plants and consequently, a significant amount of OBT still remains in the plant. Moreover, TOCATTA- $\chi$  and SOLVEG-II explicitly consider respiration in their model formulations. TOCATTA- $\chi$  considers that net OBT formation depends on leaf carbon processes, including growth, respiration, and CO<sub>2</sub> assimilation rate (net of respiration); see Eq. (47) for specific details. SOLVEG-II also considers respiration in the production of TFWT, and decomposition of NE-OBT; see Eq. (64). In the simple CERES model, the OBT formation is not based on physiological processes and consequently does not consider respiration.

Respiration is important in OBT formation during ‘plume on’, and is also important in OBT loss during ‘plume off’, because a large part of the OBT produced still remains in the plant.

For the CNSC scenario, two models (CTEM-CLASS and SOLVEG-II) calculated similar responses of HTO activity concentrations in soil following the arrival of the plume in the air, despite the models having different soil HTO module structures. This suggests the gaseous diffusion of HTO in soil has a negligible impact on the behaviour of HTO deposited to the soil. Different predictions of TFWT activity concentrations in leaves by the two models suggests that soil to plant HTO transfer depends on the vertical profile of HTO concentration in soil, and on the density profile of water-absorbing roots in the soil, and, therefore, the use of a multilayered soil model with adequate grid size is needed to precisely calculate the soil-to-plant HTO transfers. Model predictions also demonstrated that the water content in soil affects the

HTO concentration in the soil, as does the physiological activity of the standing vegetation, such as opening of the stomata and photosynthesis. This suggests that combined calculations of soil HTO, soil water, and its effect on the transfer of tritium to plants are needed in order to accurately predict tritium dynamics in atmosphere–soil–plant systems.

In the CNL and CNSC scenarios, model predictions tended to underestimate OBT concentrations in leaves both during and after arrivals of the plume. This was not the case with the IRSN scenario. This is due to the effect of wind in the Ottawa Valley which changes direction sharply due to prominent wind channelling and this results in a sharp plume shape at the receptor, with distinct arrival and departure gradients in the atmospheric activity concentration of HTO, i.e. a sharp (up to 80 fold) drop in activity concentration from the plume to the local background. Such an effect does not appear in the IRSN scenario, which is characterized by less prominent prevailing winds and a more uniform distribution of wind by sectors, suggesting that exchangeable OBT may play a minor role. Therefore, the inclusion of an exchangeable OBT pool in leaves, subsequent translocation of exchangeable OBT, and formation of non-exchangeable OBT by metabolic processes other than photosynthesis (particularly at night) are needed for proper prediction of dynamic behaviour of OBT in leaves affected by foliar deposition of HTO.

Participants of MODARIA WG7 and their colleagues from IRSN (France), CNL (Canada) and CNSC (Canada) attended the CNSC Tritium Workshop in Ottawa, Canada in April 2016. The purpose of this workshop was to discuss urgent and emerging experimental data needs and directions for future studies in the natural environment and modelling work with respect to tritium transfer in the terrestrial environment. Although the workshop was organized by CNSC outside the auspices the MODARIA programme, research areas of relevance to WG7 participants were discussed. New experimental results were presented, and ongoing field campaigns were further developed. Furthermore, new directions were identified pertaining to obtaining tritium activity concentrations in representative background areas: potentially overlooked bioavailable forms of OBT (primarily in soil) and corresponding pathways of OBT formation were also identified. Details can be found on the CNSC website and in reports published by the CANDU Owners Group (e.g. see Refs [155, 172]).





## APPENDIX I. DESCRIPTION OF MODELS USED FOR INTERCOMPARISON EXERCISE

### I.1. CTEM-CLASS

#### I.1.1. Model description

The framework of tritium transfer within the CTEM-CLASS model (see Fig. 13) is the multilayer Canadian LAnd Surface Scheme (CLASS 2.7) and the phenomenological detalization Canadian Terrestrial Ecosystem Model CTEM-CLASS of Environment Canada [161]. CTEM-CLASS can be used to explicitly model the interconnectedness of solar radiation, energy, water and carbon cycles, and has been extensively validated. Photosynthesis, stomatal conductance and energy balance are made interdependent through use of the coupled dynamic photosynthesis model, which applies the Farquhar photochemistry within the Ball-Berry and Leuning stomata-photosynthesis model [161].

Uptake of gaseous HTO by the soil–plant system, and its re-emission, which independently contributes to re-emission of HTO that is passively transported within the evapotranspiration route is defined by the exchange velocity proportional to stomatal conductance [152]:

$$\frac{dC_{leaf}}{dt} = \frac{\rho_w}{M_{leaf}} V_{ex} (C_{atm} - C_{leaf}) + E(C_{soil} - C_{leaf}) \quad (37)$$

where:

- $C_{leaf}$  is the HTO concentration in the plant water in leaf (Bq/L);
- $t$  is time (s);
- $\rho_w$  is density of water (kg/m<sup>3</sup>);
- $M_{leaf}$  is the mass of a *leaf* part of the plant per surface area (kg/m<sup>2</sup>);
- $V_{ex}$  is exchange velocity (m/s);
- $C_{atm}$  is the HTO concentration in the atmospheric moisture (Bq/L);
- $C_{soil}$  is the HTO concentration in the soil moisture (Bq/L);
- $E$  is evapotranspiration (kg m<sup>-2</sup> s<sup>-1</sup>).<sup>10</sup>

Normalized stomatal conductance  $g_{cn}$  governs the variation of exchange velocity  $V_{ex}$  during daytime:

$$V_{ex} = g_{cn} V_{ex\_max} \quad (38)$$

where:

- $V_{ex}$  is the exchange velocity during the daytime (m/s);
- $V_{ex\_max}$  is the maximum exchange velocity during the daytime (m/s) ( $V_{ex\_max} = 3 \times 10^{-3}$  m/s);
- $g_{cn}$  is the normalized stomatal conductance (dimensionless), such that:

$$g_{cn} = \frac{g_c}{g_{c\_max}} \quad (39)$$

- $g_c$  is the stomatal conductance and is calculated in CLASS using the Ball-Berry model (see Ref. [88]);
- $g_{c\_max}$  is the maximum stomatal conductance (mol m<sup>-2</sup> s<sup>-1</sup>).

---

<sup>10</sup> Evapotranspiration is measured in mm/s. Units of measured data (mm/s) can be converted to kg m<sup>-2</sup> s<sup>-1</sup>, taking account of the density of water (1 kg water = 1 L water = 10<sup>-3</sup> m<sup>3</sup>), where:

1 kg water m<sup>-2</sup> s<sup>-1</sup> ≡ 1 L water m<sup>-2</sup> s<sup>-1</sup> ≡ 10<sup>-3</sup> m<sup>3</sup> water m<sup>-2</sup> s<sup>-1</sup> ≡ 10<sup>-3</sup> m/s ≡ 1 mm/s

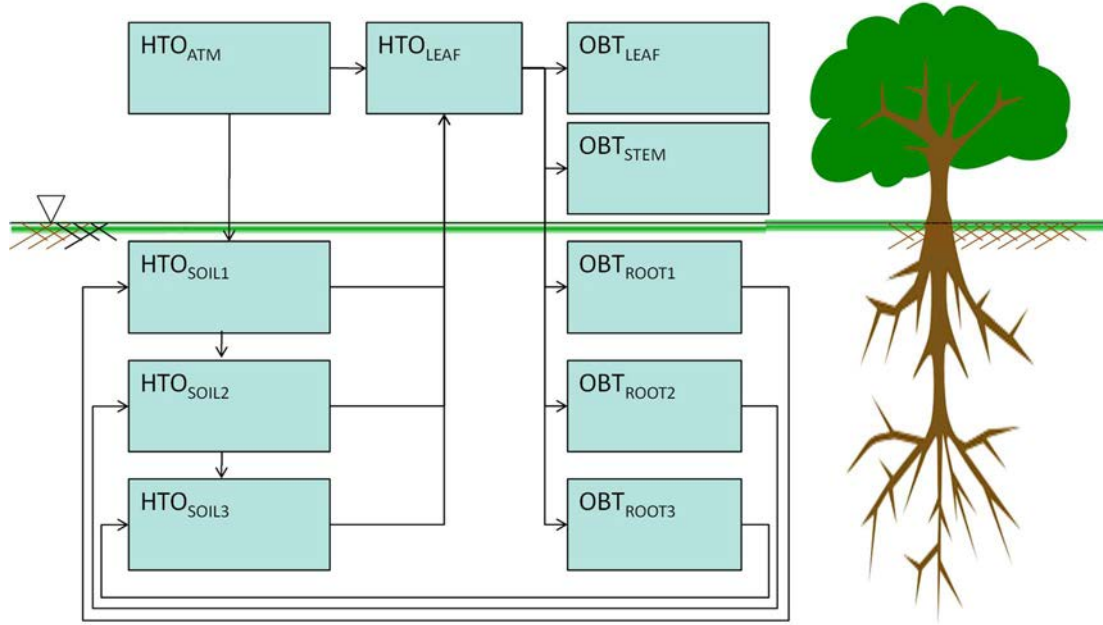


FIG. 13. Block scheme of tritium transfer as defined by the water and carbon cycles of the CTEM-CLASS model (from Ref. [152], Reprinted from *Journal of Environmental Radioactivity*, 129/March 2014, V.Y. Korolevych, S.B. Kim, P.A. Davis, OBT/HTO ratio in agricultural produce subject to routine atmospheric releases of tritium, 157-168, Copyright (2014), with permission from Elsevier).

It is assumed that  $g_{cn} = 0.1$  during dark hours to accommodate cuticle conductance when stomata and cuticles are almost, but not completely closed; see Ref. [172] for more details.

In the current version of CLASS-CTEM the gaseous exchange of HTO on the surface of soil is defined by a constant deposition velocity  $V_d$ :

$$\frac{dC_{soil}}{dt} = \frac{\rho_w}{M_{soil}} V_d (C_{atm} - C_{soil}) \quad (40)$$

where:

$C_{soil}$  is the HTO concentration in the soil water (soil moisture) of the upper soil layer (Bq/L);

$t$  is time (s);

$\rho_w$  is density of water (kg/m<sup>3</sup>);

$M_{soil}$  is the mass of soil water (soil moisture) in the upper soil layer per surface area (kg/m<sup>2</sup>);

$V_d = 0.3 \times 10^{-3}$  m/s is for soils with high clay content, and  $1.5 \times 10^{-3}$  m/s for all other cases;

$C_{atm}$  is the HTO concentration in the atmospheric moisture (Bq/L).

Wet deposition is defined by a washout ratio  $WR$ :

$$C_{precip} = WR \cdot C_{atm} \quad (41)$$

where:

$C_{precip}$  is the HTO activity concentration (Bq/L) in the precipitating water;

$C_{atm}$  is the HTO concentration in the atmospheric moisture (Bq/L);

$WR = 0.2$  (dimensionless).

It is assumed that there is no resistance for HTO uptake by plant roots from soil, and that the concentration of HTO in each soil layer is assigned directly to the corresponding fraction of the total amount of roots present in that layer, based on a distribution function for roots with depth, as defined in CTEM-CLASS.

Through consideration of the water cycle within the CTEM-CLASS model, the remaining HTO transfer within the soil–vegetation system is estimated, whereby HTO serves as a tracer (i.e. to ‘label’ water in each compartment), arriving with the incoming water, undergoing stoichiometric dilution, and leaving with outgoing water, as defined in CLASS. As a result, HTO advection is fully taken into account and HTO diffusion is assumed negligible. In particular, soil water transfer is estimated using the Green-Ampt solution, along with the numerical solution to Richards formulation for storm water flow into unsaturated media and entry into soil pores previously occupied by the existing water. Free Darcian flow is then calculated. Following water transport, soil thermodynamics are calculated using the CLASS model.

In addition to the direct uptake of HTO into the soil–vegetation system, HTO also becomes incorporated into carbohydrates that are formed in the leaf, as reflected using the Farquhar photosynthesis model (which is calculated within the CTEM-CLASS model). Through the photosynthetic process carbohydrates are labelled by the HTO in the leaf, as described by the following equation:

$$\frac{d(M_{dm}C_{OBT})}{dt} = \frac{dM_{dm}}{dt} ID_p C_{leaf} \quad (42)$$

or in equivalent form:

$$\begin{aligned} \frac{dC_{OBT}}{dt} &= \frac{d(\ln(M_{dm}))}{dt} (ID_p C_{leaf} - C_{OBT}) \\ M_{dm} &= (1 - f_w) M_{leaf} \end{aligned} \quad (43)$$

where:

$M_{dm}$  is the dry matter mass of a *leaf* part of the plant per surface area (kg/m<sup>2</sup>);

$t$  is time (s);

$f_w$  is the water fraction of *leaf* ( $f_w = 0.8$ ) (kg/kg);

$ID_p$  is the isotopic discrimination factor ( $ID_p = 0.8$ ) (dimensionless);

$C_{OBT}$  is the OBT concentration in plant tissues (Bq/kg);

$C_{leaf}$  is the HTO concentration in the plant water in leaf (Bq/kg).

Carbon compounds in different compartments become labelled with OBT labels. The OBT is carried into the plant with the incoming carbon compound, undergoing stoichiometric dilution. It then leaves the plant with the outgoing carbon compounds, as defined in the CLASS part of the model. Therefore, OBT follows the carbon cycle of CTEM-CLASS and eventually exits the system as HTO with the respiration CO<sub>2</sub> stream forecasted by CTEM-CLASS.

A certain amount of OBT remains in the litter and organic matter of the soil, where it is also slowly decomposed into HTO and CO<sub>2</sub>. OBT allocation is, therefore, modelled proportionally to the allocation of carbon within the five carbon pools that have been defined in the CTEM-CLASS model (leaf, stem, root, litter and organic soil); the model also includes maintenance and respiration. Plant growth (i.e. LAI, leaf, stem and root mass) is modelled by CTEM for nine plant phenotypes, including C3 and C4 crops for different carbon fixation in photosynthesis. Plant maintenance and respiration during growth respiration is modelled in CTEM. In doing so, it is assumed that it contributes to the re-emission flux of HTO, which contributes directly to

the HTO that is re-emitted into the atmosphere, as well as to the HTO in soil at different depths as determined by a root distribution function. HTO re-emission therefore follows the evapotranspiration route [135, 152].

## I.2. TOCATTA- $\chi$

### I.2.1. Model description

TOCATTA- $\chi$  is a dynamic compartment model developed by IRSN for pastures to simulate the transfer of tritium (and  $^{14}\text{C}$ ) in grassland ecosystems exposed to atmospheric emissions of tritium (and  $^{14}\text{C}$ ) from facilities under normal operation or accident conditions (see Fig. 14). An earlier version of the model was previously developed and tested, assuming an hourly time step for transfer of  $^{14}\text{C}$  to pasture [179, 181] and was further developed for tritium to take into account acute variations in tritium releases and meteorology [46]. The TOCATTA- $\chi$  model is being implemented in the SYMBIOSE modelling platform [182] used for operational impact studies in France.

TOCATTA- $\chi$  has a number of key features and assumptions, many of which are similar to those used for the modelling of  $^{14}\text{C}$  transfer [181]. The model runs on an hourly basis and represents the subdaily processes for the implementation of operational discharges (and potentially for accident scenarios). In particular it accounts for short and rapid kinetics that may occur in and between some compartments [46]. Atmospheric transport and dispersion processes are not explicitly modelled in TOCATTA- $\chi$ . Instead, atmospheric transport and dispersion are driven by atmospheric concentrations of HTO above the canopy and concentrations of HTO in rainwater along with weather input data for solar radiation, air temperature, relative humidity, wind speed and precipitation.

SOURCE	Gas dispersion (HTO)											
	AIR CANOPY	Soil surface (net) exchange (HTO) Wet input (HTO, via precipitation) Interception by soil Precipitation (H <sub>2</sub> O)	Foliar diffusion (TFWT) Wet input (HTO, via precipitation) Interception by plant Precipitation (H <sub>2</sub> O)								Photosynthesis (C)	
		SOIL WATER Radioactive decay	Root uptake (HTO)								Migration (HTO, H <sub>2</sub> O) Evapotranspiration (H <sub>2</sub> O)	
			PLANT WATER Biological growth Radioactive decay								Net formation (OBT)	
				PLANT DRY MATTER Biological growth Radioactive decay								
					SHOOT STRUCTURAL DRY MATTER						Ageing (C)	Cutting (C)
										ROOT STRUCTURAL DRY MATTER	Ageing (C)	
											SUBSTRATE (SAP)	Respiration (C)
										Biological growth (C)	Biological growth (C)	REST PLANT

The TOCATTA- $\chi$  model is parameterized for pasture grass only, but may be extended to vegetables and crops. Over the time period of simulation, it is assumed that pasture grass is permanently present. In addition, it is assumed that the grassland ecosystem is not being irrigated. The TOCATTA- $\chi$  model can then be used to integrate plant physiology (uptake through photosynthesis, loss via respiration, nutrient and water status, aboveground and belowground dry matter production by the plant) over the daytime–nighttime cycle. This can be done using a modelling approach that has been derived from a simplified version of the pasture simulation model (PASIM) [162]. TFWT in plant tissue is expressed as a function of:

- Foliar uptake of atmospheric HTO, assuming an exchange velocity rate, which is defined as the inverse of a sum of resistances to water loss at the leaf-to-air interface;
- Root uptake of HTO from soil after percolation of rainwater into the soil (as it is assumed that grassland ecosystems are not being irrigated).

Regarding the computation of net formation of OBT in plants, an analogy was made with the equation governing the time variation of  $^{14}\text{C}$  in the substrate compartment (sap) [181]. It is a function of leaf carbon cycling related processes, including growth, respiration and  $\text{CO}_2$  assimilation rate (net of respiration), the latter being derived from the biochemical Farquhar model [183, 184], coupled with the mechanistic stomatal conductance model given in Ref. [95]. The LAI and the solar radiation scheme have been estimated following a simplified version of the solar radiation scheme given in Ref. [162]. Similar to  $^{14}\text{CO}_2$ , the progressive incorporation of OBT into the organic matter compartment is driven by a 15 day moving average assuming instantaneously formed OBT activity, based on the mass balance between input fluxes (through photosynthesis using  $\text{CO}_2$  and TFWT) and output fluxes (through respiration and growth processes that consume sugar products to form  $\text{CO}_2$  and water) integrated on an hourly time step. This modelling approach is used to approximate the slow kinetics of OBT integration into the organic matter compartment, assuming instantaneous formation. Integration of resistances of exchange velocities at the leaf–air and soil–air interfaces can also be calculated using a physiological approach. The model integrates the hourly dynamics of soil water status based on mass water balance, with evapotranspiration estimated from the Penman-Monteith model [185]. Consequently, this new version of the model does consider the possibility of soil water stress affecting stomatal conductance and evapotranspiration. The fundamental aspects of TOCATTA- $\chi$  are summarized in Refs [181, 186]. More details on the conceptual model and the new representation of key processes are given in Ref. [46].

## 1.2.2. Key equations

### 1.2.2.1. TFWT in grass leaves

The TFWT in grass leaves is expressed as a function of:

- The net process of diffusion, assuming an exchange velocity rate that is defined as the inverse of a sum of resistances to water loss at the leaf-to-air interface;
- The root uptake of HTO from soil after percolation of rainwater into the soil.

It is assumed that the net diffusion flux is proportional to the difference in the volumetric concentrations of HTO between the atmosphere and the surface of the leaves, which can be expressed, as follows [80]:

$$THTO_{Air,P}^{Diff} = \frac{\mathcal{G}_{plant}(t)}{\chi_{Shoot\_wat}} \left\{ \rho_a [HTO]_{Air} - \frac{\rho_{sat}}{\beta} [TFWT]_P \right\} \quad (44)$$

where:

- $THTO_{Air,\rho}^{Diff}$  is the net diffusion flux ( $\text{mol L water}^{-1} \text{ s}^{-1}$ );  
 $\chi_{Shoot\_wat}$  is the aboveground water density, derived from dry density using a constant dry/fresh weight ratio for plant products ( $\text{L/m}^2$ );  
 $[HTO]_{Air}$  is the HTO concentration in the plant canopy atmosphere ( $\text{mol/L}$ ), where  $1 \text{ L} = 1 \text{ kg}$  for water;  
 $[TFWT]_P$  is the concentration of tritium in the water compartment of leaves ( $\text{mol/L}$ ), where  $1 \text{ L} = 1 \text{ kg}$  for water;  
 $\beta$  is the ratio of vapour pressure between HTO and  $\text{H}_2\text{O}$  (typically 1.1);  
 $\rho_a$  is the absolute air humidity at the reference height ( $\text{kg/m}^3$ );  
 $\rho_{sat}$  is the saturated air humidity at the vegetation temperature assumed equal to air temperature ( $\text{kg/m}^3$ );  
 $\gamma g_{plant}(t)$  is the rate of exchange of HTO from air to plant canopy ( $\text{m/s}$ );  
 $g_{plant}$  is the rate of exchange of water (or total conductance) calculated as inverse of the sum of the two resistances ( $\text{m/s}$ ) [80], as follows:

$$g_{plant} = \frac{1}{r_c + r_b} \quad (45)$$

where:

- $r_c$  is the bulk stomatal resistance of the canopy ( $\text{s/m}$ );  
 $r_b$  is the boundary layer resistance describing the mass transfer in the quasi-laminar flow layer adjacent to the canopy surface ( $\text{s/m}$ ).

The leaf stomatal conductance ( $g_s$ ) over the whole canopy leaf area is scaled up to estimate the stomatal conductance of the canopy ( $g_c = 1/r_c$ ,  $\text{m/s}$ ). In doing so, the canopy is considered to be one single leaf, applying a simplistic ‘big leaf’ approach, which uses the Huntingford model to estimate leaf stomatal conductance. The boundary layer resistance  $r_b$  is a function of LAI and wind speed at the canopy height [162]. As can be seen in Eq. (45) the aerodynamic (or atmospheric) resistance from reference height to canopy has been neglected, since the aerodynamic resistance of short grass plays a secondary role [187]. More detailed information can be found in Supplemental Data A of Ref. [46].

The uptake of soil HTO by plant roots is a function of diffusive exchange rates, as follows [80]:

$$THTO_{S,P}^{Up}(t) = g_{plant}(t) \times (\rho_{sat} - \rho_a) \frac{[HTO]_S}{\rho_w} \quad (46)$$

where:

- $THTO_{S,P}^{Up}(t)$  is the flux of HTO taken up from soil pore water by plant roots ( $\text{mol m}^{-2} \text{ s}^{-1}$ );  
 $[HTO]_S$  is the concentration of tritium in soil pore water ( $\text{mol/m}^3$  of soil pore water);  
 $g_{plant}(t)$  is the exchange rate (or total conductance) of water ( $\text{m/s}$ ) calculated in Eq. (45) above;  
 $\rho_{sat}$  is the saturated air humidity at the vegetation temperature assumed equal to air temperature ( $\text{kg/m}^3$ );  
 $\rho_a$  is the absolute air humidity at the reference height ( $\text{kg/m}^3$ );  
 $\rho_w$  is the density of water (typically  $1000 \text{ kg/m}^3$ ).

#### 1.2.2.2. OBT formation during the daytime

The net OBT formation during the daytime is related to the TFWT concentration in leaves, in addition to photosynthesis, respiration and growth rates, based on the following equation, which assumes a mass balance [80]:

$$TOBT_{P=Grass}^{NForm}(t) = \left[ \frac{TC^{Photo}}{(\chi_{Shoot} + \chi_{Root})[^{12}C]_P} WE_{eq} DI_P [TFWT]_P^* \right] - \left[ \frac{(TC^{Resp} + TC^{Gro})}{(\chi_{Shoot} + \chi_{Root})[^{12}C]_P} [OBT]_P(t) \right] \quad (47)$$

where:

- $TOBT_{P=Grass}^{NForm}(t)$  is the net OBT formation during the daytime (mol kg-dry mass<sup>-1</sup> s<sup>-1</sup>);
- $\chi_{Shoot}$  is the time dependent shoot dry biomass (kg-dry mass/m<sup>2</sup>);
- $\chi_{Root}$  is the time dependent root dry biomass (kg-dry mass/m<sup>2</sup>);
- $[^{12}C]_P$  is the stable C concentration in plant dry material (mol-C/kg dry mass);
- $WE_{eq}$  is the water equivalent factor (L/kg-dry mass);
- $[OBT]_P(t)$  is the OBT concentration in the whole plant (mol/kg dry mass);
- $[TFWT]_P^*$  is the HTO concentration in leaf water bounded by the concentration of tritium in soil water and in air humidity (mol/L);
- $TC^{Photo}$  is the stable C transfer flux through the process of canopy photosynthesis (mol-C m<sup>-2</sup> s<sup>-1</sup>);
- $TC^{Resp}$  is the stable C transfer flux through the respiration process (mol-C m<sup>-2</sup> s<sup>-1</sup>);
- $TC^{Gro}$  is the stable C transfer flux through the growth process (mol-C m<sup>-2</sup> s<sup>-1</sup>);
- $DI_P$  is the discrimination ratio (dimensionless).

As can be seen in Eq. (47), an analogy was made with the equation governing the time variation of <sup>14</sup>C in the substrate compartment (sap) [181]. This equation translates the slow kinetic of integration into the organic matter compartment. Again, by analogy with <sup>14</sup>CO<sub>2</sub>, the progressive incorporation of OBT into the organic matter compartment is driven by a 15–20 day moving average assuming instantaneously formed OBT activity [179]. More detailed information can be found in Refs [46, 179, 181].

#### 1.2.2.3. Soil HTO calculation

The concentration of HTO in soil is expressed as a function of:

- A net process of HTO exchange, assuming an exchange velocity rate that is defined as the inverse of a sum of resistances to water loss at the soil-to-air interface;
- Rainwater percolation into soil;
- Evapotranspiration (including root uptake of soil HTO).

The exchange process of HTO between the canopy atmosphere and the underlying soil horizon is expressed as follows (by analogy with Eq. (44) above):

$$THTO_{Air,S}^{SExch} = g_{soil}(t) \{ \rho_a [HTO]_{Air} - \frac{\rho_{satsurf}}{\beta} [HTO]_S \} \quad (48)$$

where:

- $THTO_{Air,S}^{SExch}$  is the exchange of HTO between the canopy atmosphere and the underlying soil horizon (mol m<sup>-2</sup> s<sup>-1</sup>);
- $g_{soil}(t)$  is the rate of exchange of water vapour between the soil surface and atmosphere at time  $t$  (m/s);
- $[HTO]_{Air}$  is the HTO concentration in the plant canopy atmosphere (mol/L), where 1 L = 1 kg for water;



$[HTO]_s$  is the concentration of HTO in soil pore water (mol/L of soil pore water), where 1 L = 1 kg for water;  
 $\rho_a$  is the absolute air humidity at the reference height (kg/m<sup>3</sup>);  
 $\rho_w$  is water density (kg/m<sup>3</sup>);  
 $\rho_{satsurf}$  is the saturated air humidity at the temperature of the soil surface (kg/m<sup>3</sup>);  
 $\beta$  is the inverse of the isotopic discrimination factor ( $\beta = 0.91$ ) (dimensionless).

The temperature of the soil surface and the soil horizon are both assumed to be equal to that of the air. Therefore,  $\rho_{satsurf}$  is calculated from the saturated vapour pressure, which is related to the air temperature according to the Magnus approximation, and  $g_{soil}$  is the rate of exchange of water vapour between the soil surface and atmosphere. By analogy to the exchange at the air–vegetation interface, this exchange rate is specified as the inverse sum of two resistances — here the aerodynamic resistance characterizes the transfer from a reference height in the free atmosphere to the soil surface [162] and the soil resistance, regulated by the HTO transport in soil and specified according to an empirical function of time (see Supplemental Data A of Ref. [46]).

The transfer of HTO in the pore solution by percolation is expressed by the following equation:

$$THTO_{S,\infty}^{Mig} = K_s(t) \times [HTO]_s \quad (49)$$

where:

$THTO_{S,\infty}^{Mig}$  is the transfer of HTO in pore solution by percolation (mol m<sup>-2</sup> s<sup>-1</sup>);  
 $[HTO]_s$  is the concentration of HTO in soil pore water (mol/m<sup>3</sup> of soil pore water);  
 $K_s$  is soil hydraulic conductivity that varies through time as a function of soil water content which also now varies through time (m/s).

The current version of the model integrates the hourly dynamics of soil water status based on mass water balance, with evapotranspiration estimated from the Penman-Monteith model [185]. Consequently, this new version of the model does consider the possibility of soil water stress affecting stomatal conductance and evapotranspiration.

### I.3. SOLVEG-II

#### I.3.1. Model description

The land surface model SOLVEG-II is a one-dimensional multilayered atmosphere–soil–vegetation model developed by the Japan Atomic Energy Agency (JAEA) for the research of material transport in vegetated ecosystems. A conceptualization of the tritium model of SOLVEG-II is illustrated in Fig. 15 and key equations are provided in Section I.3.2.

SOLVEG-II is comprised of four main modules, which are atmosphere, vegetation, soil and radiation [69, 100, 157, 188]. The model can be used to calculate transport of water, heat and CO<sub>2</sub> for a vegetated or bare land surface. The SOLVEG-II relies on meteorological input data (measured on an hourly time scale) at the upper atmospheric boundary, and calculates heat, water and CO<sub>2</sub> transport in layered atmosphere and soil with interactions with the vegetated canopy. For CO<sub>2</sub> assimilation (or organic matter production) by plants, leaf photosynthesis is calculated using Farquhar's formulation [160]. This photosynthesis is dependent on stomatal conductance by a relationship described in Refs [158, 159]. These physiological processes are parameterized by seven plant phenotypes, such as C4 grass, crop and needles [98]. For the water transport in soil, water content and flux in layered soil are explicitly calculated, by solving

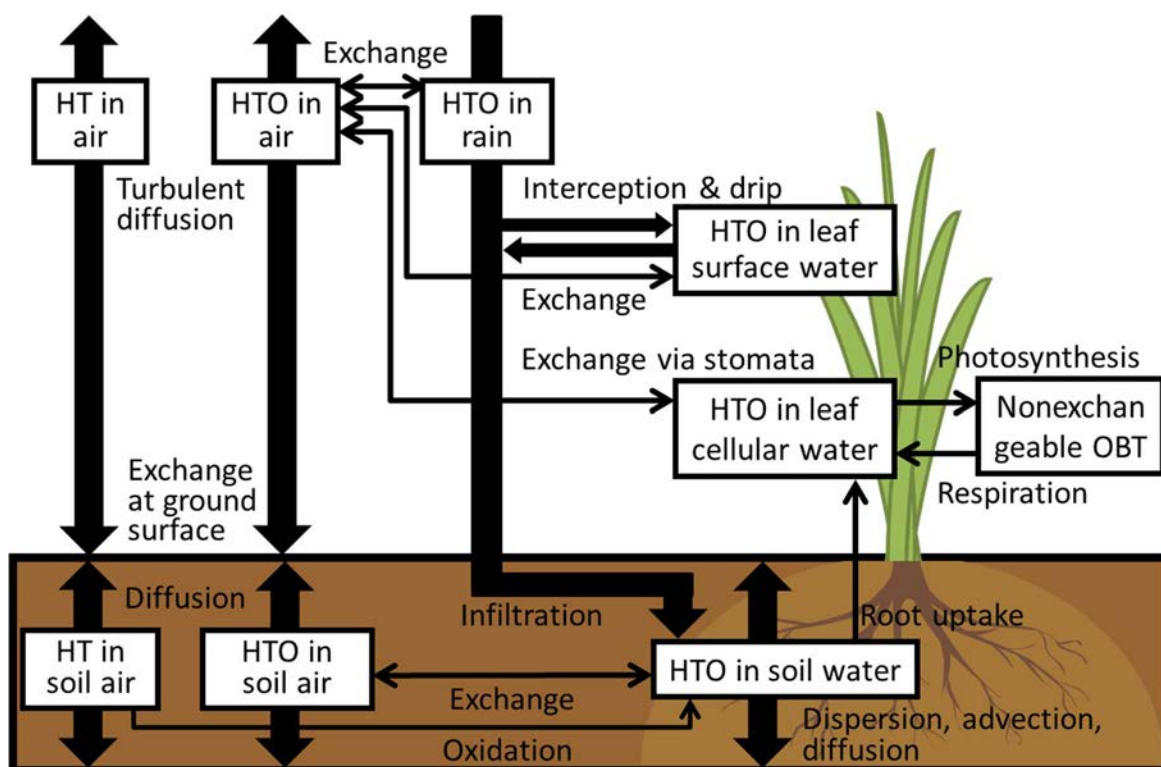


FIG. 15. Processes considered in the tritium model of SOLVEG-II (from Ref. [175], courtesy of V.Y. Korolevych).

transport equations for soil water of classical Richard's type. Hydraulic parameters of the soil are parameterized by 12 texture types as classified by the United States Department of Agriculture [157]. Verification of model predictions for processes for the transport of water, heat, CO<sub>2</sub>, fine particles, fog droplets, and other trace gases have been conducted for various types of land use, such as short vegetative field, forest, semiarid desert, rice paddy field and bare soil [29, 69, 98, 125, 175, 188–193].

The tritium model of SOLVEG-II [42, 43, 157, 194] calculates transport and exchange of HTO and HT as illustrated in Fig. 15. Calculations of the tritium transport are based on heat, water and CO<sub>2</sub> transport simulated by other modules of SOLVEG-II. The HTO model is driven by the inputs of concentrations of HTO in the air and rain at the model top atmospheric boundary. Modelled processes for HTO transport include turbulent diffusion of HTO vapour in the atmosphere and transport of HTO in the soil [157]. In soil, gaseous diffusion of HTO vapour in the soil pore space and aqueous transport of HTO by dispersion, advection and diffusion by the soil water flow are calculated. The model also considers interactions of HTO contained in rainwater [43], such as interception and drip of rain HTO by the surface of leaf within the layered vegetation canopy and exchange of HTO between the intercepted leaf surface water and air in the canopy. The remaining precipitating HTO, which is not intercepted by the canopy, is added onto the ground surface and infiltrates to the soil (see Fig. 15).

If releases of HT are considered, the HT model calculates transport of HT in the atmosphere and soil. This model is run by an input of the concentration of HT in the top atmospheric boundary. Deposition of HT to the soil (i.e. conversion of HT to HTO by microorganisms in

the soil) is calculated explicitly by solving gaseous transport of HT in the layered soil and oxidation of HT to HTO [42]. The oxidation of HT in soil is calculated using a rate constant depending on the soil temperature and water content. The modelling of HT deposition was tested against the data from a past HT release experiment at Chalk River Laboratory, Canada [42].

The vegetation tritium model calculates the TFWT content in the stomatal cavity of leaves (leaf cellular water) [43]. The processes included are shown in Fig. 15. The calculations of the transfer of HTO from the air to leaf cellular water and assimilation of TFWT to the non-exchangeable OBT in leaves have been validated [43] with data from an HTO exposure experiment with grape plants in the south of France [74].

### I.3.2. Key equations

This section briefly presents the key equations of the tritium model of SOLVEG-II. Full descriptions of this model can be found in the literature [42, 43, 194].

Transport of HTO vapour in the atmosphere is expressed by a diffusion equation:

$$\frac{\partial \chi_a}{\partial t} = \frac{\partial}{\partial z} K \frac{\partial \chi_a}{\partial z} + S \quad (50)$$

where:

- $\chi_a$  is the concentration of HTO vapour in the air (Bq/m<sup>3</sup>);
- $t$  is the time (s);
- $z$  is the vertical coordinate (height) in the atmosphere (m);
- $K$  is the vertical turbulent diffusivity calculated by a turbulent closure model of SOLVEG-II (m<sup>2</sup>/s);
- $S$  is the volumetric sink or source of HTO (Bq m<sup>-3</sup> s<sup>-1</sup>), caused by HTO exchanges between the canopy air and the leaf interior (calculated by the flux  $E_{stom}$  in Eq. (59) below) and between the canopy air and leaf surface water (rain HTO intercepted by leaf surface [194]).

Atmospheric transport of HT is calculated using:

$$\frac{\partial \chi_{aHT}}{\partial t} = \frac{\partial}{\partial z} K \frac{\partial \chi_{aHT}}{\partial z}, \quad (51)$$

where:

- $\chi_{aHT}$  is the concentration of HT in the air (Bq/m<sup>3</sup>);
- $t$  is the time (s);
- $z$  is the vertical coordinate (height) in the atmosphere (m);
- $K$  is the vertical turbulent diffusivity calculated by a turbulent closure model of SOLVEG-II (m<sup>2</sup>/s).

The soil HTO submodel of SOLVEG-II calculates the concentration of HTO vapour,  $\chi_{sa}$  (Bq/m<sup>3</sup>), in the soil pore space by:

$$\frac{\partial (\eta_{sat} - \eta_{sw}) \chi_{sa}}{\partial t} = \frac{\partial}{\partial z} D_{sa} \frac{\partial \chi_{sa}}{\partial z} - e_b \quad (52)$$

where:

- $\eta_{sat}$  is the porosity of the soil (fractional);
- $\eta_{sw}$  is the water content of the soil (vol/vol);
- $z$  is the vertical coordinate (depth) in the layered soil (m);
- $D_{sa}$  is the effective diffusivity for the HTO vapour in the soil ( $\text{m}^2/\text{s}$ );
- $e_b$  is the HTO exchange between the HTO vapour in the soil pore space and HTO contained in the soil water ( $\text{Bq m}^{-3} \text{s}^{-1}$ ).

This exchange is calculated using:

$$e_b = \frac{1}{r_b} \left\{ \chi_{sa} - q_{sat}(T_s) \frac{\rho_a}{\rho_w} \chi_{sw} \right\} \quad (53)$$

where:

- $e_b$  is the HTO exchange between the HTO vapour in the soil pore space and HTO contained in the soil water ( $\text{Bq m}^{-3} \text{s}^{-1}$ );
- $r_b$  is the resistance for condensation/evaporation of water in the soil (s);
- $q_{sat}(T_s)$  is the saturated specific humidity ( $\text{kg/kg}$ ) at the soil temperature  $T_s$  (K);
- $\rho_a$  is the density of the air ( $\text{kg/m}^3$ );
- $\rho_w$  is the density of the liquid water ( $\text{kg/m}^3$ );
- $\chi_{sw}$  is the concentration of HTO in the soil water ( $\text{Bq/m}^3$ ).

Transport of HTO in the soil water is calculated by a diffusion–advection equation:

$$\frac{\partial \eta_{sw} \chi_{sw}}{\partial t} = - \frac{\partial E_w \chi_{sw}}{\partial z} + \frac{\partial}{\partial z} D_{sw} \frac{\partial \chi_{sw}}{\partial z} + e_b - e_r + e_{oxi} \quad (54)$$

where:

- $\eta_{sw}$  is the water content of the soil (vol/vol);
- $\chi_{sw}$  is the concentration of HTO in the soil water ( $\text{Bq/m}^3$ );
- $t$  is the time (s);
- $E_w$  is the vertical flux of liquid water in the soil ( $\text{m}^3 \text{m}^{-2} \text{s}^{-1}$ );
- $D_{sw}$  is the effective diffusivity for HTO in the soil water ( $\text{m}^2/\text{s}$ );
- $e_r$  is the root uptake rate of HTO ( $\text{Bq m}^{-3} \text{s}^{-1}$ );
- $e_{oxi}$  is the HTO production in the soil due to oxidation of HT, which is applied if HT exists ( $\text{Bq m}^{-3} \text{s}^{-1}$ ).

In these soil HTO calculations, variables related to the soil water transport (e.g.  $\eta_{sw}$ ,  $D_{sa}$ ,  $E_w$ ,  $D_{sw}$ ) are calculated by the soil water model of SOLVEG-II, and soil properties (e.g.  $\eta_{sat}$ ,  $r_b$ ) are provided for each texture type of the soil [157]. Root uptake of soil HTO,  $e_r$ , at the soil depth  $z$ , is calculated using the concentration of HTO in the soil water and leaf transpiration:

$$e_r = \chi_{sw} f_r \int E_{tra}(z_c) A(z_c) dz_c \quad (55)$$

where:

- $e_r$  is the root uptake rate of HTO ( $\text{Bq m}^{-3} \text{s}^{-1}$ );
- $\chi_{sw}$  is the concentration of HTO in the soil water ( $\text{Bq/m}^3$ );
- $f_r$  is the fraction (root distribution function) of roots contained in the corresponding soil layer at the depth  $z_c$  ( $\text{m}^2/\text{m}^3$ );

$E_{tra}(z_c)$  is the transpiration per unit leaf area ( $\text{m}^3 \text{m}^{-2} \text{s}^{-1}$ ) at the aboveground height  $z_c$  in metres in the canopy;  
 $A(z_c)$  is the leaf area density in this canopy layer ( $\text{m}^2/\text{m}^3$ ) at the aboveground height  $z_c$  in metres in the canopy;  
 $z_c$  is aboveground height (m).

Variable  $E_{tra}(z_c)$  is calculated by the vegetation model of SOLVEG-II [98] and parameters  $f_r$  and  $A(z_c)$  are given as input data.

Transport of HT and oxidation of HT to HTO in the soil is calculated by:

$$\frac{\partial(\eta_{sat} - \eta_{sw})\chi_{saHT}}{\partial t} = \frac{\partial}{\partial z} D_{saHT} \frac{\partial \chi_{saHT}}{\partial z} - e_{oxi} \quad (56)$$

where:

$\eta_{sat}$  is the porosity of the soil (fractional);  
 $\eta_{sw}$  is the water content of the soil (vol/vol);  
 $\chi_{saHT}$  is the concentration of HT in the soil pore space ( $\text{Bq}/\text{m}^3$ );  
 $t$  is the time (s);  
 $z$  is the soil depth (m);  
 $D_{saHT}$  is the effective diffusivity for HT in the soil ( $\text{m}^2/\text{s}$ ) [42];  
 $e_{oxi}$  is the oxidation of HT in the soil ( $\text{Bq m}^{-3} \text{s}^{-1}$ ). This is a volume sink for HT and depends on the HT concentration in the soil pore space [42]:

$$e_{oxi} = \chi_{saHT} \rho_b \Lambda F_{st} F_{sw} f_z \quad (57)$$

where:

$\chi_{saHT}$  is the concentration of HT in the soil pore space ( $\text{Bq}/\text{m}^3$ );  
 $\rho_b$  is the dry bulk density of the soil ( $\text{kg dry mass}/\text{m}^3$ );  
 $\Lambda$  is the reference rate for the HT oxidation by a unit mass of the dry soil ( $\text{m}^3 \text{kg}^{-1} \text{s}^{-1}$ ) ( $\Lambda = 3.69 \times 10^{-5} \text{m}^3 \text{kg}^{-1} \text{s}^{-1}$  [42]);  
 $F_{st}$  is the factor representing the dependency of HT oxidation by soil microorganisms on the soil temperature [42];  
 $F_{sw}$  is the factor representing the dependency of HT oxidation by soil microorganisms on the soil water [42];  
 $f_z$  is the factor representing the dependency of soil depth [42].

The vegetation tritium model [43] can be used to calculate the activity concentration of TFWT, in leaves, by considering the budget of tritium (per unit leaf area) in the leaf cellular water:

$$\frac{\partial \eta_v \chi_v}{\partial t} = E_{stom} + E_{root} - E_{phot} + E_{res} \quad (58)$$

where:

$\eta_v$  is the amount of leaf cellular water per unit leaf area ( $\text{m}^3/\text{m}^2$ ), assumed constant at  $\eta_v = 0.154 \text{ mm}$ ;  
 $\chi_v$  is the activity concentration of TFWT in leaves ( $\text{Bq}/\text{m}^3$ );  
 $t$  is the time (s);  
 $E_{stom}$  is the flux of tritium per unit leaf area due to HTO exchange between the canopy air and the leaf cellular water via stomata ( $\text{Bq m}^{-2} \text{s}^{-1}$ );  
 $E_{root}$  is the flux of tritium per unit leaf area due to input of TFWT associated with the root uptake of HTO in the soil ( $\text{Bq m}^{-2} \text{s}^{-1}$ );

$E_{phot}$  is the flux of tritium per unit leaf area due to assimilation of TFWT to non-exchangeable OBT by photosynthesis ( $\text{Bq m}^{-2} \text{s}^{-1}$ );

$E_{res}$  is the flux of tritium per unit leaf area due to production of TFWT from decomposition of the non-exchangeable OBT by leaf respiration ( $\text{Bq m}^{-2} \text{s}^{-1}$ ).

The canopy air and leaf HTO exchange ( $E_{stom}$ ) is calculated by:

$$E_{stom} = \frac{1}{r_a + r_s} \left\{ \chi_a - q_{sat}(T_c) \frac{\rho_a}{\rho_w} \chi_v \right\} \quad (59)$$

where:

$r_a$  is the aerodynamic resistance for the leaf boundary layer transport ( $\text{s/m}$ );  
 $r_s$  is the stomata resistance ( $\text{s/m}$ );  
 $\chi_a$  is the concentration of HTO vapour in the air ( $\text{Bq/m}^3$ );  
 $q_{sat}(T_c)$  is the saturated specific humidity ( $\text{kg/kg}$ ) at the leaf temperature  $T_c$  (K);  
 $\rho_a$  is the density of the air ( $\text{kg/m}^3$ );  
 $\rho_w$  is the density of the liquid water ( $\text{kg/m}^3$ );  
 $\chi_v$  is the activity concentration of TFWT in leaves ( $\text{Bq/m}^3$ ).

$r_a$ ,  $r_s$  and  $T_c$  are the variables calculated by the radiation and vegetation model of SOLVEG-II [69, 98, 188].

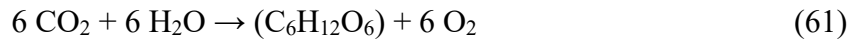
Input of TFWT by root uptake of soil water ( $E_{root}$ ) is calculated by integrating absorption of HTO by the roots over the layered soil profile:

$$E_{root} = \int f_{sc}(z_s, z) e_r(z_s) dz_s \quad (60)$$

where:

$E_{root}$  is the flux of tritium per unit leaf area due to input of TFWT associated with the root uptake of HTO in the soil ( $\text{Bq m}^{-2} \text{s}^{-1}$ );  
 $f_{sc}(z_s, z)$  represents the fraction of the absorbed HTO that is transported to the leaves at the aboveground height  $z$  in metres;  
 $e_r(z_s)$  is the root uptake rate of HTO ( $\text{Bq m}^{-3} \text{s}^{-1}$ ) at soil depth  $z_s$  in metres (see Eq. (55) above);  
 $z$  is the aboveground height  $z$  (m).

For the assimilation of non-exchangeable OBT by photosynthesis, it is assumed that 1 mol of  $\text{CO}_2$  reacts with 1 mol of free water in leaves during the photosynthesis [43]:



where  $\text{C}_6\text{H}_{12}\text{O}_6$  represents the synthesized organic matter. Therefore, the assimilation of non-exchangeable OBT by photosynthesis is calculated by:

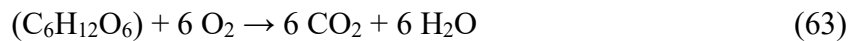
$$E_{phot} = A_{phot} f_p \frac{m_w}{\rho_w} \chi_v \quad (62)$$

where:

$E_{phot}$  is the flux of tritium per unit leaf area due to assimilation of TFWT to non-exchangeable OBT by photosynthesis ( $\text{Bq m}^{-2} \text{s}^{-1}$ );

- $A_{phot}$  is the photosynthesis flux per unit leaf area ( $\text{mol-CO}_2 \text{ m}^{-2} \text{ s}^{-1}$ ) calculated by the vegetation model of SOLVEG-II [98];
- $f_p$  is the isotopic fractionation factor for the HTO assimilation during the photosynthesis reaction ( $f_p = 0.78$ ; [9, 74]);
- $m_w$  is molar mass of water, i.e., the mass of 1 mole of  $\text{H}_2\text{O}$  ( $m_w = 18 \text{ g/mol}$ ) ( $\text{kg/mol}$ ), where the number of moles of  $\text{H}_2\text{O}$  is equal to the number of moles of  $\text{CO}_2$  (see Eq.(61));
- $\rho_w$  is the density of the liquid water ( $\text{kg/m}^3$ );
- $\chi_v$  is the activity concentration of TFWT in leaves ( $\text{Bq/m}^3$ ).

Production of TFWT ( $E_{res}$ ) due to the decomposition of organic matter (or non-exchangeable OB) by leaf respiration is calculated, assuming that the production of 1 mol of  $\text{CO}_2$  through respiration causes decomposition of 1/6 mol of  $\text{C}_6\text{H}_{12}\text{O}_6$ , as:



Therefore, the flux  $E_{res}$  is calculated by:

$$E_{res} = A_{res} \frac{1}{6} m_d r_{nexc} \quad (64)$$

where:

- $E_{res}$  is the flux of tritium per unit leaf area due to production of TFWT from decomposition of the non-exchangeable OB by leaf respiration ( $\text{Bq m}^{-2} \text{ s}^{-1}$ );
- $A_{res}$  is the respiration flux per unit leaf area ( $\text{mol-CO}_2 \text{ m}^{-2} \text{ s}^{-1}$ ) calculated by the vegetation model of SOLVEG-II [98];
- $\frac{1}{6}$  is the ratio of moles of  $\text{C}_6\text{H}_{12}\text{O}_6$ -to-moles of  $\text{CO}_2$  produced, where 1 mole of  $\text{C}_6\text{H}_{12}\text{O}_6$  results in the production of 6 moles of  $\text{CO}_2$ ;
- $m_d$  is the weight of 1 mol of  $\text{C}_6\text{H}_{12}\text{O}_6$  ( $m_d = 180 \text{ g/mol}$ ) ( $\text{kg/mol}$ );
- $r_{nexc}$  is the concentration of non-exchangeable OB in the dry matter in leaves ( $\text{Bq/kg dry mass}$ ), which is calculated by integrating the net accumulation of OB (i.e.  $E_{phot} - E_{res}$ ) and organic matter in leaves [43, 194].

#### I.4. CERES

##### I.4.1. Overall features of CERES

CERES<sup>®</sup> CBRN-E is an operational computational tool for use in atmospheric dispersion modelling and impact assessment of hazardous materials. The tool is comprised of several source term models, a variety of dispersion approaches (ranging from a Gaussian puff model to advanced four dimensional flow and dispersion computations), as well as modules to evaluate health consequence with adaptation to R-N, C or B noxious agents. CERES<sup>®</sup> CBRN-E can be used to compute atmospheric dispersion in complex environments, such as with buildings (urban areas or industrial sites), to assess the health consequences of toxic releases on a population and on first responders, and to generate operational results for use by rescue teams and decision makers in less than 15 minutes (e.g. in intervention zones or danger zones) in less than 15 minutes to. The CERES<sup>®</sup> CBRN-E Gaussian puff model is also dedicated to tritium dispersion. It takes into account processes such as deposition, re-emission, conversion of HT into HTO and conversion of HTO into OB.

The environmental compartments considered are air, soil, plants and animals. The biospheric model also covers the transfers in the food chain and exposure pathways, including direct transfer to vegetation and then to animals and animal products; dry and wet deposition to soil and then migration from soil to plants and from plants to animals and animal products.

CERES® CBRN-E can handle releases of either HT or HTO and can be used to estimate formation of OBT in plants. Final model outputs include ingestion and inhalation (including skin absorption) doses to humans, and intermediate outputs include concentrations of tritium in various environmental compartments.

## **I.4.2. Key equations or considerations**

### *I.4.2.1. Atmospheric dispersion*

Air activities are calculated using the Gaussian puff model with horizontal and vertical dispersion parameters given in Refs [195, 196]. The standard deviation depends on the atmospheric stability and the transfer duration between the source and each observation point. Key assumptions are as follows:

- The wind direction may vary with time;
- For HTO with fine weather (without rain), plume depletion due to deposition of HTO to the underlying surface is not modelled as HTO re-emitted by the soil compensates plume depletion;
- For HTO with rain, depletion is modelled using a Chamberlain equation [197];
- For HT, the air concentration is calculated taking into account the dry vapour deposition velocity whatever the meteorological conditions (with or without rain).

### *I.4.2.2. Deposition and behaviour in soil*

Dry deposition to the soil is modelled through the use of deposition velocity values which range between  $10^{-3}$  and  $10^{-2}$  m/s (HTO) and between  $10^{-5}$  and  $10^{-3}$  m/s (HT). A key assumption is that the velocity is equal to  $3 \times 10^{-3}$  m/s for HTO and to  $3 \times 10^{-4}$  m/s for HT.

Wet deposition is modelled using the following Chamberlain equation which gives the average activity of a raindrop crossing the plume. Indeed, atmospheric tritiated water vapour is easily absorbed by raindrops. For HT, there is no wet deposition:

$$C_{rain} = \beta \chi_{vap}^{atm} \left( 1 - \exp\left(-\frac{\lambda_r h_1}{v_g}\right) \right) \exp\left(-\frac{\lambda_r h_1}{v_g}\right) \quad (65)$$

where:

- $C_{rain}$  is average specific activity of the raindrops (Bq/kg-water);
- $\beta$  is ratio of the water vapour pressure to that of HTO ( $\beta = 1.1$  [198]) (dimensionless);
- $\chi_{vap}^{atm}$  is specific activity of water vapour in air (Bq/kg-vapour);
- $\lambda_r$  is the exchange constant between atmospheric water vapour and raindrop ( $s^{-1}$ );
- $h_1$  is the path length of the rain drops in the tritiated plume (charge zone) (m);
- $v_g$  is the rain drop velocity, depending on drop radius (m/s).



From the specific activity of a raindrop, HTO deposition to the soil is calculated using the rain intensity and the rain duration. Thus, deposition velocity depends on soil deposition and integrated air concentration. The specific activity of the raindrops calculated by the Chamberlain equation (see Eq. (65)) depends on: raindrop characteristics (radius, velocity, etc.) and path length of the raindrops in the plume which leads to the further concentration of tritiated water in the raindrops.

For the behaviour of tritium in soil, the key assumptions of the model are:

- Dry and wet deposition lead to tritium activity in the soil layer that contains the plant roots. A part of the tritium in the soil evaporates to the atmosphere and a part is absorbed by the roots. The tritium specific activity of soil is calculated through the integration of dry and wet deposition between the beginning and the end of the plume crossing. The HTO deposition on the soil is determined by multiplying the deposition velocity by the air concentration;
- HT dry velocity is taken at  $3 \times 10^{-4}$  m/s, then HT is converted to HTO by soil microorganisms;
- In fine weather, half of HTO (or HTO from HT conversion) deposition is re-emitted to the atmosphere;
- In wet weather, all HTO (or HTO from HT conversion) deposition goes into the soil.

#### 1.4.2.3. Tritium transfer from air to plants

The exchange of tritium from air to plants is modelled as a diffusion process which depends on the air concentration near the leaves and the exchange velocity between the air and leaves [71]. The exchange velocity is determined by dividing the leaf area index of the plant by the stomata resistance, the latter of which is assumed to be 300 s/m during the daytime, when stomata are open and 3000 s/m during nighttime, when stomata are closed.

Two steps are considered, i.e. the incorporation step (see Eq. (66)) which leads to HTO incorporation in the leaves and the transpiration step (see Eq. (67)) which leads to HTO release from plants to the atmosphere. The CERES model is used for green vegetables, fruits, cereals and grass. The model for crops assumes uptake of tritium only from soil water with the transpiration stream:

$$\frac{dA_f}{dt} = \frac{\gamma V_c}{m} \left( C_{air} - \frac{C_{water}^{sat}}{\beta} A_f \right) \quad (66)$$

and

$$\frac{dA_f}{dt} = \frac{\gamma C_{water}^{sat}}{m\beta} A_f \quad (67)$$

where:

- $A_f$  is the specific activity of tritium in leaf water (Bq/kg-water);
- $t$  is the time (s);
- $\gamma$  is the ratio of exchange velocity HTO/H<sub>2</sub>O ( $\gamma = 0.95$ ) (dimensionless);
- $V_c$  is the exchange velocity between air and leaves (m/s);
- $m$  is water mass in leaves per soil surface unit (kg-water/m<sup>2</sup> of soil);
- $C_{air}$  is the specific activity of tritium in the water vapour near the leaves (Bq/m<sup>3</sup>);
- $C_{water}^{sat}$  is the concentration of saturated water vapour concentration (kg-water/m<sup>3</sup>);
- $\beta$  is the ratio of the water vapour pressure to that of HTO ( $\beta = 1.1$  [198]) (dimensionless).

#### I.4.2.4. Air concentration due to re-emission

Tritium in air activity concentrations from re-emission are not calculated. The plume depletion is not taken into account as it is considered that HTO re-emitted by the soil (and the leaves of vegetables) compensates for the plume depletion.

#### I.4.2.5. Organically bound tritium formation in plants

The OBT production model is based on a simple approach which considers that:

- All organic matter is ‘organically bound tritium’;
- Organic matter is continuously produced and depends essentially on climatic factors irrespective of the type of vegetable;
- There is a relationship between the tritium activity in the organic matter and HTO activity in the free water of plants. The model predicts an average tritium incorporation rate in organic matter taking into account the plant yield at the harvest, the dry matter rate and the time of growth, as follows:

$$\tau_{inc} = 0.53 \frac{\tau_{ms}^{vg} Y}{86400 \Delta t_{growth}} \quad (68)$$

where:

- |                     |  |
|---------------------|--|
| $\tau_{inc}$        | is the incorporation rate of tritium in organic matter (kg-water m-soil <sup>-2</sup> s <sup>-1</sup> ); |
| 0.53                | is the weighting coefficient (kg-water/kg-dry plant);  |
| $\tau_{ms}^{vg}$    | is the plant dry matter ratio (kg-dry plant/kg-fresh plant);   |
| $Y$                 | is the plant yield at the time of harvest (kg-fresh plant/m <sup>2</sup> soil);                          |
| 86400               | is the time conversion factor (s/day);   |
| $\Delta t_{growth}$ | is the time of growth of the plant (day).  |

The dry matter produced is assumed to have a T/H ratio of 0.95. To calculate the exchangeable tritium part, the dry matter is weighted by a factor of 0.53. This factor corresponds to the T–H ratio multiplied by the molecular weight of (H<sub>2</sub>O)<sub>5</sub> (since there are 5 H<sub>2</sub>O molecules in one cellulose molecule) over the molecular weight of cellulose (C<sub>6</sub>H<sub>10</sub>O<sub>5</sub>)<sub>n</sub>, which is equivalent to 0.95 × (90/162).

## APPENDIX II. INTERCOMPARISON OF RESULTS AND DETAILED DISCUSSION

### II.1. INTRODUCTION

The following sections of this appendix present comparisons of the calculation results of the four models (CTEM-CLASS, TOCATTA- $\chi$ , SOLVEG-II and CERES) and the three scenarios (IRSN-EDF, CNL and CNSC scenarios) used during the study. In these intercomparisons, particular focus is placed on deposition of HTO from the atmosphere to leaves, assimilation of OBT in leaves, and deposition of HTO from the atmosphere to soil. The aim of the intercomparisons was to clarify the importance of the processes involved in controlling these tritium transfers in order to help suggest simple approaches to predict the behaviour of tritium in an atmosphere–plant–soil system.

Firstly, the comparison of the results of modelling the IRSN-EDF scenario are presented, where each model was run for a yearlong simulation of tritium transfer at a grassland ecosystem affected by chronic tritium releases from a nearby nuclear facility (i.e. AREVA (now Orano)-NC's La Hague reprocessing plant: see Section 3.1).

For the CNL scenario, model predictions of the short term dynamics of tritium in cultivated plots were compared with data from extensive measurements during and immediately after the passage of a plume (see Section 3.2). In these scenarios, predictions of foliar deposition of atmospheric HTO and formation of OBT were extensively analyzed, as the experimental sites were affected by the frequent arrivals of a tritium plume [152, 199]. All four models, which have different calculation schemes of foliar uptake of HTO, participated in these scenarios.

Finally, for the CNSC scenario, model predictions under different irrigation regimes (see Section 3.3) were compared, and processes important for soil to plant HTO transfer, which extensively occurred under irrigation conditions with high tritium water at the site, were discussed [156]. Two models, CTEM-CLASS and SOLVEG-II, which have different structures of the soil HTO model, participated in the CNSC scenario.

### II.2. IRSN-EDF SCENARIO

#### II.2.1. TFWT in leaves

##### II.2.1.1. Results

The calculated results of TFWT concentration in grass plant leaves in the IRSN-EDF scenario are shown in Fig. 16(a). Measurements of TFWT concentration and hourly inputs of HTO concentration in the air are also presented. Among the four model predictions, results by TOCATTA- $\chi$ , CERES and SOLVEG-II revealed dynamic variations for the TFWT concentration in leaves. During the daytime, rapid variations of TFWT concentrations were calculated, with TFWT quickly responding to the changes in the HTO concentration in the air, e.g. the daytime results on 1 and 2 August 2013 shown in Fig. 17. During the nighttime, slow evolutions of TFWT concentrations against arrivals of the plume were calculated, e.g. increases in the calculated TFWT concentrations around 00:00 on 3 August 2013. These predictions of TFWT concentrations by TOCATTA- $\chi$ , SOLVEG-II and CERES agreed well with the measurements throughout the simulation period.

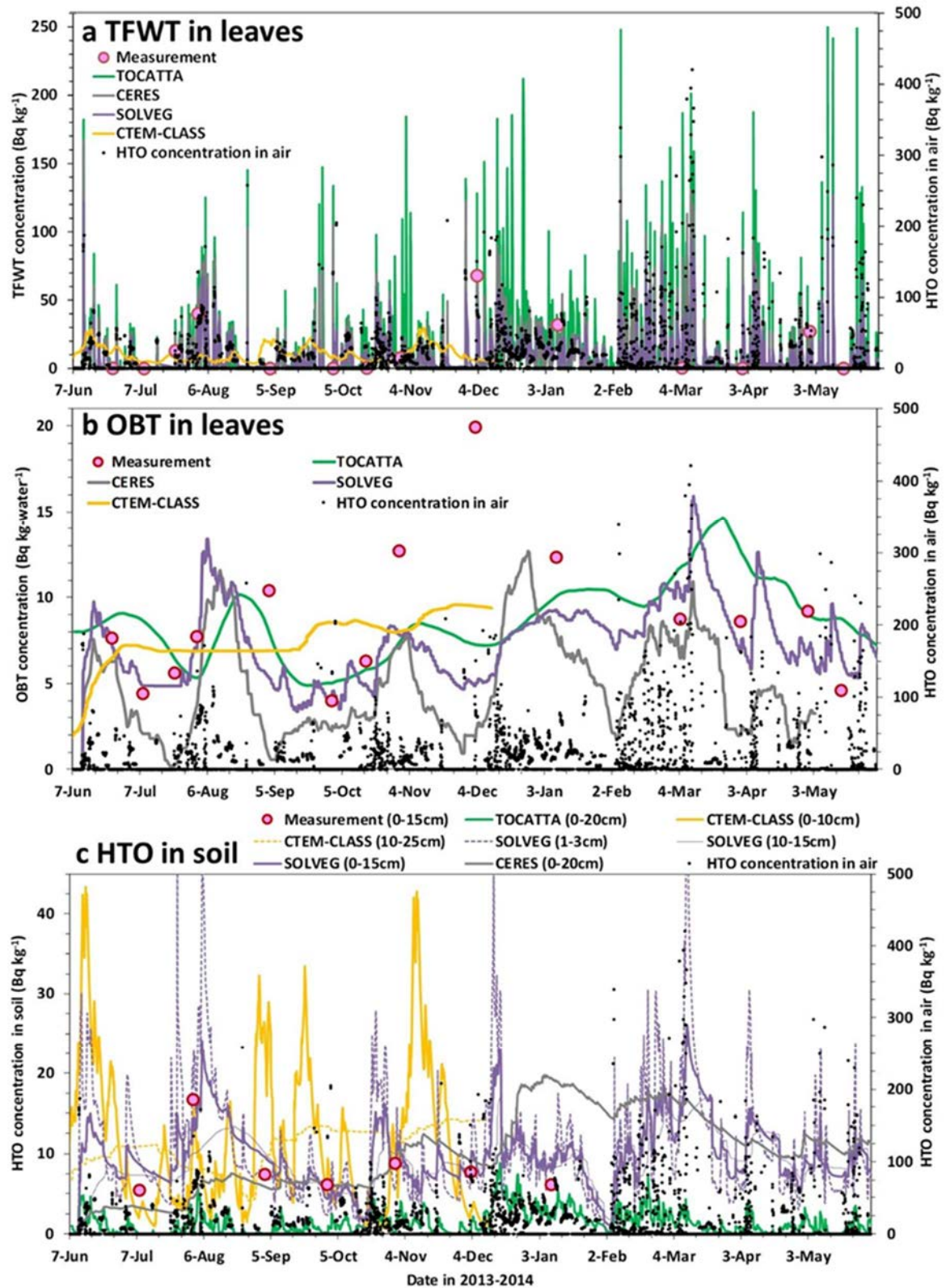


FIG. 16. Hourly input of HTO concentration in the air and predicted and measured TFWT (a) and OBT concentrations (b) in grass plant's leaves and HTO concentrations in soil (c) for the IRSN-EDF scenario. Values in the parentheses in the legend in (c) represent the depths of the soil used in each model for comparison with the measurement.

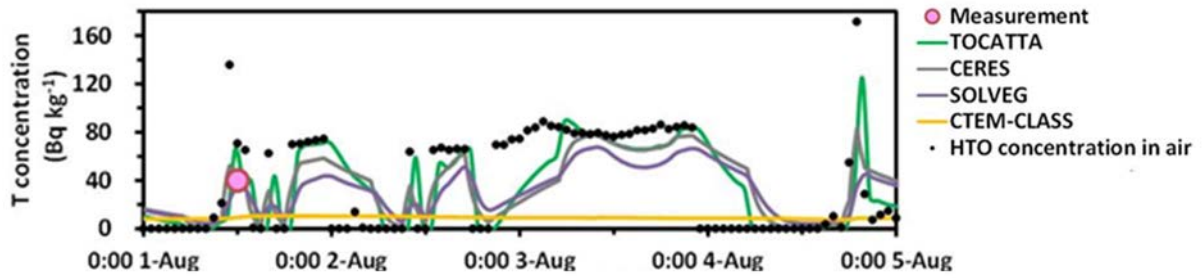


FIG. 17. Hourly input of HTO concentration in the air and measured and predicted and measured TFWT for a 5-day interval.

In contrast, predictions by CTEM-CLASS revealed moderate variabilities of the TFWT concentration, less affected by the changes in the HTO concentration in the air. Increases of TFWT concentration during arrivals of the plume in daytime hours were small, for example, the results during the daytime on 1 and 2 August 2013 shown in Fig. 17. Furthermore, TFWT concentrations calculated by the CTEM-CLASS model stayed elevated even under the absence of the plume, e.g. at the end of November (Fig. 16(a)).

#### II.2.1.2. Discussion

The TFWT concentrations in grass plant leaves after the arrival of the plume differed between the predictions made using the four models (Fig. 16(a)). For calculations of air–leaf HTO exchange, all four models rely on a similar approach, i.e. a net exchange approach that uses exchange velocity and difference in the HTO concentrations between the air and leaves (see Section 4.2). However, the derivation of the exchange velocity differs between models. Therefore, the differences, or similarities, in the predicted TFWT concentrations are mainly attributable to the model calculations of the exchange velocity.

In these models, exchange velocity extensively depends on the stomatal resistance (see Sections I.1.1, I.2.1 and I.3.1). With this in mind, the comparison of predictions by TOCATTA- $\chi$ , SOLVEG-II and CTEM-CLASS indicates that precise calculations of stomatal conductance (or resistance) are primarily important for accurate predictions of TFWT concentration in leaves. In TOCATTA- $\chi$  and SOLVEG-II the stomatal resistance is time dependent and calculated from a relationship between the stomatal resistance and photosynthesis calculated by Farquhar's model. The similarity in the calculation of stomatal resistance likely led to similar predictions of TFWT concentrations by these two models (Fig. 16(a)). In CTEM-CLASS, stomatal resistance (and thus the exchange velocity) is dynamically calculated by using the relationship between the stomata resistance and photosynthesis (Section I.1.1). However, TFWT concentration calculated by this model showed much less variability and frequently appeared nearly constant (Fig. 16(a)). In the CTEM-CLASS calculation, the predicted exchange velocity is truncated by a user specified threshold value so that uptake of the atmospheric HTO by leaves does not exceed 8% per hour of the atmospheric HTO (Section I.1.1). This kept the exchange velocity small in the CTEM-CLASS' calculation, which made TFWT concentrations less affected by the changes in the atmospheric HTO concentration. These different responses in the predicted TFWT concentrations indicate that precise calculations of stomatal resistance are primarily important for calculating responses of TFWT in leaves against arrivals of HTO plumes.

An interesting result from the intercomparison shown in Fig. 16(a) is the accurate performance of the relatively simple CERES model. For the air–leaf HTO exchange, CERES simply assumes a fixed exchange velocity which fully relies on a specified stomatal resistance of 300 s/m during the day and a cuticle resistance of 3000 s/m during the night (Section I.4.2). Even with such a simple assumption, TFWT concentration predicted by CERES revealed dynamic variabilities similar to predictions by other complex models, such as TOCATTA- $\chi$  and SOLVEG-II, and reproduced measurements well (Fig. 16(a)). This finding will be useful for simplification of complex models as well as for development of a simple approach to calculate foliar deposition of HTO, but only after the processes involved in air–leaf exchange, which are complex, are well understood and sensitivity and uncertainty analysis for the most relevant parameters are carried out. The simplification of complex models like TOCATTA- $\chi$ , SOLVEG-II and other models in literature cannot be done considering prescribed values of stomatal resistance for day and night as default values.

Comparison of the predictions made using three complex models further demonstrates that air–leaf HTO exchange is extensively regulated by stomata (or cuticle) resistance, and aerodynamic leaf boundary layer resistance is of lesser importance. TOCATTA- $\chi$  and SOLVEG-II calculate resistance of the air–leaf HTO exchange as a sum of the time dependent stomatal resistance and aerodynamic leaf boundary layer (laminar flow) resistance. The simplest model, CERES, only considers a constant stomatal resistance to calculate the exchange velocity. Comparable predictions of TFWT concentrations by these three models (Fig. 16(a)) imply that air–leaf exchanges of HTO at the experimental plot were mostly regulated by the stomatal (or cuticle) resistance, and leaf boundary layer transport was not the rate limiting process (it can, therefore, be disregarded).

Another important finding from this intercomparison is that the TFWT concentration calculated by CTEM-CLASS remained elevated even under the long absence of the tritium plume (Fig. 16(a)). As mentioned previously, CTEM-CLASS used truncated small exchange velocities to calculate atmosphere–leaf HTO exchange and this exchange velocity was also applied to HTO exchange at the atmosphere–soil interface (Section I.1.1). Consequently, concentrations of TFWT calculated by the CTEM-CLASS model for close to local background conditions were consistent with the concentration of HTO in the soil (shown in Fig. 16(a) and 16(c) and discussed in Section II.2.3). Predicted TFWT concentration, therefore, remained elevated even in the absence of the plume due to support from HTO previously deposited to the soil. In contrast, TFWT concentrations predicted by TOCATTA- $\chi$ , SOLVEG-II and CERES decreased to nearly zero when the plume was not present at the experimental site (Fig. 16(a)). This is because the exchange velocity at the air–leaf interface was larger than that at the air–soil interface in the calculations of these models and therefore TFWT concentration followed HTO concentration in the atmosphere rather than the HTO concentration in the soil. These results indicate that accurate predictions of exchange velocities for both air–leaf and air–soil interfaces are necessary to calculate the TFWT concentration in leaves.

## **II.2.2. OBT in leaves**

### *II.2.2.1. Results*

Concentrations of OBT (non-exchangeable OBT) in grass plants' leaves calculated by the four models are shown in Fig. 16(b). Predictions by CERES and SOLVEG-II revealed high variabilities of OBT concentration which largely increased during the arrivals of the plume at the site, e.g. the first week of August 2013. When the plume was not present at the experimental site, OBT concentrations calculated by these models showed significant decreases, e.g. the latter half of August 2013 and the latter half of March 2014. Pronounced differences in the time trends

of OBT concentration predicted by these two models were found in July 2013; OBT concentration calculated by CERES decreased while results from SOLVEG-II remained unchanged.

TOCATTA- $\chi$  also calculated relatively large seasonal variations of OBT concentration, with increases during arrivals and decreases during long absences of the plume (Fig. 16(b)). Compared with the previously mentioned predictions by CERES and SOLVEG-II, OBT concentration calculated by the TOCATTA- $\chi$  model showed slower variations, yet the model generally followed the predictions made using CERES and SOLVEG-II with certain time lags.

In the prediction made using the CTEM-CLASS model, much more moderate variabilities of OBT concentration were calculated. Concentration of OBT calculated by the CTEM-CLASS model showed continuous increases in most of the simulation period, with no pronounced decreases even under the long absences of the plume, e.g. the latter half of August 2013.

#### *II.2.2.2. Discussion*

Clear differences were observed among the long term (i.e. season to season) predictions of OBT concentration by the four models. These different time trends of model calculated OBT concentrations provide important insights to the processes controlling the assimilation of OBT in the vegetation affected by frequent arrivals of the HTO plume. Comparison of results obtained from CTEM-CLASS, TOCATTA- $\chi$  and SOLVEG-II's calculations suggest that precise prediction of TFWT concentration, rather than photosynthesis, is crucial to calculate the OBT assimilation. These models use the same Farquhar photosynthesis model to calculate dry matter production (thus, assimilation of OBT from TFWT) (see Section 4.2). Given that the calculations of the dry matter production by these three models were similar, differences in the predicted OBT concentrations are expected to have arisen from variabilities in the predicted TFWT concentrations. In the simulation by the CTEM-CLASS model, TFWT concentration remained elevated throughout the simulation period (Fig. 16(a)). Therefore, the OBT concentration predicted by this model showed continuous increases, approaching the TFWT concentration (Fig 16(b)). In contrast, TFWT concentrations predicted by TOCATTA- $\chi$  and SOLVEG-II changed more dynamically (Fig. 16(a)), which caused high variabilities of the OBT concentrations throughout the entire simulation period (Fig. 16(b)). This intercomparison indicates that variability of the OBT concentration in leaves was mainly caused by those in the TFWT concentration rather than dry matter production, and therefore accurate predictions of the TFWT concentration is primarily important to calculate the OBT concentration in leaves. This conclusion can also be deduced from the results obtained by the calculation with CERES (Fig. 16(b)). CERES simply assumes a constant dry matter production rate during each sectioned interval of plant growth (Section 4.2). Therefore, variations in the predicted OBT concentration by CERES came from those in the predicted TFWT concentration, not from variations in the dry matter production rate. Similarity between the predictions of OBT concentrations by CERES, SOLVEG-II and TOCATTA- $\chi$  again indicate that the variability of the OBT concentration was mostly caused by those in the TFWT concentration.

Similar predictions of OBT concentrations by simple and complex models further demonstrate that short term (i.e. diurnal scale) variations of photosynthesis are less important in the long term (i.e. over seasons) accumulation of OBT in leaves. CERES and SOLVEG-II use different approaches to calculate the dry matter production (thus the assimilation of TFWT to OBT). SOLVEG-II dynamically calculates the dry matter production at every time step by using a sophisticated Farquhar photosynthesis model, whereas CERES just assumes an averaged dry matter production rate during each interval of plant growth (Section 4.2). Similar predictions of the long term trends of OBT concentrations made using the two models (Fig. 16(b)) imply



that simple averaging of photosynthesis during the growth interval is applicable to calculate long term OBT accumulation, given that TFWT concentrations in leaves were well predicted — this condition was achieved in calculations of CERES and SOLVEG-II by similar predictions of TFWT concentration by two models (Fig. 16(a)).

In contrast, an intercomparison of the predictions by CERES and SOLVEG-II indicates that a dynamic prediction of the dry matter production is certainly needed to calculate the assimilation of OBT during periods where large variabilities in photosynthesis are expected. At the experimental site, there were few rain events during a one-month period, i.e. from 28 June to 25 July 2013 (referred from the input meteorological data). This caused drying of the surface soil; observation of the soil water content in the top 15 cm horizon decreased from 0.26 to 0.11 vol/vol in this period. In the calculation by SOLVEG-II, surface soil became dried; soil water content in the surface 1 cm horizon decreased from 0.15 to 0.03 vol/vol. Consequently, in the calculation by SOLVEG-II, grass plant leaves ceased photosynthesis in this period due to drought stress by the dried soil and neither the dry matter production nor OBT assimilation was calculated. As a result, the OBT concentration predicted by SOLVEG-II remained constant during this period, which reproduced nearly unchanged OBT concentrations measured on 7 July and 22 July 2013 (Fig. 16(b)). In contrast, for the predictions by CERES, dry matter production continued during this period because CERES assumes a constant dry matter production during each growth period. This calculation led to a dilution of OBT in the leaf dry matter pool and OBT concentrations calculated by CERES underestimated the measured values at the end of this period (22 July 2013 shown in Fig. 16(b)). These contrasting predictions demonstrate that dynamic predictions of dry matter production are necessary to calculate the assimilation of OBT under a situation where photosynthesis has large variabilities.

Similar time trends of OBT concentrations during absences of the plume that were predicted by CERES, SOLVEG-II and TOCATTA- $\chi$  imply that respiration has minor impact on the dynamics of OBT in leaves. SOLVEG-II and TOCATTA- $\chi$  consider loss of tritium from the leaf OBT pool due to decomposition of tritium containing dry matter by respiration (Section 4.2). Therefore, in calculations with these two models, OBT concentration decreases during absences of the plume due to the respirational loss and dilution by the addition of newly formed tritium free (or low tritium) dry matter to the leaf organic matter pool. On the other hand, in the calculation of CERES, the decrease in OBT concentration during the absences of the plume was caused only by the effect from the dilution because CERES does not account for the respirational loss of OBT (Section 4.2). The similar decreasing trend of OBT concentration calculated by these three models during long absences of the plume (e.g. the latter half of August 2013 and latter half of March 2014 as shown in Fig. 16(b)) suggest that respirational loss of OBT has a minor impact on the dynamics of OBT in leaves. Indeed, past experimental studies [74] and model exercises [43] have suggested minor roles for respiration in controlling OBT concentrations in leaves. Respiration is a key process that leads to carbon fixation by plants. In addition to producing biosynthetic precursors, respiration is necessary for energy production by plants and may also serve to balance cellular energy budgets, both in the light and in darkness [200] and consequently contribute to OBT formation during the day, but mostly at night. Experiments show that leaves preserve OBT, while at exposure time and afterwards, growth does not occur; only maintenance respiration occurs. Experiments with radio markers demonstrate that respiration has a fast ( $\sim 2 \text{ d}^{-1}$ ) and slow ( $\sim 0.3 \text{ d}^{-1}$ ) component, respectively [201]. The fast component uses predominantly the new assimilate, while the slow component uses mostly the old assimilate [202]. Respiration is very important for OBT formation at night, especially for those plants using more starch at night [130].



### II.2.3. HTO in soil

#### II.2.3.1. Results

Model calculations and measurement of HTO concentration in soil for the IRSN-EDF scenario are shown in Fig. 16(c). Predictions by CTEM-CLASS, SOLVEG-II and TOCATTA- $\chi$  revealed dynamic variabilities for the HTO concentration in the surface horizons affected by the arrivals and departures of the tritium plume at the experimental site. The CTEM-CLASS model calculated the most dynamic variabilities in the HTO concentration for the surface 10 cm horizon (results of ‘CTEM-CLASS (0–10 cm)’). SOLVEG-II also predicted dynamically varying HTO concentrations for the top 15 cm horizon (‘SOLVEG (0–15 cm)’). Predictions by these two models satisfactorily reproduced measurements of HTO concentration in the top 15 cm soil.

Predictions by TOCATTA- $\chi$  also showed rapid changes in the HTO concentration in the 20 cm thick soil (see Fig. 16(c) above), in which the time trend was similar to the above predictions of HTO concentrations by CTEM-CLASS and SOLVEG-II. However, the HTO concentration calculated by TOCATTA- $\chi$  remained extensively low, compared to the results from other models, and systematically underestimated the measurements. In predictions made using CERES, the HTO concentration in the top 20 cm thick soil showed moderate variations, with small increases during the arrivals of the plume and slow decreases at the post-plume phases.

Figure 16(c) also presents HTO concentrations at different horizons in the soil calculated by multilayered models (i.e. CTEM-CLASS and SOLVEG-II). In the predictions by CTEM-CLASS, HTO concentration in the second layer, 10–25 cm in depth, showed much more moderate variabilities, compared to the result at the first 10 cm horizon (see ‘CTEM-CLASS (10–25 cm)’ and ‘CTEM-CLASS (0–10 cm)’). Slower responses of HTO concentration in deeper horizons of the soil were also calculated by SOLVEG-II (see the results of ‘SOLVEG (10–15 cm)’ and ‘SOLVEG (1–3 cm)’).

#### II.2.3.2. Discussion

The four models used for the intercomparison calculated different responses of HTO concentrations in the surface horizon of the soil against the arrivals of the tritium plume. Comparison of the predictions by TOCATTA- $\chi$  and those by the other three models provides important insights into the land surface tritium dynamics subjected to tritium releases from a reprocessing plant. Soil HTO concentration calculated by the TOCATTA- $\chi$  model remained low and underestimated the observations at all measurement points (see Fig. 16(c)). Such systematic underestimations were not found in the predictions made using the other models. As for the deposition of atmospheric tritium, CTEM-CLASS, SOLVEG-II and CERES consider dry and wet depositions of HTO and dry deposition of HT, whereas TOCATTA- $\chi$  considers dry and wet depositions of HTO only (Section 4.2). Therefore, systematic underestimation of the soil HTO concentration by the TOCATTA- $\chi$  model was likely attributable to the effect of HT deposition at the experimental site. In the simulation of SOLVEG-II, gross deposition of tritium during the whole simulation period was calculated at 5.4 kBq/m<sup>2</sup>, 4.5 kBq/m<sup>2</sup> and 6.2 kBq/m<sup>2</sup> for the dry deposition of HTO, dry deposition of HT and wet deposition of HTO, respectively. Clearly, deposition of HT had a large impact on the input of tritium to the soil at the site. These results suggest that not only the dynamics of HTO, but also those of HT need to be considered when calculating the land surface tritium transfer near a fuel reprocessing plant (AREVA (now Orano)-NC’s La Hague reprocessing plant in this scenario).

Different variabilities of HTO concentration calculated at different horizons of the soil indicate that the multilayer soil model is effective when predicting the dynamics of tritium in atmosphere–soil–plant systems. In calculations of CTEM-CLASS and SOLVEG-II, HTO concentrations in the upper soil layers were extensively elevated during and immediately after the arrivals of plume (see Fig. 16(c)). After departures of the plume, HTO concentration in the upper horizons rapidly decreased and became smaller than those in the deeper horizons. These calculations indicate that deposition and re-emission of atmospheric tritium (HTO and HT) extensively occurred within the surface horizon of the soil and HTO was supplied from the deeper horizon of the soil when the plume was absent for long periods of time. This result suggests that the multilayered model that can simulate such vertical transport of HTO in the soil profile is needed in order to effectively calculate both short and long term dynamics of deposited tritium in the soil (thus re-emission and root uptake of HTO).

Another implication from this intercomparison is that the thickness of the modelled soil layer is important to predict dynamics of the deposited tritium. For example, TOCATTA- $\chi$  and CERES uses a 20 cm thick soil layer and deposited HTO is lost from this layer due to downward infiltration of water (Section 4.2). On the other hand, predictions by SOLVEG-II demonstrated that most of the deposited HTO did not infiltrate the soil below the depth of 10 cm during and shortly after the arrivals of the plume (i.e. increases in the HTO concentration in the 10–15 cm horizon were quite small during and soon after plume arrivals (see ‘SOLVEG (10–15 cm)’ in Fig. 16(c)). This result suggests that the use of a thick soil layer (or layers) exceeding the depth scale of tritium deposition may result in inaccurate predictions of HTO concentration in the soil and therefore HTO re-emission to the air. Overall, the predictions suggest that the multilayer soil model with an adequate grid size is needed to precisely predict concentrations of HTO in the soil and thus soil–plant HTO transfer in vegetated ecosystems.

## II.3. CNL SCENARIO

### II.3.1. TFWT in leaves

Numerous plant compartments were measured during CNL experiments and it appears convenient to have them aggregated, based on the following assumptions:

- **Assumption 1:** The tritium contents of the aboveground parts of the plant can be represented by tritium in the leaves, i.e. leaf TFWT (or leaf HTO) and leaf OBT are offered for comparison with model predictions;
- As per **Assumption 1** TFWT in the fruit compartment was not presented separately and a composite of leaf, stem and fruit HTO was offered to modellers;
- **Assumption 2:** Generic values apply for LAI timeline, rooting depth, dry matter partition, partition to tuber, partition to fruits, initiation of tuber and fruits, initial amount of dry matter, soil stratification and other parameters not specified in the CNL scenario.

#### II.3.1.1. Results

Modelled and measured TFWT concentrations in the leaves of tomato and potato plants in the CNL scenario are shown in Fig. 18(a), together with the input data of HTO concentration in the atmosphere. Predictions by all four models revealed a reasonable time trend of TFWT concentration affected by the HTO plume arrival at the site. Of the four model predictions, CERES and SOLVEG-II showed high variabilities in the TFWT concentration, with rapid increases during the plume arrivals and decreases during the post-plume phases. Conversely, predictions by TOCATTA- $\chi$  and CTEM-CLASS revealed moderate variabilities and remained relatively high in the absences of the plume.

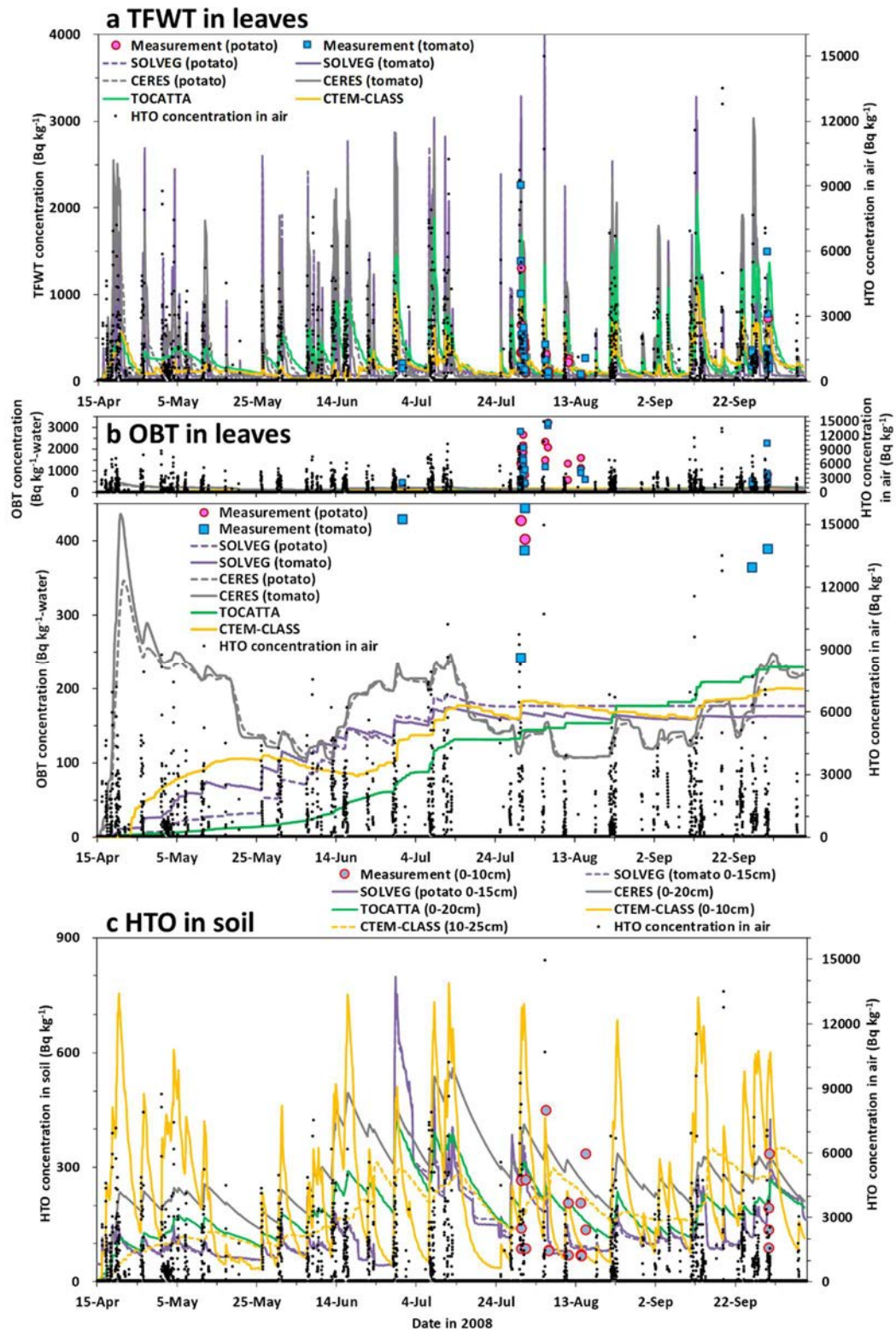


FIG. 18. Half hourly inputs of HTO concentration in the air and measured and calculated concentrations of TFWT (a) and OBT (b) in leaves, and concentrations of HTO in soil (c) for the CNL scenario.

Note: In Fig. 18, the graphs in (b) have different scales for 'OBT concentration' (left axis). Values in the parentheses in the legend in (c) represent the depths of the soil.

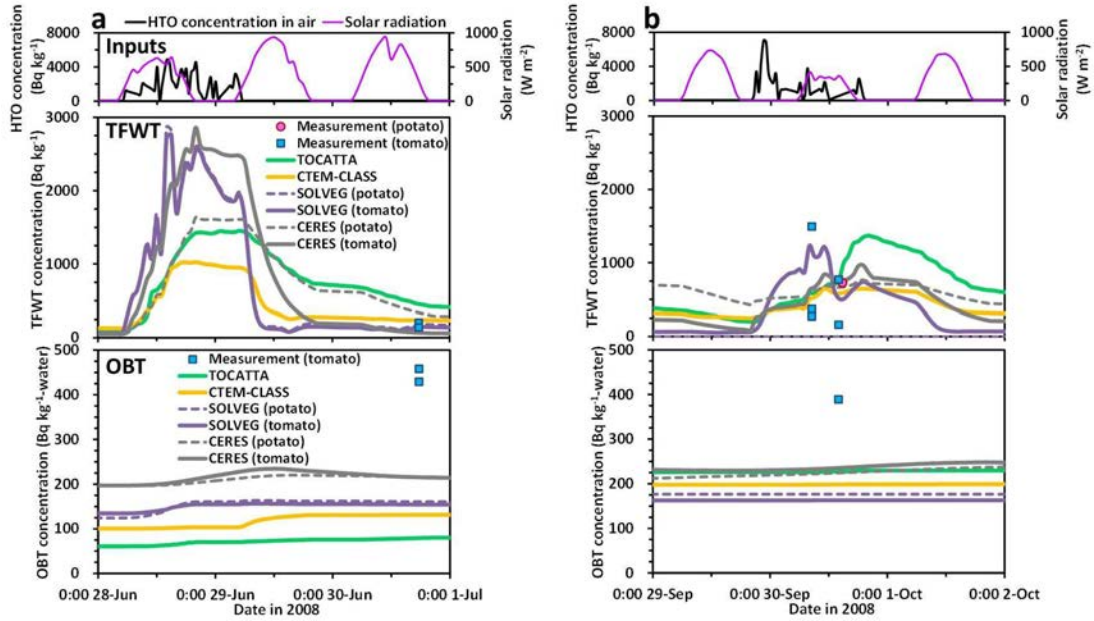


FIG. 19. Inputs of solar radiation and HTO concentration in the air (small graphs at the top) and results of TFWT (middle graphs) and OBT concentrations (bottom graphs) in leaves during the two selected three-day periods of the CNL scenario.

Dynamics of TFWT concentrations during and immediately after passages of the plume are compared in Fig. 19 for the selected periods where the input data of HTO concentration in the air were reliable with low uncertainties (see Section 5). Moreover, Fig. 19 also illustrates inputs of solar radiation. During the daytime, rapid responses in the TFWT concentrations against the arrivals of the tritium plume were calculated by all four models. For example, during 28 June 2008 (Fig. 19(a)), the HTO concentration in the air was often elevated and the model predicted TFWT concentrations rapidly increased. When the plume disappeared during the subsequent morning (~06:00 on 29 June 2008), TFWT concentrations decreased accordingly, which reproduced the low TFWT concentrations measured on the following day (17:30 on 30 June 2008 in Fig. 19(a)).

During the nighttime, the model predictions revealed slower responses of TFWT concentrations against the changes in the HTO concentration in the air. For example, the plume arrived at approximately 21:00 on 29 September 2008 (Fig. 19(b)) and the model calculated TFWT concentrations increased moderately. Interesting results were found for the arrival and the departure of the plume during the dusk period. On 30 September 2008 (Fig. 19(b)), the plume arrived during the daytime and then disappeared by 19:00. Thereafter, the predicted TFWT concentrations remained elevated until the next morning (i.e. morning of 1 October 2008), nevertheless HTO concentration in the air remained at the background (low) level during the night.

### II.3.1.2. Discussion

The models gave reasonable predictions of the TFWT concentration in leaves against arrivals of the HTO plume at the site. During the daytime, the results of all four models showed high variabilities for TFWT concentration (Fig. 19(a)) which rapidly followed the changes in the

HTO concentration in the air. In contrast, during the nighttime, slow responses of TFWT concentrations against arrivals of the plume were calculated (Fig. 19(b)). These variabilities in the simulated TFWT concentrations indicate that the four models used for the intercomparison adequately calculated the air–leaf exchanges of HTO, which are largely controlled by the opening and closing of stomata during the day and night, respectively.

The evolutions of TFWT concentrations during nighttime hours in the four model predictions suggest that cuticle resistance is more important than aerodynamic leaf boundary layer resistance for air–leaf HTO exchanges at night. During the nighttime, similar slow responses of TFWT concentrations against changes in the atmospheric HTO concentration were calculated by all four models (Fig. 19(b)). In the calculation of air–leaf HTO exchanges at night, CTEM-CLASS and CERES use an exchange velocity which fully relies on a constant cuticle resistance. TOCATTA- $\chi$  and SOLVEG-II consider cuticle resistance plus aerodynamic leaf boundary layer resistance (see Section 4.2). Generally, wind is calm at night and therefore resistance is increased for transport of trace gases in the atmosphere and the laminar layer surrounding leaf surfaces [203, 204]. However, well agreed slow responses of TFWT concentrations in the predictions made using the four models indicate that the leaf boundary layer transport was not the rate limiting process for the air–leaf HTO exchange, even at nighttime for the site. In other words, large cuticle resistance regulated the air–leaf HTO exchanges during nighttime hours.

Another important finding from this intercomparison is that TFWT concentration remained elevated during the night once the leaves were subjected to the plume during the dusk period. Predictions by the four models showed that after the arrival of the HTO plume at dusk, TFWT concentrations in the leaves remained elevated throughout the following night. Nevertheless, HTO concentration in the air was at the background level (Fig. 19(b)). This retention of TFWT in the leaves throughout the night was maintained by the regulated release of the deposited HTO (TFWT) from the leaves due to the closure of the stomata (i.e. by large cuticle resistances). This retention of TFWT in leaves throughout the night is important to recognize, considering that non-exchangeable OBT can be formed even at night through metabolic processes that are independent of light (see Section II.3.2 for a detailed discussion on this process), although this process is currently not included in the models used for the intercomparison. These predictions of the nighttime dynamics of TFWT imply that models are needed to accurately calculate (or parameterize) not only the daytime stomatal resistance but also the nighttime cuticle resistance.

The predictions of TFWT (HTO) are not only close to the observations, but the predictions made using the different models are also quite similar. This indicates the validity of Assumption 1.

### II.3.2. OBT in leaves

The following assumptions were made to justify the use of total OBT:

- **Assumption 3:** The contribution of E-OBT to total OBT activity concentration is negligible;
- **Assumption 4:** The total OBT can be approximated by the net photosynthate produced during the course of the day and by the corresponding activity concentration of NE-OBT;
- **Assumption 5:** Due to rapid exchange of tritium between the E-OBT and TFWT, the E-OBT concentration can be modelled (if need be) as a dependent variable equal to a certain fraction of TFWT concentration.

The validity of these assumptions is assessed through the comparison of model predictions with observations. Total OBT was measured in dried, but not rinsed plant samples.

### *II.3.2.1. Results*

Model predictions of NE-OBT concentration in leaves for the CNL scenario are compared in Fig. 18(b) above. Predictions by CTEM-CLASS and SOLVEG-II showed similar seasonal trends of OBT concentration, with relatively large variations during the first half of the simulation period (until middle July 2008) and low variabilities in the subsequent period. In the TOCATTA- $\chi$  calculation, OBT concentration continued to increase over the entire period. CERES predicted high variability of OBT concentration during the whole simulation period, with the maximum value in April 2008.

These predictions of NE-OBT concentration made using the four models systematically underestimated the measurement of the total (exchangeable and non-exchangeable) OBT concentration in the leaves (see upper, small graph in Fig. 18(b)). Lower panels in Fig. 19 also show the results of OBT concentrations during and immediately after passages of the plume where the inputs of HTO concentrations in the air were reliable (Section 5). Predictions made using the four models underestimated the total OBT concentration measured during the arrival of the plume: see results on 30 September 2008 in Fig. 19(b). Even under the absence of the plume, model predictions of NE-OBT concentration underestimated measurements: see results on 30 June 2008 in Fig. 19(a).

### *II.3.2.2. Discussion*

In the CNL scenario, predictions of NE-OBT concentrations made using the four models systematically underestimated the total OBT concentration observed during the passage of the plume (Fig. 19(b)) and a few hours after the plume passage, i.e., in the absence of the plume (Fig. 19(a)). As for the underestimation in the predicted OBT concentrations during the passage of the plume, the effects from E-OBT contained in the leaves can be considered. In plant tissues, hydrogen atoms contained in the exchangeable portions of the organic matter quickly exchange with the hydrogen (thus tritium) atoms in the surrounding free water [9, 180]. Therefore, the total OBT measured during and shortly after the passage of a plume in this dataset probably contained a significant amount of E-OBT in the leaves, which came from the temporally elevated TFWT concentrations (e.g. see middle graph in Fig. 19(b)). None of the participating models include an exchangeable OBT pool (Section 4.2) and therefore likely failed to reproduce such elevated amounts of exchangeable (and hence the total) OBT in leaves.

Another possible reason for the model underestimations of OBT concentration, particularly during absences of the plume, is the formation of NE-OBT by metabolic processes other than photosynthesis. In plant leaves, NE-OBT can be formed not only by photosynthesis, but also by other metabolic processes such as hydrolysis of organic compounds [99]; see Section 2.5. This process is independent of light and therefore occurs during the day and night [78, 128]. The models do not consider the formation of OBT by the hydrolysis of organic compounds (Section 4.2). Overall, comparison of the observations and the model predictions suggest that modelling of OBT assimilation by processes other than photosynthesis and exchange of TFWT and OBT will be important to calculate dynamic behaviour of total OBT in leaves during and immediately after passages of an HTO plume. To clarify whether a longer retention of elevated levels of E-OBT is at all possible (i.e. whether the observations in the CNL scenario shown in Fig. 19 are affected by an overlooked source (i.e. are not an artifact of incomplete measurements)), an independent and better instrumented field study is warranted.

Despite the uncertainties, comparing model predictions of OBT concentration can be beneficial for a better understanding and modelling of land surface tritium dynamics. Differences in the seasonal trends of OBT concentration predicted by SOLVEG-II and CERES suggest that plant growth affects the long term consequence of OBT accumulation. Predictions made using SOLVEG-II revealed relatively large variation of OBT concentration for the first half of the simulation period, and variability in the OBT concentration became smaller in the latter half of the simulation period (Fig. 18(b)). These seasonal variations in the OBT concentration were attributable to the assumed decrease in the leaf area index and leaf colour change (death of leaves) from green to yellow in the SOLVEG-II calculation (Section 4.2). In contrast, OBT concentration calculated by the CERES model showed dynamic variability throughout the entire simulation period (Fig. 18(b)). This was attributable to the setting of the plant growth (the dry matter production) in CERES, which assumed the same dry matter production rate during every sectioned growth interval, without any seasonal variation in the dry matter production rate (Section 4.2). The different seasonal evolutions of OBT concentrations between these two model predictions, therefore, indicate that the growth status of plants has an impact on the long term accumulation of OBT and needs to be adequately parameterized within models.

In general, all model predictions of NE-OBT agreed well, with differences being only ~14%. Given the extensive validation of some of the models against both controlled experiments and field data [42, 43], it is reasonable to assume that modelled NE-OBT effectively represented missing observations of actual NE-OBT, because during quasi-stationary periods between episodes of plume presence, the modelled NE-OBT and observed total OBT (exchangeable and non-exchangeable) are quite similar. Therefore, Assumptions 3 and 4 appear to be valid for these periods.

However, for 2008, when field samples were consistently collected on a short timescale during the narrow plume departure phases, observations of total OBT (i.e. non-rinsed, with E-OBT included) deviated substantially from modelled NE-OBT and presumably from actual NE-OBT (as shown in Fig. 18(b)). This finding is in striking contrast to the current view that E-OBT does not contribute much to total OBT, and it is this view that provides the justification for the simplified method of measuring OBT samples in the lab, in which rinsing is omitted. It is important, therefore, what is measured: total OBT or NE-OBT, rinsed OBT (as NE-OBT containing buried tritium). In any case, total OBT is higher than the rinsed OBT by a factor less than 2 [152, 205]. NE-OBT comprises a variable fraction of total OBT and is dependent on plant type, irrigation conditions and treatment of samples in taking OBT measurements [178].

During the plume departure, at which time frequent samples were taken in 2008, the total OBT concentration pattern (timeline) closely followed that for the TFWT (plant HTO). Given the nearly constant NE-OBT, this is only possible if E-OBT follows the plant HTO concentration very closely. On the other hand, during the quasi-stationary periods between episodes of plume presence (e.g. for samples collected in 2011 as illustrated in Fig. 19 (bottom graphs)), the total OBT converged to the NE-OBT, indicating that the E-OBT became small (i.e. close to atmospheric HTO which dropped to its background level). Based on this, an empirical algorithm for E-OBT quantification can be proposed.



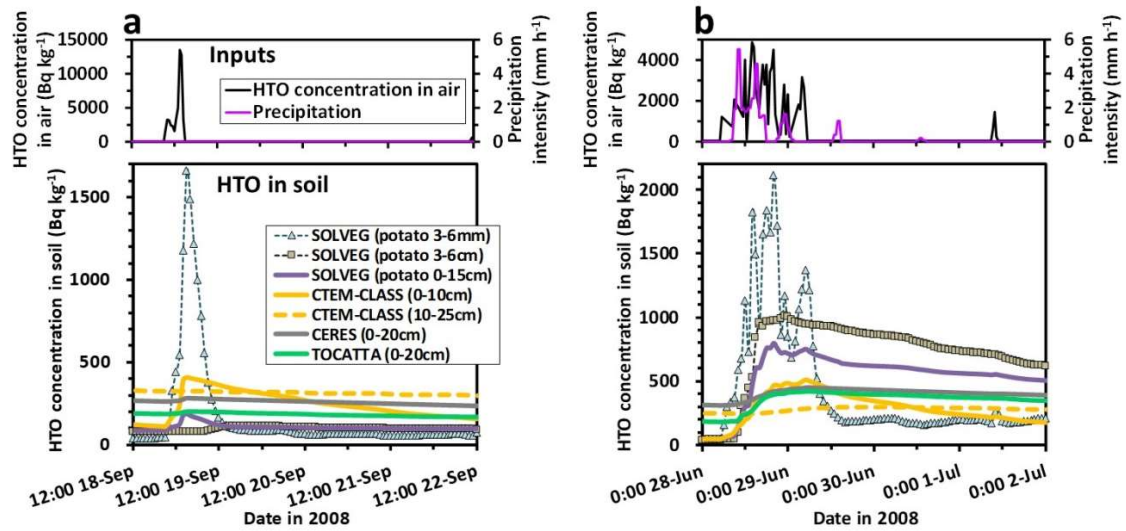


FIG. 20. Inputs of precipitation intensity and HTO concentration in the air (small upper graphs) and calculated HTO concentrations in soil (lower graphs) during selected four-day periods of the CNL scenario.

Note: In Fig 20, the values given in parentheses in the legend represent the depths of the soil layers used in the respective model.

### II.3.3. HTO in soil

#### II.3.3.1. Results

The calculated results of HTO concentrations in the soil for the CNL scenario are shown in Fig. 18(c). Among the four model predictions, results by CTEM-CLASS revealed the most dynamic variabilities for the HTO concentration in the surface horizon (top 10 cm of soil), affected by the arrivals of HTO plumes at the site. SOLVEG-II also calculated high variabilities of HTO concentrations for the top 15 cm surface horizon. In the predictions made using TOCATTA- $\chi$  and CERES, HTO concentration in the 20 cm thick soil varied similarly throughout the simulation period, with relatively moderate decreases at the post-plume phases.

These predictions of soil HTO concentrations made using the four models agreed with measurements in the 10 cm surface horizon, falling within the same order of magnitude, although it is important to note that most of the measurements were conducted during the periods when uncertainties can be expected in inputs of HTO concentration in the air (see Section 5.3.3).

Predictions of soil HTO concentrations during and immediately after the plume arrivals on a fine day (i.e. with no rain) and a rainy day are shown in Figs 20(a) and 20(b), respectively. Maximum predicted values in peaks are not shown as peaks are invariably narrow and never directly correspond to observations. In these figures, inputs of HTO concentration in the air and precipitation intensity are also shown. After the deposition of HTO during fine weather (i.e. 18–19 September 2008 in Fig. 20(a)), the soil HTO concentrations calculated by SOLVEG-II (‘SOLVEG (potato 0–15 cm)’) showed a rapid decrease, while soil HTO concentration predicted by CTEM-CLASS showed a slower decrease (‘CTEM-CLASS (0–10 cm)’). In contrast, after the depositions of HTO during a rain event (28–29 June 2008 in Fig. 20(b)), HTO concentration in the soil predicted by SOLVEG-II decreased more moderately than predictions made using CTEM-CLASS, i.e. compare ‘SOLVEG (potato 0–15 cm)’ with ‘CTEM-CLASS (0–10 cm)’ in Fig. 20(b).



### *II.3.3.2. Discussion*

The four model predictions of soil HTO concentration for the CNL scenario (see Fig. 18(c)) revealed different responses of HTO concentrations in the surface soil against arrivals of the plume at the site. Predictions by CTEM-CLASS and SOLVEG-II that have a multilayered soil submodel, again suggest the effectiveness of a thin multilayer soil model to calculate the behaviour of HTO in the soil — a conclusion obtained from the model to model comparison for the IRSN-EDF scenario (see Section II.2.1). Results of SOLVEG-II during deposition of HTO during fine weather (Fig. 20(a)) showed that HTO concentration in the upper horizons (i.e. a depth of 3–6 mm) varied more than that in deeper horizons (i.e. depth of 3–6 cm). This result indicates that deposition of HTO occurred at the very shallow layer of the soil, mostly within the top 1 cm horizon, and most of the deposited HTO was re-emitted shortly after the departure of the plume without being transported to the deeper layers. Moreover, this also indicates that the use of a thick soil layer (or layers) that exceeds the depth scale of HTO deposition will result in inadequate predictions of HTO concentrations in the soil.

In contrast, after deposition of HTO occurred during rainfalls, the decrease in the soil HTO concentration predicted by SOLVEG-II became more moderate (Fig. 20(b)). The different time trends of HTO concentration in the post-plume phases after the HTO depositions during fine and rainy weather were caused by the different depth scales of deposition. Simulation of SOLVEG-II shown in Fig. 20(b) indicates that HTO concentration in the deeper horizons of the soil increased as rapidly as that in the surface horizon for the HTO deposition during rain (see ‘SOLVEG (3–6 mm)’ and ‘SOLVEG (3–6 cm)’). These results indicate that deposited HTO was transported deeply into the soil due to large water flux caused by infiltration of rainwater. Consequently, HTO was lost (emitted) from the soil to the atmosphere slowly in the post-plume phase, because the deeply distributed HTO needed to be transported to the surface via aqueous diffusion to be emitted to the atmosphere. These results also indicate that transport of HTO within the soil profile regulated the re-emission of HTO. Clearly, concurrent predictions of the transport of water and HTO in the soil profile are needed to accurately predict such soil water driven dynamics of soil HTO, particularly for the deposition of HTO during rain (or, wet deposition of HTO).

## **II.4. CNSC SCENARIO**

### **II.4.1. HTO in soil**

#### *II.4.1.1. Results*

The predictions of the HTO concentration in soil by CTEM-CLASS and SOLVEG-II for three different irrigation treatments of the CNSC scenario are shown in Figs 21(b)–21(d). In Figs 21(a)–21(d), measurements of HTO concentration in the soil and the inputs of HTO concentration in the air are also plotted. In the natural meadow soil with no irrigation treatment (Fig. 21(b)), CTEM-CLASS and SOLVEG-II predicted roughly similar variations of HTO concentration in the surface 10–20 cm horizon (‘CTEM-CLASS (grass, meadow, 0–10 cm)’ and ‘SOLVEG (grass, meadow, 0–20 cm)’), which showed rapid increases during the arrivals of the tritium plume (i.e. spikes in the input HTO concentration in the air) and decreases following the departures of the plume. Predicted soil HTO concentrations also revealed decreases when the soil received precipitations (e.g. rainfall on both 13 June and 10 September 2012 as shown in Fig. 21(a)). These model predictions roughly agreed with the measurements in this meadow soil (blue squares). SOLVEG-II predictions of HTO concentration in barrel soil with no irrigation treatment (‘SOLVEG (potato, barrel, 0–20 cm)’),

which are presented in Fig. 21(b)) remained lower than the result calculated for the meadow soil during the first half of the simulation period (i.e. 'SOLVEG (grass, meadow, 0–20 cm)' shown in Fig. 21(b)). This is due to the model assumption of low initial HTO concentration in the barrel soil. This trend of predicted HTO concentration in the barrel soil agreed with the measured low HTO concentrations (red circles).

Figure 21(c) shows the model predicted HTO concentrations in the barrel soils that were irrigated with low tritium tap water (i.e. HTO concentration of 5 Bq/kg; as described in Section 3.3.3.1). In this soil, predictions of HTO concentrations by CTEM-CLASS and SOLVEG-II also revealed large increases due to the arrivals of the plume. Compared with the results in the soil with no irrigation (see Fig. 21(b)), drops of the HTO concentrations during the rainfalls became smaller in the irrigated soils (e.g. results during rainfalls on 13 June and 10 September 2012). On the other hand, decreases in the soil HTO concentration during the absences of the plume became pronounced in the irrigated soil (e.g. compare 'SOLVEG (potato, barrel, 0–20 cm)' shown in Figs. 21(b) and 21(c)). As a result of these pronounced decreases, HTO concentrations predicted for the irrigated soil by the two models remained lower than those for the soil with no irrigation. The simulated trends of low HTO concentration in the irrigated soil agreed well with lower HTO concentrations measured in this soil (see Fig. 21(c)).

Figure 21(d) shows the model predictions of HTO concentrations in barrel soils irrigated with high activity concentration tritium well water (i.e. HTO concentration of 10 kBq/L; as described in Section 3.3.3.1). Concentrations of HTO calculated by CTEM-CLASS and SOLVEG-II revealed short term spikes which were caused by the modelled inputs of HTO via irrigation. As a result, predicted HTO concentrations remained elevated throughout the entire simulation period, which agreed with the observations to the same order of magnitude. Predicted HTO concentrations in this irrigated soil showed large drops when the soil received rainfall (e.g. results for 6 August and 10 September 2012). Conversely, HTO concentrations in this soil became less affected by arrivals of the plume. For example, large increases of HTO concentrations were calculated during plume arrivals on 21 July and 8 August 2012 in soils with the other two treatments (see Figs 21(b) and 21(c)), while no significant increases of the HTO concentrations were calculated on these dates in the soil irrigated with high activity concentration tritium well water (see Fig. 21(d)).

#### *II.4.1.2. Discussion*

Model predictions of HTO concentrations in soils with three different irrigation treatments provide important insights into the role of soil related processes in the tritium dynamics in atmosphere–vegetation–soil systems. Model predictions showed that responses of the soil HTO concentrations against changes in the HTO concentration in the air differed between the soils irrigated with low and high tritium water (Figs. 21(c) and 21(d)). In the soil irrigated with low tritium tap water (see Fig. 21(c)), HTO concentrations calculated by CTEM-CLASS and SOLVEG-II showed large increases during passages of the plume. These pronounced depositions of atmospheric HTO to the soil were caused by the fact that the HTO concentration in the air (plume) was much higher than that in the irrigated soil which was kept low due to the repeated additions of low tritium water.

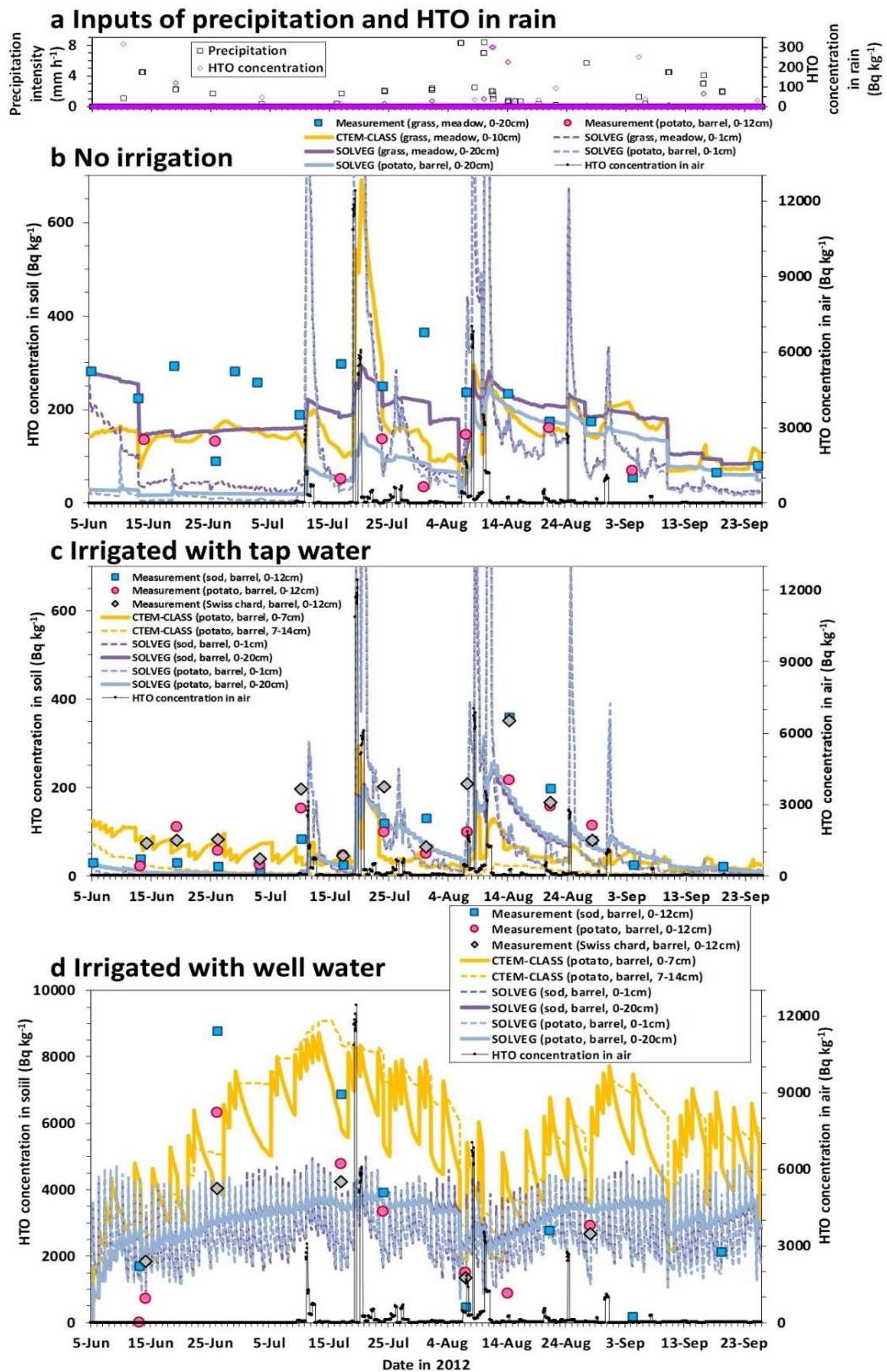


FIG. 21. Hourly inputs of precipitation intensity and HTO concentration in rain (a), and inputs of HTO concentration in the air and results of soil HTO concentrations (b-d) for the CNSC scenario.

Note: In Fig. 21, the depths in the legends represent the depths of the soil in the models and measurements.

In contrast, in the soil irrigated with high activity concentration tritium well water (Fig. 21(d)), dry deposition of HTO did not occur (or was quite small) even during passages of the plume, but HTO was emitted from the soil to the atmosphere for most of the simulation period. This continuous HTO emission from the soil was driven by the elevated HTO concentrations in this soil due to repeated additions of high activity concentration tritium water. These contrasting responses of soil HTO to the arrivals of the plume imply that irrigation with tritium containing water alters the fluxes of HTO at the atmosphere–soil interface, and therefore, need to be considered in models to predict the dynamics of tritium in such cultivated (irrigated) plots.

The difference in the simulated dynamics of HTO in soils with and without irrigation treatment (Figs. 21(b) and 21(c)), also suggests that the soil water status regulates the dynamics of deposited HTO in the soil. During absences of the plume, decreases of HTO concentrations were more pronounced in the soil irrigated with low activity concentration tritium tap water (Fig. 21(c)) than the soil with no irrigation (Fig. 21(b)). The difference can be attributable to the different water regime between the two soils. In the soil without irrigation, decreases of HTO concentration were mostly caused by the emission of deposited HTO to the atmosphere. Conversely, in the soil irrigated with the low activity concentration tritium water, HTO concentration in the surface soil was also reduced by the effect from dilution via additions of low activity concentration tritium water, which appeared in the stepwise decreases of HTO concentrations calculated by SOLVEG-II and CTEM-CLASS as shown in Fig. 21(c). These results again indicate that irrigation treatment affects the activity concentration of HTO in the soil, even for irrigation with tritium free water, and therefore, needs to be carefully be considered in predictions of tritium dynamics on cultivated plots.

Different dynamics of soil HTO predicted under irrigation conditions with low and high activity concentration tritium water also imply that wet deposition of HTO by rain will be highly important for a situation when HTO concentration in the precipitating water is higher than that in the air (plume). As discussed previously, under irrigation conditions with high activity concentration tritium well water (Fig. 21(d)), soil acted as a source of HTO by emitting the added HTO to the atmosphere. This result indicates that wet deposition of HTO is particularly important in controlling land surface tritium dynamics in a situation where HTO concentration in the precipitating water is higher than that in the air. Such a situation can certainly be expected in a real environment (e.g. sites near a high altitude HTO-releasing stack). Near a high-altitude stack which releases HTO, the concentration of HTO in the air at ground level is generally low [57, 58] because the release point is high. Meanwhile, the HTO concentration in the precipitating rainwater can be great because large amounts of HTO are contained in the air column near the releasing point and can be scavenged by the rain [57, 58]. In such a situation, soil will be a strong source of HTO, as demonstrated by the predictions presented in this report for irrigation with high activity concentration tritium water (see Fig. 21(d)), and therefore, this needs to be highlighted in predicting tritium dynamics for land surfaces.

Comparison of soil HTO concentrations predicted by CTEM-CLASS and SOLVEG-II shows the importance of each elemental process in the HTO dynamics in soil. Similarity in HTO concentrations in the soil with no irrigation (Fig. 21(b)) predicted by the two models suggests that gaseous diffusion of HTO had minor impact on the soil HTO dynamics. During arrivals of the plume almost the same increases of HTO concentration in the soil were calculated by the two models (see ‘CTEM-CLASS (grass, meadow, 0–10 cm)’ and ‘SOLVEG (grass, meadow, 0–20 cm)’ shown in Fig. 21(b)). Decreases in HTO concentration in these surface horizons during post-plume phases were also similar in the two model predictions. When calculating HTO concentration in the soil, CTEM-CLASS considers transport of HTO as tritiated water only. SOLVEG-II considers transports of tritiated water and tritiated water vapour (see Section 4.2). Similar behaviours of soil HTO concentrations predicted by these two models

indicate that gaseous diffusion of HTO was not the rate limiting process for the dry deposition and the re-emission of HTO (thus it can be neglected). This conclusion is also supported by the results in the soil irrigated with the low activity concentration tritium water (see Fig. 21(c)). CTEM-CLASS and SOLVEG-II again predicted similar variabilities in HTO activity concentration in this soil, in which resistance to the gaseous diffusion of HTO was anticipated to be larger than that in the soil with no irrigation due to the reduced air filled porosity in the irrigated wet soil.

Another important result obtained from these predictions is that responses of the soil HTO concentration to rainfalls differed between the soils with different irrigation treatments. Concentrations of HTO predicted by CTEM-CLASS and SOLVEG-II in soils with no irrigation, and soils irrigated with high activity concentration tritium well water, revealed decreases during rainfall (Figs 21(b) and 21(d)). In contrast, in the soil irrigated with low activity concentration tritium tap water, HTO concentrations were less affected by the inputs of the rain (see Fig. 21(c)). The difference was caused by the fact that the HTO concentration in the soil irrigated with low activity concentration tritium tap water remained low, being almost comparable to the HTO concentrations in the rainwater (Fig. 21(a)). Thus, the HTO concentration in this soil was neither decreased nor increased by the inputs of rainwater (thus HTO) to the soil. This result indicates that the response of soil HTO to wet deposition of HTO depends on the relative relationship between the HTO concentrations in the rainwater and the soil, which suggests that accurate calculations of soil HTO are needed in order to calculate land surface tritium dynamics affected by wet deposition of HTO (e.g. sites near the stack as described above).

## **II.4.2. TFWT in leaves**

### *II.4.2.1. Results*

Concentrations of TFWT in leaves calculated by CTEM-CLASS and SOLVEG-II for the grass plants grown in the natural meadow and potato plants cultivated in barrels with no irrigation treatments are shown in Fig. 22(a). The results of the selected 8 day period for the natural meadow are also shown in Fig. 23(a). In the natural meadow, TFWT concentrations predicted by SOLVEG-II revealed high variabilities, with large increases during arrivals of the plume and rapid decreases after departures of the plume (see ‘SOLVEG (grass, meadow)’ shown in Fig. 22(a)), satisfactorily reproduced the measured TFWT concentrations (e.g. elevated values on 7 August 2012). Meanwhile, in the predictions made using CTEM-CLASS (see ‘CTEM-CLASS (grass, meadow)’ shown in Fig. 22(a)), increases and decreases of TFWT concentration during the arrivals and departures of the plume were relatively small. When the plume was long absent, TFWT concentrations predicted by CTEM-CLASS remained elevated, compared with the result of SOLVEG-II (see Fig. 22(a)). In predictions by SOLVEG-II, daily peaks of TFWT concentrations appeared, while no such daily spikes were found in the predictions made using CTEM-CLASS (see ‘SOLVEG, TFWT, grass, meadow’ and ‘CTEM-CLASS, TFWT, grass, meadow’ shown in Fig. 23(a)).

Figure 22(b) shows the model calculated TFWT concentrations in the leaves of potato plants and sod cultivated in barrels irrigated with low activity concentration tritium tap water. In this case, TFWT concentrations predicted by the two models showed dynamic variability affected by the arrivals of the plume. Compared with the results for the no irrigation treatment (Fig. 22(a)), TFWT concentrations predicted by CTEM-CLASS and SOLVEG-II in the absences of the plume became lower under this irrigation treatment. Furthermore, in the predictions by SOLVEG-II, increases of TFWT concentrations during the plume arrivals on 11 and 19 July 2012 became more pronounced under irrigation treatments (e.g. compare ‘SOLVEG (grass, meadow)’ in Fig. 22(a) and ‘SOLVEG (sod, barrel)’ in Fig. 22(b)).

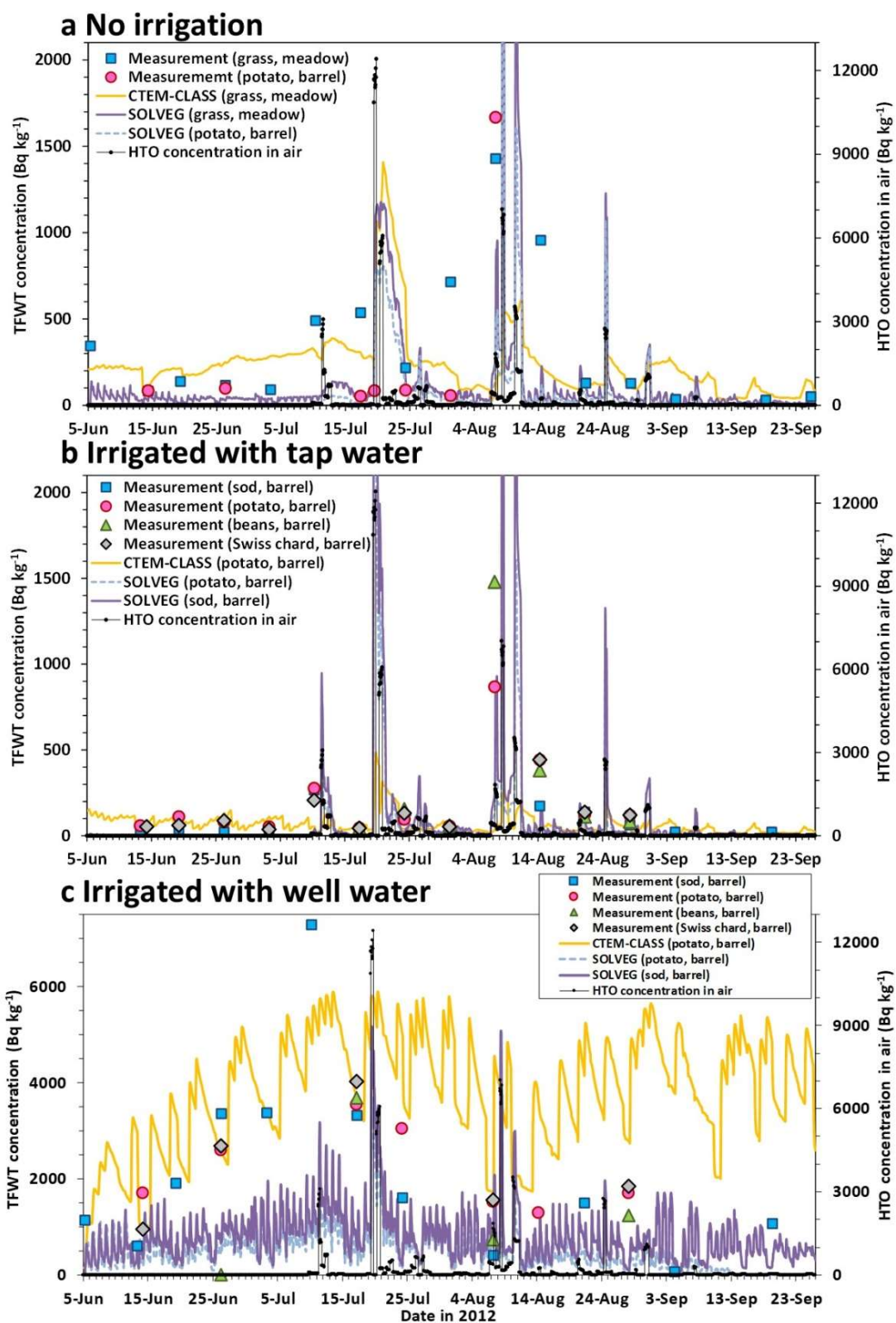


FIG. 22. Hourly inputs of HTO concentration in the air and results of TFWT concentrations in leaves for the CNSC scenario.



Under irrigation with high activity concentration tritium well water (Fig. 22(c)), TFWT concentrations predicted by CTEM-CLASS and SOLVEG-II became significantly different as compared to results from the above two treatments. Concentrations of TFWT predicted by the two models under well water treatment were an order, or more, of magnitude larger than those in the other two treatments (see Figs 22(a) and 22(b)). In particular, under this irrigation treatment, TFWT concentrations remained elevated even in the absences of the plume. Again, in the predictions made using SOLVEG-II, diurnal peaks of TFWT concentrations appeared, while no such diurnal peaks appeared in the predictions of CTEM-CLASS (see ‘SOLVEG, TFWT, potato, barrel’ and ‘CTEM-CLASS, TFWT, potato, barrel’ in Fig. 23(c)).

#### *II.4.2.2. Discussion*

Modelled concentrations of TFWT in leaves were significantly different in their magnitudes and time evolutions between the three irrigation treatments, indicating that the irrigation activities have significant impacts, not only on the soil HTO (as demonstrated in Section II.4.1), but also on TFWT levels in the standing vegetation. In the plants cultivated under irrigation with low activity concentration tritium tap water, TFWT concentrations predicted by CTEM-CLASS and SOLVEG-II showed dynamic responses to the arrivals of the plume (Figs 22(b) and 23(b)). This result indicates that input of tritium to leaves for this cultivation regime was mainly caused by the foliar deposition of atmospheric HTO. In contrast, predictions by the two models for irrigation with high activity concentration tritium well water showed that TFWT concentrations were almost independent of the HTO concentration in the air (Figs 22(c) and 23(c)) and remained elevated throughout the entire period. These TFWT concentrations are well over the atmospheric HTO level under this treatment and were caused by the transport of HTO from the contaminated soil via root uptake (see Fig. 21(d)). Clearly, irrigation treatment with water having different concentrations of HTO causes different dynamics of tritium in atmosphere–soil–plant systems.

A comparison of the model predicted dynamics of TFWT during the absences of the plume by CTEM-CLASS and SOLVEG-II demonstrates that soil–plant HTO transfer largely depends on the distribution of the deposited HTO in the soil. During absences of the plume, TFWT concentrations calculated by CTEM-CLASS were larger than those calculated by SOLVEG-II under all three treatments (see Figs 22(a)–22(c)). The difference was attributable to the different effect of root uptake of HTO in the simulations by the two models. Detailed results of soil HTO by SOLVEG-II showed that HTO concentration in the first 0–1 cm layer varied more dynamically than those averaged over the thicker 0–20 cm horizon in all three cases (Figs 21(b)–21(d)). This result indicates that deposited HTO (from the plume, rain and irrigation water) mostly occurred in the surface horizon (i.e. several centimeters) of the soil in all three cases. In the calculation of SOLVEG-II, water uptake by the roots occurred extensively in the top several 10 cm soil, with an assumed depth scale of the root distribution at 10 cm. Consequently, concentration of HTO in the water streaming from the soil to the aboveground leaves, via the root water uptake, became low due to dilution from the uptake of low HTO water in the deeper horizon of the soil. This resulted in relatively low TFWT concentrations during absences of the plume in the predictions made by SOLVEG-II (see Fig. 22). Conversely, in the calculation of CTEM-CLASS, the deposited HTO was apportioned to the thick surface layer (i.e. 10 cm in the natural meadow and 7 cm in the barrels) in which root water uptake extensively occurred. Therefore, in the calculations of CTEM-CLASS, HTO concentrations in the water streaming from the soil to leaves were relatively high, which elevated TFWT concentrations during the absences of the plume (see Fig. 22). Clearly, soil–plant transfer of HTO depends on the vertical profiles of the deposited HTO and water absorbing roots in soil. This finding again suggests that the use of a multilayered soil model with an adequate grid size

is needed in order to precisely calculate soil–plant HTO transfer (and therefore leaf TFWT concentration in leaves). This conclusion also implies that root distribution, which exerts large variabilities depending on climate, plant type, etc. [206, 207], is a critical factor affecting the soil to plant HTO transfer and therefore needs to be accurately parameterized in tritium models.

For SOLVEG-II predictions, different seasonal trends of deposition of atmospheric HTO to leaves were calculated for the plants cultivated with and without irrigation. Without irrigation, increases in TFWT concentration during the plume arrivals on 11 and 19 July 2012 were small (see Fig. 22(a)), while TFWT concentration showed efficient increases on these dates for irrigation with low activity concentration tritium water (Fig. 22(b)). The difference was caused by the occurrence of drought stress on the plants cultivated under the no irrigation treatment. During July 2012, there was no rainfall at the site (inferred from the input meteorological data). Therefore, the surface soil dried during this period (e.g. soil water content in the top 1 cm layer decreased below 0.05 vol/vol in the calculation of SOLVEG-II). This drying of the soil reduced the activity of grass and potato plants cultivated in this unirrigated soil, which caused limited openings of stomata (i.e. reduced stomata conductance) and regulated deposition of HTO to leaves during July 2012 (Fig. 22(a)). In contrast, under the irrigation treatment, soil remained sufficiently wet (e.g. soil water content in the top 1 cm layer remained greater than 0.25 vol/vol throughout the entire simulation period in the SOLVEG-II calculations). Therefore, no drought stress occurred on the standing vegetation, which enabled rapid exchange of HTO between the atmosphere and leaves (see Fig. 22(b)). These contrasting responses of foliar deposition of atmospheric HTO indicate that soil water status has a large impact on land surface HTO transfer by affecting physiological activity of vegetation. Therefore, combined calculations of soil water and its effect on plant activity (stomata resistance and photosynthesis, etc.) are needed to effectively predict HTO transfer in atmosphere–soil–plant systems, particularly in a situation where the water content of the soil can have large variabilities.

An interesting difference was found in the diurnal variations of TFWT concentrations calculated by CTEM-CLASS and SOLVEG-II. Under the irrigation treatment with high activity concentration tritium well water (see Fig. 23(c)), the TFWT concentrations calculated by SOLVEG-II revealed daily peaks in the afternoon (not the timing of the modelled daily irrigation from 07:00–08:00, see Section II.4.2.1). Similar diurnal peaks of TFWT concentrations were also calculated in the absences of the plume for the other two cases by SOLVEG-II (see Figs 23(a) and 23(b)). These small diurnal peaks were caused by the input of HTO to leaves via root uptake of HTO in the soil, which was driven by leaf transpiration during daytime hours. In contrast, such diurnal peaks of TFWT concentrations were not calculated by CTEM-CLASS (Fig. 23). The different diurnal variations of TFWT between the two model predictions originate from the parameterization of HTO exchanges at air–leaf and air–soil interfaces. In CTEM-CLASS, the exchange velocity for air–leaf HTO exchange was assumed to be the same as that of the air–soil HTO exchange (see Section 4.2). As a result, the HTO concentration in the soil and the TFWT concentration in leaves varied similarly in the calculations of CTEM-CLASS (as shown by the solid and broken yellow lines in Figs 23(a)–23(c)). In this situation, the TFWT concentration becomes unaffected by the inputs of HTO from the soil via the root water uptake. In contrast, SOLVEG-II independently calculates the depositions of HTO from the atmosphere to leaves and soil with different exchange velocities at air–leaf and air–soil interfaces (see Section 4.2). As a result, in the simulations by SOLVEG-II, the HTO concentration in the surface soil (rooting zone) remained higher than the TFWT concentration in leaves for most of the simulation period (see solid broken blue lines in Figs 23(a)–23(c)).



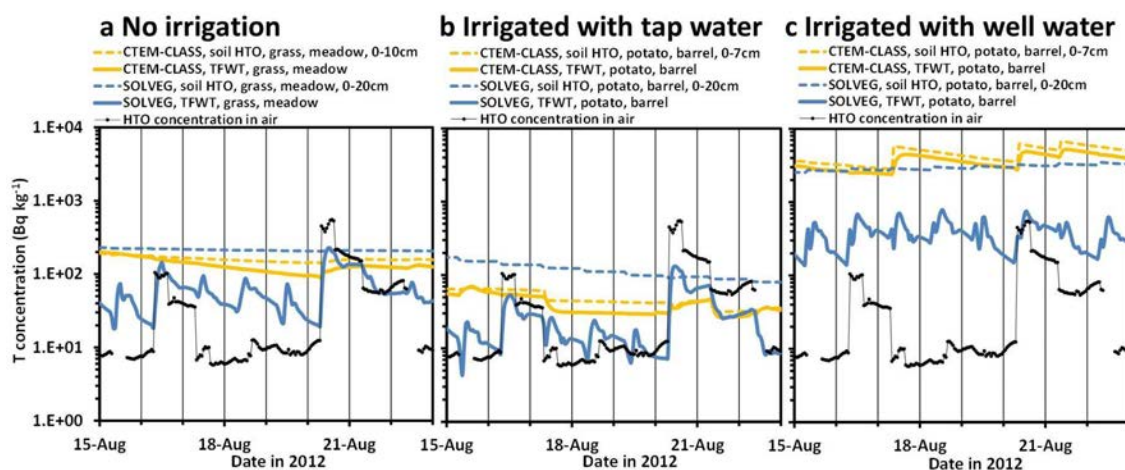


FIG. 23. Comparison of concentrations of HTO in soil, TFWT in leaves and HTO in the air (hourly inputs) during the selected eight days in the CNSC scenario. Reproduced from Ref. [175] under a Creative Commons licence.

Therefore, TFWT concentrations increased in the daytime due to HTO fluxes from the soil via the root uptake (i.e. TFWT concentrations became closer to soil HTO concentrations). These contrasting simulations from CTEM-CLASS and SOLVEG-II indicate that the effect of belowground root uptake of HTO on TFWT concentration in leaves depends on the relative relationship of HTO concentrations at the two sites (i.e. soil and leaf). This finding again demonstrates that simultaneous predictions of the vertical profile of the deposited HTO in the rooting zone and root water uptake in the soil profile are needed to accurately calculate TFWT concentrations in leaves.

### II.4.3. OBT in plants

#### II.4.3.1. Results

Modelled and measured results of OBT concentrations in grass and potato plants cultivated under the no irrigation treatments for the CNSC scenario are shown in Fig. 24(a). The concentration of OBT in grass plant leaves predicted by CTEM-CLASS showed continuous increases until 20 July 2012 and thereafter remained at around 250 Bq/kg. In the predictions made using SOLVEG-II, OBT concentrations in leaves of grass and potato plants revealed more dynamic variability, with large increases during arrivals of the plume (e.g. on 8 August 2012) and decreases during absences of the plume. These predictions of NE-OBT concentrations by the two models significantly underestimated the observations of total OBT concentration in the leaves (see the upper graph in Fig. 24(a)). In contrast, OBT concentration in the potato tubers calculated by SOLVEG-II showed better agreement with observations, with low values until the end of July 2012 and elevated values after August 2012 (Fig. 24(a)).

The predicted OBT concentrations in leaves of sod and potato plants cultivated with irrigation with low tritium tap water are shown in Fig. 24(b). Compared with the results under the no irrigation treatment (see Fig. 24(a)), the predictions made using CTEM-CLASS showed lower values under this irrigation treatment. In the predictions made using SOLVEG-II, large differences appeared between the two treatments during plume arrivals on 11 and 19 July 2012, i.e. increases of the OBT concentrations calculated assuming irrigation with tap water became much more pronounced than those calculated under the no irrigation treatments. Again, assuming irrigation with tap water, these OBT concentrations in leaves predicted using CTEM-CLASS and SOLVEG-II significantly underestimated the observations (see the upper graph of Fig. 24(b)).

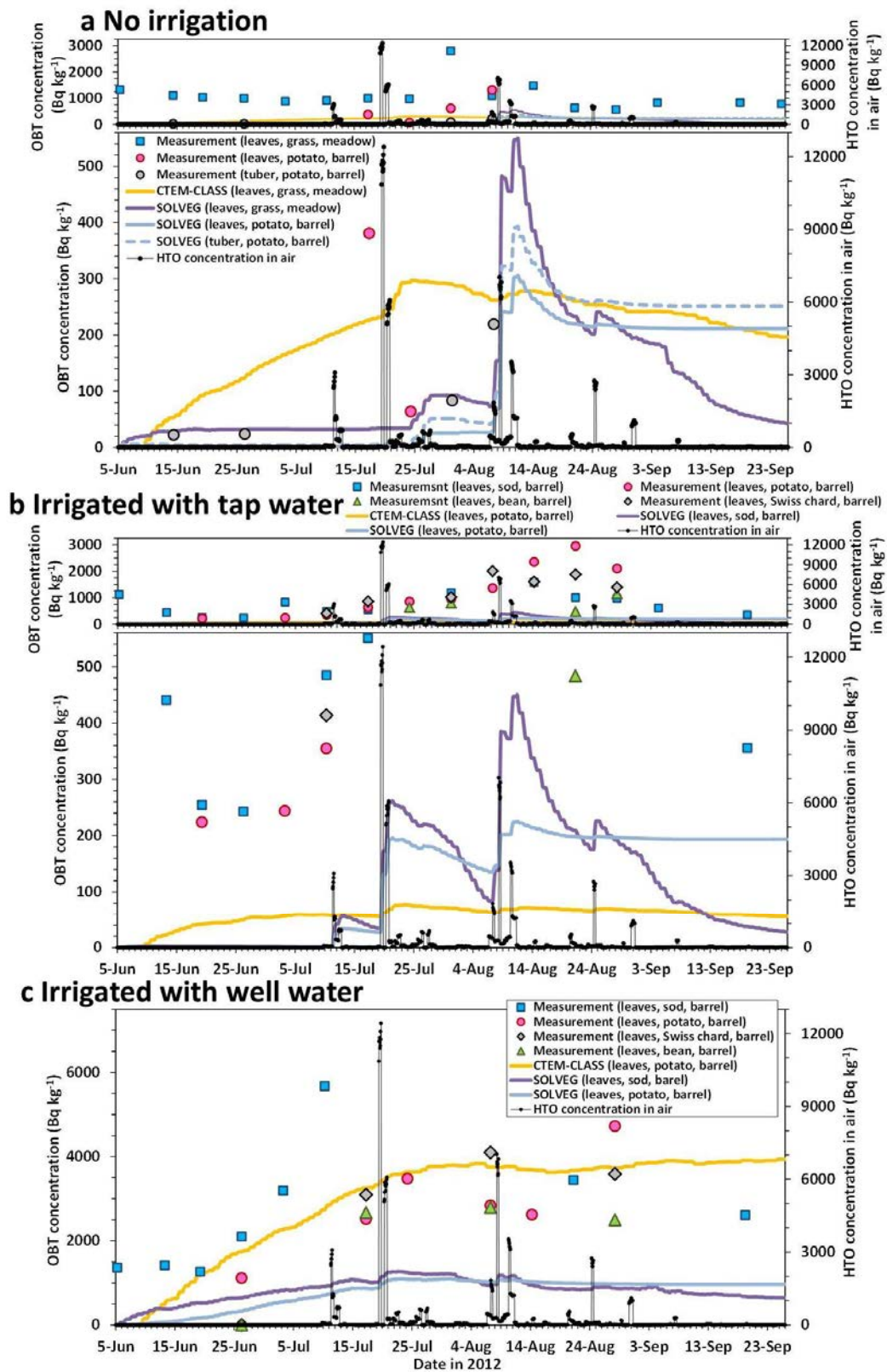


FIG. 24. Hourly inputs of HTO concentration in the air and results of OBT concentrations in plants for the CNSC scenario.

Note: The two figures presented in 24(a) and 24(b) above have different scales for 'OBT concentration' (left axis).

For irrigation with high activity concentration tritium well water (shown in Fig. 24(c)), the magnitude and seasonal trends of OBT concentrations in the leaves became significantly different from those calculated for the other two treatments (Figs 24(a) and 24(b)). The model predicted OBT concentrations assuming irrigation with high activity concentration tritium water became an order of magnitude higher than those under the other two treatments. Both the predictions by CTEM-CLASS and SOLVEG-II showed similar seasonal evolutions of OBT concentrations in the leaves; OBT concentrations continuously increased during the first two months (i.e. June and July 2012) and remained roughly constant in the subsequent period (see Fig. 24(c)). For the SOLVEG-II predictions, moderate evolutions of OBT concentration calculated under the irrigation with the high activity concentration tritium well water (see Fig. 24(c)) were significantly different from the dynamic variabilities of OBT concentrations calculated for the other two cases (Figs 24(a) and 24(b)).

#### *II.4.3.2. Discussion*

Predictions of OBT concentrations revealed large differences between the three irrigation treatments conducted during the CNSC scenario and these results have important insights into the roles of irrigation activities and soil related processes in the tritium assimilation in vegetation. Among the three treatments, the largest OBT concentration was calculated under the irrigation with high activity concentration tritium well water (Fig. 24(c)), which were clearly attributable to the elevated TFWT concentrations in the leaves in this treatment (see Fig. 22(c) above) caused by the soil–plant HTO transfer which extensively occurred in the tritium contaminated soil (see Fig. 21(d)). Clearly, irrigation with high activity concentration tritium water result in elevation of not only HTO concentration in the soil, but also TFWT concentration and assimilation of OBT in the standing vegetation.

Under the cultivation conditions with no irrigation and irrigation with low activity concentration tritium tap water, predictions of OBT concentrations in the leaves by CTEM-CLASS and SOLVEG-II significantly underestimated the observations (see Figs 24(a) and 23(b)). The significant difference between the model predictions and observations may be attributable to the effect of the E-OBT contained in the leaves and the non-photosynthetic formation of OBT (as suggested in the results of the CNL scenario, summarized in Section 3.2). Both CTEM-CLASS and SOLVEG-II do not consider the E-OBT pool in plants and assimilation of OBT through non-photosynthetic process, and therefore likely underestimated the amount of total OBT in the leaves. Again, it is highly recommended that models include an E-OBT pool and non-photosynthetic OBT formation to calculate total OBT concentration in plants.

In contrast, for irrigation with high activity concentration tritium well water (see Fig. 24(c)), model predictions were in better agreement with the observations (i.e. of the same order of magnitude) than the other two cases (Figs 24(a) and 24(b)). This result indicates that the contribution of E-OBT to the total OBT in leaves might differ between the conditions of irrigation with high tritium well water and the other two treatments. For irrigation with high activity concentration tritium water, predictions by CTEM-CLASS and SOLVEG-II showed that the TFWT concentration and NE-OBT concentration in the leaves maintained almost similar levels for most of the simulation period (as can be seen when comparing the results shown in Figs 22(c) and 24(c)). This result indicates that NE-OBT and TFWT in the leaves were in quasi-equilibrium in this case. In such a situation, E-OBT does not largely affect the total OBT concentration, because the concentration of the E-OBT essentially equals the concentration of TFWT (and thus NE-OBT in this situation) [9, 100]. This expected behaviour of OBT and TFWT in leaves suggests that the impact of the E-OBT becomes less important if

NE-OBT and TFWT are equilibrated (e.g. an environment that has been contaminated with HTO over a long period of time).

The predicted behaviour of OBT under no irrigation and irrigation with low activity concentration tritium water emphasizes the importance of water status of the soil in regulating the assimilation of tritium by plants. In the predictions of SOLVEG-II under treatments with no irrigation and irrigation with low activity concentration tritium tap water, significant differences appeared in the increases of OBT concentrations during the plume arrivals on 11 and 19 July 2012 (see Figs 24(a) and 24(b)). Again, low activity concentration OBT assimilation calculated at the no irrigation case was caused by the limited stomata opening, plus low photosynthesis due to drought stress on the plants in this month (see Section II.2.2.2 'TFWT in leaves'). Therefore, water status in soil has impacts not only on the transfer of HTO from the atmosphere to leaves by affecting the stomata openings, but also on the assimilation of OBT by affecting photosynthesis, and this needs to be adequately considered in tritium models.

The importance of soil related processes in determining the dynamics of OBT in leaves is also indicated by the different long term evolutions of OBT in the leaves predicted by CTEM-CLASS and SOLVEG-II. In the prediction by CTEM-CLASS, the OBT concentration in the leaves of plants cultivated with no irrigation and irrigation with low activity concentration tritium tap water showed continuous increases during the first months (see Figs 24(a) and 24(b)) and thereafter remained roughly constant. In the predictions by SOLVEG-II, the OBT concentrations in the leaves under these cultivation regimes revealed dynamic variability throughout the entire simulation period (see Figs 24(a) and 24(b)). The difference in the long term dynamics of OBT between the two models' predictions was attributable to the different impact of root uptake of HTO. As discussed in Section II.4.2.2 above, TFWT concentrations calculated by CTEM-CLASS remained elevated over the entire simulation period due to the large soil-plant HTO transfer. Consequently, in the calculation of CTEM-CLASS, the OBT concentration in the leaves continuously increased after the start of the calculation and reached a level similar to TFWT concentration several months later (see Figs 24(a) and 24(b)). In this quasi-equilibrium state, the concentration of OBT in leaves became unchanged, because the concentration of newly synthesized OBT is similar to the concentration of OBT already present in the organic matter pool in leaves. In the SOLVEG-II calculations, such equilibrium of OBT and TFWT in leaves can certainly be seen under irrigation with high activity concentration tritium well water (shown in Figs 22(c) and 24(c)) in which the TFWT concentration remained constant over the simulation period and hence the OBT concentration reached the equilibrium level by the end of July 2012. However, under no irrigation and irrigation with the low activity concentration tritium tap water, OBT and TFWT concentrations in leaves did not reach an equilibrium state in the SOLVEG-II calculations (see Figs 22 and 24), because of the dynamic variability of TFWT concentrations in leaves calculated by this model throughout the simulation period. Overall, these results indicate that the OBT concentration in leaves reaches an equilibrium state if the TFWT concentration in leaves is maintained at a certain level over an extended period and the OBT concentration in leaves at the equilibrium state is determined by the TFWT concentration. In this respect, soil related processes (i.e. root uptake) need to be considered as a process that determines steady state OBT concentrations under a situation where ecosystems are contaminated with HTO over a long period of time.

Another interesting result gleaned from this intercomparison is a relatively accurate agreement between the model predictions and observations for the OBT concentration in the tubers of potato plants. Under the cultivation with no irrigation treatments, OBT concentrations in leaves of potato plants predicted by the two models significantly underestimated the observations, while the predicted OBT concentrations in the tubers showed better agreement with the

observations (see Fig. 24(a)). The contrasting results for OBT between the tubers and leaves imply that the behaviour of E-OBT could differ between the two parts of the plant. Given that the underestimations of OBT concentrations in the model predictions were due to the effect of the E-OBT contained in the leaves, it is believed that the impact of E-OBT on the total OBT will be less pronounced in the tubers than in the leaves. The result suggests a possibility that the dynamics of exchanges of TFWT and OBT differ between leaves and tubers, although more studies are needed to better generalize this phenomena and model it in more detail.



## REFERENCES

- [1] INTERNATIONAL ATOMIC ENERGY AGENCY, Modelling of Marine Dispersion and Transfer of Radionuclides Accidentally Released from Land Based Facilities, Report of Working Group 10, Modelling of Marine Dispersion and Transfer of Radionuclides Accidentally Released from Land Based Facilities, MODARIA Topical Heading Marine Modelling, Modelling and Data for Radiological Impact Assessments (MODARIA) Programme, IAEA-TECDOC-1876, IAEA, Vienna (2019).
- [2] INTERNATIONAL ATOMIC ENERGY AGENCY, Development of a Common Framework for Addressing Climate and Environmental Change in Post-closure Radiological Assessment of Solid Radioactive Waste Disposal, Report of Working Group 6, Common Framework for Addressing Environmental Change in Long Term Safety Assessments of Radioactive Waste Disposal Facilities, MODARIA Topical Heading Uncertainties and Variability, Modelling and Data for Radiological Impact Assessments (MODARIA) Programme, IAEA-TECDOC-1904, IAEA, Vienna (2020).
- [3] INTERNATIONAL ATOMIC ENERGY AGENCY, Approaches for Modelling of Radioecological Data to Identify Key Radionuclides and Associated Parameter Values for Human and Wildlife Exposure Assessments, Report of Working Group 4, Analysis of Radioecological Data in IAEA Technical Reports Series Publications to Identify Key Radionuclides and Associated Parameter Values for Human and Wildlife Exposure Assessment, MODARIA Topical Heading Uncertainties and Variability, Modelling and Data for Radiological Impact Assessments (MODARIA) Programme, IAEA-TECDOC-1950, IAEA, Vienna (2021).
- [4] INTERNATIONAL ATOMIC ENERGY AGENCY, Assessment of Radioactive Contamination in Urban Areas, Report of Working Group 9, Urban Areas of EMRAS II, Topical Heading: Approaches for Assessing Emergency Situations, Environmental Modelling for Radiation Safety (EMRAS II) Programme, IAEA-TECDOC-1941, IAEA, Vienna (2021).
- [5] INTERNATIONAL ATOMIC ENERGY AGENCY, Soil–Plant Transfer of Radionuclides in Non-temperate Environments, Report of Working Group 4 Transfer Processes and Data for Radiological Impact Assessment, Subgroup 3 on Non-temperate Data, IAEA Programme on Modelling and Data for Radiological Impact Assessments (MODARIA II), IAEA-TECDOC-1979, IAEA, Vienna (2021).
- [6] INTERNATIONAL ATOMIC ENERGY AGENCY, Radiation Protection of Wildlife: Modelling the Exposure and Effects, A Joint Summary Report by MODARIA I Working Groups 8, Biota Modelling: Further Development of Transfer and Exposure Models and Application to Scenarios, MODARIA I Working Group 9, Models for Assessing Radiation Effects on Populations of Wildlife Species, MODARIA II Working Group 5, Exposure and Effects on Biota, IAEA Programmes on Modelling and Data for Radiological Impact Assessments (MODARIA I and II), IAEA-TECDOC-1986, IAEA, Vienna (in press).
- [7] INTERNATIONAL ATOMIC ENERGY AGENCY, Modelling the environmental transport of tritium in the vicinity of long term atmospheric and sub-surface sources, IAEA-BIOMASS-3, IAEA, Vienna (2003).

- [8] INTERNATIONAL ATOMIC ENERGY AGENCY, Transfer of Tritium in the Environment after Accidental Releases from Nuclear Facilities, IAEA-TECDOC-1738, IAEA, Vienna (2014).
- [9] DIABATE, S., STRACK, S., Organically bound tritium, *Health Phys.* **65** (1993) 698–712.
- [10] YAMAZAWA, H., OTA, M., MORIIZUMI, J., Realistic and practical modeling of tritium deposition to bare soil, *Fusion Sci. Technol.* **60** (2011) 1224–1227.
- [11] TÄSCHNER, M., BUNNENBERG, C., CAMUS, H., BELOT, Y., Investigations and modeling of tritium reemission from soil, *Fusion Technol.* **28** (1995) 976–981.
- [12] McFARLANE, J.C., ROGERS, R.D., BRADLEY JR., D.V., Tritium oxidation in surface soils, A survey of soils near five nuclear fuel reprocessing plants, *Environ. Sci. Technol.* **13** (1979) 607–608.
- [13] FOERSTEL, H., LEPA, K., TRIERWEILER, H., Re-emission of HTO into the atmosphere after HT/HTO conversion in the soil, *Fusion Technol.* **14** (1988) 1203–1208.
- [14] TÄSCHNER, M., BUNNENBERG, C., RASKOB, W., Measurements and modeling of tritium reemission rates after HTO deposition at sunrise and sunset, *J. Environ. Radioactiv.* **36** (1997) 219–235.
- [15] YOKOYAMA, S., NOGUCHI, H., ICHIMASA, Y., ICHIMASA, M., Re-emission of heavy water vapour from soil to the atmosphere, *J. Environ. Radioact.* **71** (2004) 201–213.
- [16] GARLAND, J.A., COX, L.C., The absorption of tritium gas by English soils, plants and the sea, *Water Air Soil Pollut.* **14** (1980) 103–114.
- [17] GARLAND, J.A., The absorption and evaporation of tritiated water vapor by soil and grassland, *Water Air Soil Pollut.* **13** (1980) 317–333.
- [18] RASKOB, W., Modeling of tritium behavior in the environment, *Fusion Technol.* **21** (1992) 636–645.
- [19] FEINHALS, J., BUNNENBERG, C., Laboratory investigations of HTO deposition to soils, *Fusion Technol.* **14** (1988) 1253–1257.
- [20] YOKOYAMA, S., NOGUCHI, H., ICHIMASA, M., ICHIMASA, Y., FUKUTANI, S., Deposition of heavy water on soil and reemission to the atmosphere, *Fusion Eng. Des.* **42** (1998) 141–148.
- [21] BELOT, Y., GUENOT, J., CAPUT, C., Emission of tritiated water formed at soil surface by oxidation of HT, *Fusion Technol.* **14** (1988) 1231–1234.
- [22] WIENER, B., TÄSCHNER, M., BUNNENBERG, C., HTO reemission from soil after HT deposition and dose consequences of HT releases, *Fusion Technol.* **14** (1988) 1247–1252.
- [23] McFARLANE, J.C., ROGERS, R.D., BRADLEY JR., D.V., Environmental tritium oxidation in surface soil, *Environ. Sci. Technol.* **12** (1978) 590–592.
- [24] ICHIMASA, M., ICHIMASA, M., AZUMA, Y., KOMURO, M., FUJITA, K., AKITA, Y., Oxidation of molecular tritium by surface soils, *J. Radiat. Res.* **29** (1988) 144–151.



- [25] BROWN, R.M., OGRAM, G.L., SPENCER, F.S., Field studies of HT behaviour in the environment I, Dispersion and oxidation in the atmosphere, *Fusion Technol.* **14** (1988) 1165–1169.
- [26] BROWN, R.M., OGRAM, G.L., SPENCER, F.S., Oxidation and dispersion of HT in the environment: the August 1986 field experiment at Chalk River, *Health Phys.* **58** (1990) 171–181.
- [27] PETERSON, S.-R., DAVIS, P.A., Tritium doses from chronic atmospheric releases: a new approach proposed for regulatory compliance, *Health Phys.* **82** (2002) 213–225.
- [28] BUNNENBERG, C., FEINHALS, J., WIENER, B., Differences in the behaviour of HTO and H<sub>2</sub>O in soil after condensation from the atmosphere and conversion of HT to HTO and OBT in soil relative to moisture content and pore volume, *Radiat. Prot. Dosim.* **14** (1986) 83–87.
- [29] OTA, M., YAMAZAWA, H., MORIIZUMI, J., IIDA, T., Measurement and modeling of oxidation rate of hydrogen isotopic gases by soil, *J. Environ. Radioactiv.* **97** (2007) 103–115.
- [30] SWEET, C.W., MURPHY, C.E., Tritium deposition in pine trees and soil from atmospheric releases of molecular tritium, *Environ. Sci. Technol.* **18** (1984) 358–361.
- [31] FOERSTEL, H., Uptake of elementary tritium by the soil, *Radiat. Prot. Dosim.* **16(1-2)** (1986) 75–81.
- [32] SPENCER, F.S., OGRAM, G.L., BROWN, R.M., Field studies of HT behavior in the environment: 3. Tritium deposition and dynamics in vegetation, *Fusion Technol.* **14** (1988) 1176–1181.
- [33] AMANO, H., ATARASHI, M., NOGUCHI, H., YOKOYAMA, S., ICHIMASA, Y., ICHIMASA, M., Formation of organically bound tritium in plants during the 1994 chronic HT release experiment at Chalk River, *Fusion Technol.* **28** (1995) 803–808.
- [34] TÄSCHNER, M., WIENER, B., BUNNENBERG, C., HT dispersion and deposition in soil after experimental releases of tritiated hydrogen, *Fusion Technol.* **14** (1988) 1264–1269.
- [35] AMIRO, B.D., DAVIS, P.A., JOHNSTON, F.L., WORKMAN, W.J.G., Theoretical and practical aspects of a free-atmosphere tritium exposure system, *J. Environ. Radioact.* **36** (1997) 141–156.
- [36] KIM, S.B., STUART, M., BREDLAW, M., FESTARINI, A., BEATON, D., HT to HTO conversion and field experiments near Darlington Nuclear Power Generating Station (DNP GS) Station, *J. Environ. Radioact.* **132** (2014) 73–80.
- [37] ICHIMASA, Y., ICHIMASA, M., JIANG, H., KATSUNO, K., In vitro determination of HT oxidation activity and tritium concentration in soil and vegetation during chronic HT release experiment at Chalk River, *Fusion Technol.* **28** (1995) 877–882.
- [38] DAVIS, P.A., GALERIU, D.C., SPENCER, F.S., AMIRO, B.D., Evolution of HTO concentrations in soil, vegetation and air during an experimental chronic HT release, *Fusion Technol.* **28** (1995) 833–839.

- [39] DUNSTALL, T.G., OGRAM, G.L., SPENCER, F.S., Elemental tritium deposition and conversion in the terrestrial environment, *Fusion Technol.* **8** (1985) 2551–2556.
- [40] NOGUCHI, H., MATSUI, T., MURATA, M., Tritium behavior observed in the Canadian HT release study, *Fusion Technol.* **14** (1988) 1187–1192.
- [41] ICHIMASA, M., SUZUKI, M., OBAYASHI, H., SAKUMA, Y., ICHIMASA, Y., In vitro determination of oxidation of atmospheric tritium gas in vegetation and soil in Ibaraki and Gifu, Japan, *J. Radiat. Res.* **40** (1999) 243–251.
- [42] OTA, M., NAGAI, H., KOARASHI, J., Importance of root HTO uptake in controlling land-surface tritium dynamics after an-acute HT deposition: A numerical experiment, *J. Environ. Radioactiv.* **109** (2012) 94–102.
- [43] OTA, M., NAGAI, H., Development and validation of a dynamical atmosphere–vegetation–soil HTO transport and OBT formation model, *J Environ. Radioactiv.* **102** (2011) 813–823.
- [44] LE DIZÈS, S., AULAGNIER, C., HENNER, P., SIMON-CORNU, M., TOCATTA: a dynamic transfer model of  $^3\text{H}$  from the atmosphere to soil–plant systems, *J. Environ. Radioact.* **124** (2013) 191–204.
- [45] CONNAN, O., MARO, D., HÉBERT, D., SOLIER, L., CALDEIRA IDEAS, P., LAGUIONIE, P., ST-AMANT, N., In situ measurements of tritium evapotranspiration ( $^3\text{H}$ -ET) flux over grass and soil using the gradient and eddy covariance experimental methods and the FAO-56 model, *J. Environ. Radioact.* **148** (2015) 1–9.
- [46] LE DIZÈS, S., AULAGNIER, C., MARO, D., ROZET, M., VERMOREL, F., HÉBERT, D., VOISEUX, C., SOLIER, L., GODINOT, C., FIEVET, B., LAGUIONIE, P., CONNAN, O., CAZIMAJOU, O., MORILLON, M., The VATO Project: Development and Validation of a Dynamic Transfer Model of Tritium in Grassland Ecosystem, *J. Environ. Radioact.* **171** (2017) 83–92.
- [47] DANA, M.T., WOGMAN, N.A., WOLF, M.A., Rain scavenging of tritiated water (HTO), A field experiment and theoretical considerations, *Atmos. Environ.* **12** (1978) 1523–1529.
- [48] BELOVODSKI, L.F., GAEVOY, V.K., A.V., KOSHELEVA, T.A., Tritium oxide wash-out by drops', *J. Environ. Radioact.* **36(2-3)** (1997) 129–139.
- [49] TOKUYAMA, H., OONISHI, M., Precipitation washout of tritiated water vapor from a nuclear reactor, *J. Environ. Radioact.* **34** (1997) 59–68.
- [50] RASKOB, W., BARRY P., Importance and variability in processes relevant to environmental tritium ingestion dose models, *J. Environ. Radioactiv.* **36** (1997) S237–S251.
- [51] MURATA, M., NOGUCHI, H., Dose Delivered by Unit Amount of Tritium Released into the Environment, *J. Nucl. Sci. Technol.* **34** (1997) 176–184.
- [52] RUSSELL, S.B., OGRAM, G.L., ETMOD: A New Environmental Tritium Model, *Fusion Technol.* **21** (1992) 645–650.
- [53] YOKOYAMA, S., NOGUCHI, H., KUROSAWA, N., Development of dose assessment code for accidental tritium releases, *ACUTRI, Hoken Butsuri* **40(4)** (2005) 376–384.

- [54] GOLUBEV, V.S., LAWRIK, J.H., GROISMAN, P.Y., SPERANSKAYA, N.A., ZHURAVIN, S.A., MENNE, M.J., PETERSON, T.C., MALONE, R.W., Evaporation changes over the contiguous United States and the former USSR: A reassessment, *Geophys. Res. Lett.* **28** (2001) 2665–2668.
- [55] HALES, J.M., Fundamentals of the theory of gas scavenging by rain, *Atmos. Environ.* **6** (1972) 635–659.
- [56] OGRAM, G.L., Precipitation scavenging of tritiated water vapour (HTO), Technical report, Ontario Hydro research division, Canada (1985).
- [57] BELOT, Y., Derivation of parameters for use in tritium washout predictions, Presented at the Workshop of the IAEA Task Group on Tritium Safety and Environmental Effects, 11–12 May 1998, held at AECL, Chalk River, Canada (1998a).
- [58] BELOT, Y., Development of parameters for use in tritium washout predictions, Proceedings of the IEA Task Group on Tritium Safety and Environmental Effects, 11–12 May 1998, AECL, Chalk River, Canada (1998b).
- [59] ASTON, A.R., Rainfall interception by eight small trees, *J. Hydrol.* **42(3)** (1979) 383–396.
- [60] NOILHAN, J., PLANTON, S., A simple parameterization of land surface processes for meteorological models, *Mon. Wea. Rev.* **117** (1989) 536–549.
- [61] JACKSON, L.J., Relationship between rainfall parameters and interception by tropical forest, *J. Hydrol.* **24** (1975) 215–238.
- [62] TANAKA, K., Multi-layer model of CO<sub>2</sub> exchange in a plant community coupled with the water budget of leaf surfaces, *Ecological Modelling* **147** (2002) 85–104.
- [63] BRUDENELL, A.J.P., COLLINS, C.D., SHAW, G., Dynamics of tritiated water (HTO) uptake and loss by crops after short-term atmospheric release, *J. Environ. Radioact.* **36** (1997) 197–218.
- [64] VANDECASTEELE, C.M., BAKER, S., FORSTEL, H., MUZINSKY, M., MILLAN, R., MADOZ-ESCANDE, C., TORMOS, J., SAURAS, T., SCHULTE, E., COLLE, C., Interception, retention and translocation under greenhouse conditions of radiocaesium and radiostrontium from a simulated accidental source, *Sci. Total Environ.* **278** (2001) 199–214.
- [65] PRÖHL, G., Interception of dry and wet deposited radionuclides by vegetation, *J. Environ. Radioact.* **100** (2009) 675–682.
- [66] CHAMBERLAIN, A.C., Interception and retention of radioactive aerosols by vegetation, *Atmos. Environ.* **4** (1970) 57–78.
- [67] LLORENS, P., GALLART, F., A simplified method for forest water storage capacity measurement, *J. Hydrol.* **240** (2000) 131–144.
- [68] DEARDORFF, J.W., Efficient prediction of ground surface temperature and moisture, with inclusion of layer of vegetation, *J. Geophys. Res.* **93(4)** (1978) 1889–1903.
- [69] NAGAI, H., Validation and sensitivity analysis of a new atmosphere-soil-vegetation model, *J. Appl. Meteorol.* **41** (2002) 160–176.

- [70] KLINE, J.R., STEWART, M.L., Tritium uptake and loss in grass vegetation which has been exposed to an atmospheric source of tritiated water, *Health Phys.* **26(6)** (1974) 567–573.
- [71] BELOT, Y., GAUTHIER, D., CAMUS, H., CAPUT, CL., Prediction of the flux of tritiated water from air to plant leaves, *Health Phys.* **37** (1979) 575–583.
- [72] GARLAND, J.A., COX L.C., Uptake of tritiated water vapor by bean leaves, *Water Air Soil Pollut.* **17** (1982) 207–212.
- [73] COUCHAT, P., PUARD, M., LASCEVE, G., Tritiated water vapor exchange in sunflowers, *Health Phys.* **45(3)** (1983) 757–764.
- [74] GUENOT, J., BELOT, Y., Assimilation of  $^3\text{H}$  in photosynthesizing leaves exposed to HTO, *Health Phys.* **47** (1984) 849–855.
- [75] SPENCER, F.S., Tritiated water uptake kinetics in tissue-free water and organically-bound fractions of tomato plants, Report No. 84-69-K., Ontario Hydro Research Division (1984).
- [76] BELOT, Y., CAPUT, C., GAUTHIER, D., Distribution of the organically bound tritium in vegetation exposed to fall-out, *Radiat. Proc. Dos.* **16** (1986) 111–113.
- [77] MURPHY, C.E., Tritium transport and cycling in the environment, *Health Phys.* **65(6)** (1993) 683–697.
- [78] DIABATE, S., STRACK, S., Organically bound tritium in wheat after short-term exposure to atmospheric tritium under laboratory conditions, *J. Environ. Radioactiv.* **36** (1997) 157–175.
- [79] JIANG, M., ZHANG, J., Water stress-induced abscisic acid accumulation triggers the increased generation of reactive oxygen species and up-regulates the activities of antioxidant enzymes in maize leaves, *J. Exp. Bot.* **53(379)** (2002) 2401–2410.
- [80] BELOT, Y., Comportement du tritium dans l'environnement, In: BELOT, Y., ROY, M., METIVIER, H., (Dir), *Le Tritium de l'Environnement à l'Homme*, Institut de Protection et de Sûreté Nucléaire, Les Editions de Physique, France, (1996) 39–76 (in French).
- [81] ATARASHI, M., AMANO, H., ICHIMASA, M., KANEKO, M., ICHIMASA, Y., Uptake of heavy water vapor from atmosphere by plant leaves as a function of stomatal resistance, *Proceedings of International Meeting on Influence of Climatic Characteristics upon Behavior of Radioactive Elements*, Rokkasho, Aomori, Japan, 14–16 October 1997 (OHMOMO, Y., SAKURAI, N., Eds), IES (1997) 236–242.
- [82] ICHIMASA, M., WENG, C., ARA, T., ICHIMASA, Y., Organically bound deuterium in rice and soybean after exposure to heavy water vapor as a substitute for tritiated water, *Fusion Sci. Technol.* **41** (2002) 393–398.
- [83] ICHIMASA, M., MAEJIMA, T., SEINO, N., ARA, T., MASUKURA, A., NISHIHIRO, S., TAUCHI, H., ICHIMASA, Y., Organically bound deuterium in soybean exposed to atmospheric D<sub>2</sub>O vapor as a substitute for HTO under different growth phase, *Proceedings of the International Symposium: Transfer of Radionuclides in Biosphere – Prediction and Assessment*, Mito, 18–19 December 2002, JAERI-Conf 2003-010 (2003) 226–232.

- [84] ICHIMASA, Y., SASAJIMA, E., MAKIHARA, H., TAUCHI, H., UDA, T., ICHIMASA, M., Uptake of Heavy Water and Loss by Tangerine in the Heavy Water Vapor Release Experiment in a Greenhouse as a Substitute for Tritiated Water, *Fusion Sci. Technol.* **48** (2005) 775–778.
- [85] MURPHY, C.E., Jr., The relationship between tritiated water activities in air, vegetation and soil under steady-state conditions, *Health Phys.* **47** (1984) 635–639.
- [86] MELINTESCU, A., GALERIU, D., A versatile model for tritium transfer from atmosphere to plant and soil, *Radioprotection* **40** (2005) S437–S442.
- [87] DAMOUR, G., SIMONEAU, T., COCHARD, H., URBAN, L., An overview of models of stomatal conductance at the leaf level, *Plant Cell Environ.* **33** (2010) 1419–1438.
- [88] JARVIS, P.G., The interpretation of the variations in leaf water potential and stomatal conductance found in canopies in the field, *Philos. T. R. Soc. B* **273** (1976) 593–610.
- [89] BALL, M.C., WOODROW, I.E., BERRY, J.A., A Model Predicting Stomatal Conductance and its Contribution to the Control of Photosynthesis under Different Environmental Conditions, *Progress in Photosynthesis Research* (BIGGINS, J., Ed.), Martinus Nijhoff Publishers, Dordrecht, Netherlands (1987) 221–224.
- [90] LEUNING, R., A critical appraisal of a combined stomatal-photosynthesis model for C<sub>3</sub> plants, *Plant Cell Environ.* **18** (1995) 339–355.
- [91] JACOBS, C.M.J., Direct impact of atmospheric CO<sub>2</sub> enrichment on regional transpiration, PhD. Thesis, Agricultural University, Wageningen (1994).
- [92] CALVET, J.C., Investigating soil and atmospheric plant water stress using physiological and micrometeorological data, *Agricultural and Forest Meteorology* **103** (2000) 229–247.
- [93] RONDA, R.J, DE BRUIN, H.A.R., HOLTSLAG, A.A.M., Representation of the canopy conductance in modeling the surface energy budget for low vegetation, *J. Appl. Meteorol.* **40** (2001) 1431–1444.
- [94] MEDLYN, B.E., DUURSMA, R.A., EAMUS, D., ELLSWORTH, D.S., PRENTICE, I.C., BARTON, C.V.M., CROUS, K.Y., DE ANGELIS, P., FREEMAN, M., WINGATE, L., Reconciling the optimal and empirical approaches to modelling stomatal conductance, *Global Change Biology* **17**(6) (2011) 2134–2144.
- [95] HUNTINGFORD, C., SMITH, D.M., DAVIES, W.J., FALK, R., SITCH, S., MERCADO, L.M., Combining the [ABA] and net photosynthesis-based model equations of stomatal conductance, *Ecol. Model.* **300** (2015) 81–88.
- [96] MERCADO, L.M., HUNTINGFORD, C., GASH, J.H.C., COX, P.M., JOGIREDDY, V., Improving the representation of radiation interception and photosynthesis for climate model applications, *Tellus Ser. B.* **59** (2007) 553–565.
- [97] DING, R., KANG, S., DU, T., HAO, X., ZHANG, Y., Scaling up stomatal conductance from leaf to canopy using a dual-leaf model for estimating crop evapotranspiration, *PLOS ONE*, **9**(4) (2014) e95584.  
<https://doi.org/10.1371/journal.pone.0095584>.

- [98] NAGAI, H., Incorporation of CO<sub>2</sub> exchange processes into a multiplayer atmosphere-soil-vegetation model, *J. Appl. Meteorol.* **44** (2005) 1574–1592.
- [99] KIM, S.B., WORKMAN, W.G., KOROLEVYCH, V., DAVIS, P.A., Field measurements of key parameters associated with nocturnal OBT formation in vegetables grown under Canadian conditions, *J. Environ. Radioact.* **104** (2012) 94–100.
- [100] KIM, S.B., BAGLAN, N., DAVIS, P.A., Current understanding of organically bound tritium (OBT) in the environment, *J. Environ. Radioact.* **126** (2013) 83–91.
- [101] BOGEN, D.C., WELFORD, G.A., Fallout tritium distribution in the environment, *Health Phys.* **30** (1976) 203–208.
- [102] TINDALL, J.A., KUNKEL, J.R., Unsaturated zone hydrology. Prentice-Hall, Inc., New Jersey (1999).
- [103] FOURRÉ, E., BAUMIER, D., DAPOIGNY, A., BONTÉ, P., CLAVEL, B., JEAN-BAPTISTE, P., Environmental tritium in the vicinity of Creys-Malville nuclear power plant, *Radioprotection, Suppl. 1*, **40** (2005) S765–S770.
- [104] MOMOSHIMA, N., KAKIUCHI, H., OKAI, T., HISAMATSU, S., Tritium in a pine forest ecosystem: Relation between fresh pine needles, organic materials on a forest floor and atmosphere, *J. Radioanal. Nucl. Chem.* **243** (2000) 479–482.
- [105] PAPKE, H., FÖRSTEL, H., Formation rate of nonexchangeable organically bound tritium from tritiated soil water, *Health Phys.* **60** (1991) 773–779.
- [106] DIABATÉ, S., HONIG, D., Conversion of molecular tritium to HTO and OBT in plants and soils, *Fusion Technol.* **14** (1988) 1235–1239.
- [107] HISAMATSU, S., KATSUMATA, T., TAKIZAWA, Y., Tritium concentrations in pine needle, litter and soil samples, *J. Radiat. Res.* **39** (1998) 129–136
- [108] KIM, S.B., BREDLAW, M., KOROLEVYCH, V.Y., Organically bound tritium (OBT) in soil at different depths around Chalk River Laboratories (CRL), Canada, *AECL Nuclear Review* **2** (2013) 17–26.
- [109] JEAN-BAPTISTE, P., BAUMIER, D., FOURRE, E., DAPOIGNY, A., CLAVEL, B., The distribution of tritium in the terrestrial and aquatic environments of the Creys-Malville nuclear power plant (2002–2005), *J. Environ. Radioactiv.* **94** (2007) 107–118.
- [110] THOMPSON, P.A., KWAMENA, N.-O.A., ILIN, M., WILK, M., CLARK, I.D., Levels of tritium in soils and vegetation near Canadian nuclear facilities releasing tritium to the atmosphere: implications for environmental models, *J. Environ. Radioact.* **140** (2015) 105–113.
- [111] JENKINSON, D.S., HARKNESS, D.D., VANCE, E.D., ADAMS, D.E., HARRISON, A.F., Calculating net primary production and annual input of organic matter to soil from the amount and radiocarbon content of soil organic matter, *Soil Biol. Biochem.*, **24** (1992) 295–308.
- [112] BAISDEN, W.T., AMUNDSON, R., BRENNER, D.L., COOK, A.C., KENDALL, C., HARDEN, J.W., A multiisotope C and N modeling analysis of soil organic matter turnover and transport as a function of soil depth in a California annual grassland soil chronosequence, *Glob. Biogeochem. Cycles* **16**(4) (2002) 82-1–82-26.

- [113] LÜTZOW, M.V., KÖGEL-KNABNER, I., EKSCHMITT, K., MATZNER, E., GUGGENBERGER, G. MARSCHNER, B. FLESSA, H., Stabilization of organic matter in temperate soils: mechanisms and their relevance under different soil conditions – a review, *European Journal of Soil Science*, **57(4)** (2006) 426–445.
- [114] KOARASHI, J., ATARASHI-ANDOH, M., ISHIZUKA, S., MIURA, S., SAITO, T., HIRAI, K., Quantitative aspect of heterogeneity in soil organic matter dynamics in a cool-temperate Japanese beech forest: a radiocarbon-based approach, *Glob. Change Biol.* **15** (2009) 631–642.
- [115] TORN, M.S., TRUMBORE, S.E., CHADWICK, O.A., VITOUSEK, P.M., HENDRICKS, D.M., Mineral control of soil organic carbon storage and turnover, *Nature* **389** (1997) 170–173.
- [116] TORN, M.S., SWANSTON, C.W., CASTANHA, C., TRUMBORE, S.E., Storage and Turnover of Organic Matter in Soil, In: *Biophysico-Chemical Processes Involving Natural Nonliving Organic Matter in Environmental Systems* (SENESE, N., XING, B., HUANG, P.M.m Eds), John Wiley and Sons (2009) 219–272.
- [117] TRUMBORE, S.E., Potential responses of soil organic carbon to global environmental change, *Proc. Natl. Acad. Sci. USA* **94(16)** (1997) 8284–8291.
- [118] FRÖBERG, M., HANSON, P.J., TRUMBORE, S.E., SWANSTON, S.E., TODD, D.E., Flux of carbon from <sup>14</sup>C-enriched leaf litter throughout a forest soil mesocosm, *Geoderma* **149** (2009) 181–188.
- [119] SCHMIDT, B.H.M., WANG, C.P., CHANG, S.C., MATSNER, E., High precipitation causes large fluxes of dissolved organic carbon and nitrogen in a subtropical montane *Chamaecyparis* forest in Taiwan, *Biogeochemistry* **101** (2010) 243–256.
- [120] RUBINO, M., LUBRITTO, C., D’ONOFRIO, A., TERRASI, F., GLEIXNER, G., COTRUFO, M.F., An isotopic method for testing the influence of leaf litter quality on carbon fluxes during decomposition, *Oecologia*, **154** (2007) 155–166.
- [121] PARTON, W.J., SCHIMEL, D.S., COLE, C.V., OJIMA, D.S., Analysis of factors controlling soil organic matter levels in great plains grasslands, *Soil Sci. Soc. Am. J.* **51** (1987) 1173–1179.
- [122] PARTON, W.J., SCURLOCK, J.M.O., OJIMA, D.S., GILMANOV, T.G., SCHOLES, R.J., SCHIMEL, D.S., KIRCHNER, T., MENAUT, J-C., SEASTEDT, T., GARCIA MOYA, E., KAMNALRUT, A., KINYAMARIO, J.I., Observations and modeling of biomass and soil organic matter dynamics for the grassland biome worldwide, *Global Biogeochem. Cycles* **7** (1993) 785–809.
- [123] ELZEIN, A., BALESDENT, J., Mechanistic simulation of vertical distribution of carbon concentrations and residence times in soils, *Soil Sci. Soc. Am. J.* **59** (1995) 1328–1335.
- [124] KOARASHI, J., HOCKADAY, W.C., MASIELLO, C.A., TRUMBORE, S.E., Dynamics of decadal cycling carbon in subsurface soils, *J. Geophys. Res.* **117** (2012) G03033.
- [125] OTA, M., NAGAI, H., KOARASHI, J., Root and dissolved organic carbon controls on subsurface soil carbon dynamics: A model approach, *J. Geophys. Res.: Biogeosciences* **118** (2013) 1646–1659.

- [126] ELIASSON, P.E., McMURTRIE, R.E., PEPPER, D.A., STRÖMGREN, M., LINDER, S., ÅGREN, G.I., The response of heterotrophic CO<sub>2</sub> flux to soil warming, *Global Change Biology* **11(1)** (2005) 167–181.
- [127] DAVIDSON, E., JANSSENS, I., Temperature sensitivity of soil carbon decomposition and feedbacks to climate change, *Nature* **440** (2006) 165–173.
- [128] BOYER, C., VICHOT, L., FROMM, M., LOSSET, Y., TATIN-FROUX, F., GUÉTAT, P., BADOT, P.M., Tritium in plants: A review of current knowledge, *Environ. Exp. Bot.* **67** (2009) 34–51.
- [129] MELINTESCU, A., GALERIU, D., DIABATÉ, S., STRACK, S., Preparatory steps for a robust dynamic model for OBT dynamics in agricultural crops, *Fusion Sci. Technol.* **67** (2015) 479–482.
- [130] GALERIU, D., MELINTESCU, A., Relevance of Night Production of OBT in Crops, *Fusion Sci. Technol.* **71(4)** (2017) 595–599.
- [131] BARRY, P.J., WATKINS, B.M., BELOT, Y., DAVIS, P.A., EDLUND, O., GALERIU, D., RASKOB, W., RUSSELL, S., TOGAWA, O., Intercomparison of model predictions of tritium concentrations in soil and foods following acute airborne HTO exposure, *J. Environ. Radioactiv.* **42** (1999) 191–207.
- [132] GALERIU, D., DAVIS, P., RASKOB, W., MELINTESCU, A., Recent progresses in tritium radioecology and dosimetry, *Fusion Sci. Technol.* **54(1)** (2008) 237–242.
- [133] GALERIU, D., MELINTESCU, A., STRACK, S., ATARASHI-ANDOH, M., KIM, S.B., An overview of organically bound tritium experiments in plants following a short atmospheric HTO exposure, *J. Environ. Radioact.* **118** (2013) 40–56.
- [134] MURPHY, C.E., Jr., Modelling tritium transport in the environment, *Radiat. Prot. Dosim.* **16(1-2)** (1986) 51–58.
- [135] KOROLEVYCH, V., KIM, S.B., Modelling and validation of OBT formation in tomato and potato plants, *Fusion Sci. Technol.* **60** (2011) 1288–1291.
- [136] STRACK, S., DIABATÉ, S., MÜLLER, J., RASKOB, W., Organically Bound Tritium Formation and Translocation in Crop Plants, Modelling and Experimental Results, *Fusion Technol.* **28** (1995) 951–956.
- [137] STRACK, S., DIABATÉ, S., RASKOB, W., Organically bound tritium in plants: insights gained by long-term experience in experimental and modelling research, *Fusion Sci. Technol.* **48** (2005) 767–770.
- [138] ATARASHI-ANDOH, M., AMANO, H., KAKIUCHI, H., ICHIMASA, M., ICHIMASA, Y., Formation and retention of organically bound deuterium in rice in deuterium water release experiment, *Health Phys.* **82** (2002) 863–868.
- [139] RASKOB, W., Enhancement of accident consequence assessment model for tritium UFOTRI to include a wider variety of human foodstuffs, The Sixth International Conference on Tritium Science and Technology, 11–16 November 2001, Tsukuba, Japan, *Fusion Sci. Technol.* **41(3, Part 2)** (2002) 346–350.
- [140] MOSES, V., CALVIN, M., Photosynthesis studies with tritiated water, *Biochim. Biophys. Acta.* **33** (1959) 297–312.



- [141] THOMPSON, R.G., NELSONS, C.D., Photosynthetic assimilation and translocation of  $^3\text{H}$ - and  $^{14}\text{C}$ -organic compounds after  $^3\text{HHO}$  and  $\text{iC}_2\text{O}_2$  were simultaneously offered to a primary leaf of soybean, *Can. J. Bot.* **49** (1971) 757–766.
- [142] BELOT, Y., Tritium in plants: a review, *Radiat. Prot. Dosim.* **16** (1986) 101–105.
- [143] FONDY, B., GEIGER, D.R., Diurnal pattern of translocation and carbohydrate metabolism in source leaves of *Beta vulgaris* L, *Plant Physiol.* **70** (1982) 671–676.
- [144] KIM, S.B., KOROLEVYCH, V., Quantification of exchangeable and non-exchangeable organically bound tritium (OBT) in vegetation, *J. Environ. Radioact.* **118** (2013) 9–14.
- [145] MELINTESCU, A., GALERIU, D. Exchange Velocity Approach and the Role of Photosynthesis for Tritium Transfer from Atmosphere to Plants, *Fusion Sci. Technol.* **60(3)** (2011) 1179–1182.
- [146] GALERIU, D., MELINTESCU, A., Relevance of Night Production of OBT in Crops, Oral Presentation at 11<sup>th</sup> International Conference on Tritium Science and Technology (TRITIUM 2016), accepted to *Fusion Sci. Technol.* (2016) FST16-174R1.
- [147] GALERIU, D., MELINTESCU, A., Carbon-14 dynamics in rice: an extension of the ORYZA2000 model, *Radiat. Environ. Biophys.* **53** (2014) 187–202.
- [148] MARO, D., VERMOREL, F., ROZET, M., AULAGNIER, C., HÉBERT, D., LE DIZÈS, S., VOISEUX, C., SOLIER, L., COSSONNET, C., GODINOT, C., FIÉVET, B., LAGUIONIE, P., CONNAN, O., CAZIMAJOU, O., MORILLON, M., LAMOTTE, M., The VATO project: An original methodology to study the transfer of tritium as HT and HTO in grassland ecosystem, *J. Environ. Radioact.* **167** (2017) 235–248.
- [149] KOROLEVYCH, V., KIM, S.B., Relation between the tritium in continuous atmospheric release and the tritium contents of fruits and tubers, *J. Environ. Radioact.* **118** (2013) 113–120.
- [150] INTERNATIONAL ATOMIC ENERGY AGENCY, Modelling the Environmental Transfer of Tritium and Carbon-14 to Biota and Man, Report of the Tritium and Carbon-14 Working Group of EMRAS Theme 1, The Potato Scenario, p. 226–246, Report included on the Companion CD to:  
INTERNATIONAL ATOMIC ENERGY AGENCY, Environmental Modelling for Radiation Safety (EMRAS) — A Summary Report of the Results of the EMRAS Programme (2003–2007), IAEA-TECDOC-1678, IAEA, Vienna (2012).  
<https://www-ns.iaea.org/downloads/rw/projects/emras/draft-final-reports/emras-tritium-wg.pdf>
- [151] DINGMAN, S.L., Physical Hydrology: Third Edition (2015) 643 pp.
- [152] KOROLEVYCH, V., KIM, S.B., DAVIS, P.A., OBT/HTO ratio in agricultural produce subject to routine atmospheric releases of tritium, *J. Environ. Radioact.* **129** (2014) 157–168.
- [153] CANADIAN NUCLEAR SAFETY COMMISSION, Radioactive Release Data from Canadian Nuclear Power Plants 2001-10 INFO-0210/Rev. 14, CNSC, Ottawa (2012).

- [154] CANADIAN NUCLEAR SAFETY COMMISSION, Tritium Activity in Garden Produce from Pembroke in 2007 and Dose to the Public, CNSC, Ottawa (2010).
- [155] CANADIAN NUCLEAR SAFETY COMMISSION, Environmental Fate of Tritium in Soil and Vegetation, Part of the Tritium Studies Project, CNSC, Canada (2013).
- [156] MIHOK, S., WILK, M., LAPP, A., ST-AMANT, N., KWAMENA, N.-O.A., CLARK, I.D., Tritium dynamics in soils and plants grown under three irrigation regimes at a tritium processing facility in Canada, *J. Environ. Radioact.* **153** (2016) 176–187.
- [157] YAMAZAWA, H., A one-dimensional dynamical soil-atmosphere tritiated water transport model, *Environ. Model. Softw.* **16** (2001) 739–751.
- [158] COLLATZ, G.J., BALL, J.T., GRIVET, C., BERRY, J.A., Physiological and environmental regulation of stomatal conductance, photosynthesis, and transpiration: a model that includes a laminar boundary layer, *Agricultural and Forest Meteorology* **54** (1991) 107–136.
- [159] COLLATZ, G.J., RIVBAS-CARDO, M., BERRY, J.A., Coupled photosynthesis-stomatal conductance model for leaves of C4 plants, *Aust. J. Plant Physiol.* **19** (1992) 519–538.
- [160] FARQHAR, G.D., VON CAEMMERER, S., BERRY, A., A biochemical model of photosynthetic CO<sub>2</sub> assimilation in leaves of C3 species, *Planta* **149** (1980) 78–90.
- [161] ARORA, V.K., Simulating energy and carbon fluxes over winter wheat using coupled land surface and terrestrial ecosystem models, *Agricultural and Forest Meteorology* **118** (2003) 21–47.
- [162] RIEDO, M., GRUB, A., ROSSET, M., FUHRER, J., A pasture simulation model for dry matter production and fluxes of carbon, nitrogen, water and energy, *Ecol. Model.* **105** (1998) 141–183.
- [163] WARE, A., ALLOTT, R.W., Review of methods for the Analysis of Total Tritium and Organically Bound Tritium, NCAS/TR/99/003 (1999).
- [164] WORKMAN, W.J.G., KIM S.B., KOTZER T.G., Inter-laboratory comparison of organically bound tritium measurements in environmental samples, *Fusion Sci. Technol.* **48** (2005) 763–766.
- [165] POINTURIER, F., BAGLAN N., ALANIC, G., CHIAPPINI, R., Determination of organically bound tritium background level in biological samples from a wide area in the south-west of France, *J. Environ. Radioactiv.* **68** (2003) 171–189.
- [166] POINTURIER, F., BAGLAN N., ALANIC, G., A method for the determination of low-level organic-bound tritium activities in environmental samples, *Appl. Radiat. Isot.* **61** (2004) 293–298.
- [167] PALOMO, M., PENALVER, A., AGUILAR, C., BORRULL, F., Tritium activity levels in environmental water samples from different origins, *Appl. Radiat. Isot.* **65** (2007) 1048–1056.
- [168] STANGA, D., CASSETTE, P., Improved method of measurement for tritiated water standardization by internal gas proportional counting, *Appl. Radiat. Isot.* **64** (2006) 160–162.

- [169] KIM, M-A., BAUMGÄRTNER, F., Equilibrium and non-equilibrium partition of tritium between organics and tissue water of different biological systems, *Appl. Radiat. Isot.* **45** (1994) 353–360.
- [170] FUMA, S., INOUE, Y., Simplified and Sensitive Analysis of Organically Bound Tritium in Tree Rings to Retrospect Environment Tritium Levels, *Appl. Radiat. Isot.* **46** (1995) 991–997.
- [171] MARO, D., ST-AMAND, N., KWAMENA, N.O., HEBERT, D., SOLIER, L., CONNAN, O., Campagne d’intercomparaison réalisée au Canada pour la mesure du tritium dans l’environnement, étude IRSN-CCSN, Rapport IRSN/PRP-ENV/SERIS/2014-00035 (2014) p. 31 (in French).
- [172] KIM, S.B., DAVIS, P.A., OBT/HTO Ratios in Plants, COG report, COG-06-3053 (2007).
- [173] KIM, S.B., OLFERT, J., BAGLAN, N., St-AMAND, N., CARTER, B., CLARK, I., BUCUR, C., Canadian inter-laboratory organically bound tritium (OBT) analysis exercise, *J. Environ. Radioactiv.* **150** (2015) 236–241.
- [174] BAGLAN, N., COSSONNET, C., ROCHE, E., KIM, S.B., CROUDACE, I., WARWICK, P., Feedback of the third interlaboratory exercise organised on wheat in the framework of the OBT working group, *J. Environ. Radioact.* **181** (2018) 52–61.
- [175] OTA, M., KWAMENA, N.A., MIHOK, S., KOROLEVYCH, V., Role of soil-to-leaf tritium transfer in controlling leaf tritium dynamics: Comparison of experimental garden and tritium-transfer model results, *J Environ Radioact.* **178-179** (2017) 212–231.
- [176] JEAN-BAPTISTE, P., FOURRE, E., BAUMIER, D., DAPOIGNY, A., Environmental OBT/TFWT Ratios Revisited, *Fusion Sci. Technol.* **60(4)** (2011) 1248–1251.
- [177] MARO, D., MASSON, M., FIEVET, B., BAILLY DU BOIS, P., CONNAN, O., BOUST, D., GERMAIN, P., Analyse critique des données disponibles de carbone 14 et de tritium dans le Nord Cotentin et en Manche, Rapport IRSN/DEI/SECRE/2008-006, In GRNC Report (2006) 215–270 (in French).
- [178] MELINTESCU, A., GALERIU, D., Uncertainty of current understanding regarding OBT formation in plants, *J. Environ. Radioact.* **167** (2017) 134–149.
- [179] AULAGNIER, C., LE DIZÈS, S., MARO, D., HÉBERT, D., LARDY, R., MARTIN, R., GONZE, M.-A., Modelling the transfer of  $^{14}\text{C}$  from the atmosphere to grass: A case study in a grass field near AREVA-NC La Hague, *J. Environ. Radioact.* **112** (2012) 52–59.
- [180] WASSENAAR, L.I., HOBSON, K.A., Improved method for determining the stable-hydrogen isotopic composition ( $\delta\text{D}$ ) of complex organic materials of environmental interest, *Environ. Sci. Technol.* **34** (2000) 2354–2360.
- [181] AULAGNIER, C., LE DIZÈS, S., MARO, D., HÉBERT, D., LARDY, R., MARTIN, R., The TOCATT- $\chi$  model for assessing  $^{14}\text{C}$  transfers to grass: an evaluation for atmospheric operational releases from nuclear facilities, *J. Environ. Radioact.* **120** (2013) 81–93.

- [182] GONZE, M.-A., MOURLON, C., GARCIA-SANCHEZ, L., LE DIZÈS, S., NICOULAUD, V., MÉTIVIER, J.-M., SIMON-CORNU, M., GERBER P.-P., VERMOREL, F., SYMBIOSE: A Simulation Platform for Performing Radiological Risk Assessments, ICRER 2011, 19–24 June 2011, Hamilton (2011).
- [183] FARQUHAR, G.D., VON CAEMMERER, S., Modelling of photosynthetic response to environmental conditions. In: Encyclopedia of Plant Physiology, N.S., vol. 12B: Physiological plant ecology II, Water relations and carbon assimilation (LANGE, O.L., NOBEL, P.S., OSMOND, C.B., ZIEGLER, H., Eds) Springer, Berlin Heidelberg New York (1982) 549–588.
- [184] VON CAEMMERER, S., A model of photosynthetic CO<sub>2</sub> assimilation and carbon-isotope discrimination in leaves of certain C3–C4 intermediates, *Planta* **178** (1989) 463–474.
- [185] ALLEN, R.G., PEREIRA, L.S., RAES, D., SMITH, M., Crop evapotranspiration: guidelines for computing crop water requirements, FAO Irrigation and Drainage Paper 56, FAO, Rome, **300(9)** (1998) p. D05109.
- [186] LIMER, L.M.C., LE DIZÈS-MAUREL, S., KLOS, R., MARO, D., NORDÉN, M., Impacts of <sup>14</sup>C discharges from a nuclear fuel reprocessing plant on surrounding vegetation: comparison between grass field measurements and TOCATTA- $\chi$  and SSPAM<sup>14</sup>C model computations, *J. Environ. Radioact.* **147** (2015) 115–124.
- [187] RANA, G., KATERJI, N., MASTRORILLI, M., EL MOUJABBER, M., Evapotranspiration and canopy resistance of grass in a Mediterranean region, *Theor. Appl. Climatol.* **50(1–2)** (1994) 61–71.
- [188] NAGAI, H., Validation and sensitivity analysis of a new atmosphere-soil-vegetation model. Part II: Impacts on in-canopy latent heat flux over a winter wheat field determined by detailed calculation of canopy radiation transmission and stomatal resistance, *J. Appl. Meteorol.*, **42** (2003) 434–451.
- [189] KATATA, G., NAGAI, H., UEDA, H., AGAM, N., BERLINER, P.R., Development of a land surface model including evaporation and adsorption processes in the soil for the land–air exchange in arid regions, *J. Hydrometeorology* **8** (2007) 1307–1324.
- [190] KATATA, G., NAGAI, H., WRZESINSKY, T., KLEMM, O., EUGSTER, W., BURKARD, R., Development of a land surface model including cloud water deposition on vegetation, *J. Appl. Meteo. Clim.* **47** (2008) 2129–2146.
- [191] KATATA, G., KAJINO, M., HIRAKI, T., AIKAWA, M., KOBAYASHI, T., NAGAI, H., A method for simple and accurate estimation of fog deposition in a mountain forest using a meteorological model, *J. Geophys. Res.* **116** (2011) D20102.
- [192] KATATA, G., HAYASHI, K., ONO, K., NAGAI, H., MIYATA, A., MANO, M., Coupling atmospheric ammonia exchange process over a rice paddy field with a multi-layer atmosphere-soil-vegetation model, *Agricultural and Forest Meteorology*, **180** (2013) 1–21.
- [193] KATATA, G., KAJINO, M., MATSUDA, K., TAKAHASHI, A., NAKAYA, K., A numerical study of the effects of aerosol hygroscopic properties to dry deposition on a broad-leaved forest, *Atmos. Environ.* **97** (2014) 501–510.

- [194] OTA, M., NAGAI, H., HTO transport and OBT formation after nighttime wet deposition of atmospheric HTO onto land surface, *Radioprotection* **46** (2011) S417–S422.
- [195] DOURY, A., Pratiques françaises en matière de prévision quantitative de la pollution atmosphérique potentielle Liée aux activités nucléaires, Proceedings of the CEC Seminar on Radioactive Releases and their Dispersion in the Atmosphere following a Hypothetical Reactor Accident, Volume 1, RISO, 22–25 April 1980, Commission of the European Communities, Luxembourg (1980) 403–448 (in French).
- [196] PASQUILL, F., Atmospheric Diffusion, A study of the dispersion of windborne material from industrial and other sources, Second Edition, Horwood Ellis Ltd., London (1974).
- [197] CHAMBERLAIN, A.C., EGGLETON, E.J., Washout of tritiated water vapour by rain, *Air Water Pollution* **8** (1964) 135–149.
- [198] SEPALL, O., MASON, S.G., Vapor-liquid partition of tritium in tritiated water, *Can. J. Chem.* **38** (1960) 2024–2025.
- [199] LE DIZÈS, S., MARO, D., ROZET, M., HÉBERT, D., Modeling and validating tritium transfer in a grassland ecosystem in response to  $^3\text{H}$  releases, *Fusion Sci. Technol.*, **67** (2015) 447–450.
- [200] LEWIS, C.E., NOCTOR, G., CAUSTON, D., FOYER, C.H., Regulation of assimilate partitioning in leaves, *Aust. J. Plant Physiol.* **27** (2000) 507–519.
- [201] THORNLEY, J., FRANCE, J., Mathematical Models in Agriculture: Quantitative Methods for the Plant, Animal and Ecological Sciences, CAB International, Wallingford, UK (2007).
- [202] CARBONE, M.S., TRUMBORE, S.E., Contribution of new photosynthetic assimilates to respiration by perennial grasses and shrubs: residence times and allocation patterns, *New Phytol.* **176**(1) (2007) 124–135.
- [203] MARTIN, T.A., HINCKLEY, T.M., MEINZER, F.C., SPRUGEL, D.G., Boundary layer conductance, leaf temperature and transpiration of *Abies amabilis* branches, *Tree Physiology* **19** (1999) 435–443.
- [204] AMENU, G.G., KUMAR, P., A model for hydraulic redistribution incorporating coupled soil-root moisture transport, *Hydrology and Earth System Sciences* **12** (2008) 55–74.
- [205] KIM, S.B., WORKMAN, W.J.G., DAVIS, P.A., Experimental investigation of buried tritium in plant and animal tissues, *Fusion Sci. Technol.* **54** (2008) 257–260.
- [206] CANADELL, J., JACKSON, R.B., EHLERINGER, J.R., MOONEY, H.A., SALA, O.E., SCHULZE, E.D., Maximum rooting depth of vegetation types at the global scale, *Oecologia* **108** (1996) 583–595.
- [207] JACKSON, R. B., CANADELL, J., EHLERINGER, J.R., MOONEY, H.A., SALA, O.E., SCHULZE, E.D., A global analysis of root distributions for terrestrial biomes, *Oecologia*, **108** (1996) 389–411.



## LIST OF ABBREVIATIONS

ABA	abscisic acid
ARS	acid rain site
BIOMASS	IAEA Programme on Biosphere Modelling and Assessment, 1996–2001
BWB	Ball-Woodrow-Berry (computer model)
CNL	Canadian National Laboratories
CNSC	Canadian Nuclear Safety Commission
EMRAS	IAEA programme on Environmental Modelling for Radiation Safety, 2003–2007
EMRAS II	follow-up to EMRAS, 2009-2011
E-OBT	exchangeable organically bound tritium
HT	tritium gas
HTO	tritiated water
IRSN	Institut de Radioprotection et de Sûreté Nucléaire
LAI	leaf area index
MODARIA	IAEA programme on Modelling and Data for Radiological Impact Assessments, 2012–2015
OBT	organically bound tritium
NE-OBT	non-exchangeable organically bound tritium
PASIM	PAsture SImulation Model
RMSE	root mean square error
SOC	soil organic carbon
TFWT	tissue free water tritium





## CONTRIBUTORS TO DRAFTING AND REVIEW

Aulainger, C.	Electricité de France, France
Galeriu, D. <sup>†</sup>	“Horia Hulubei” National Institute of Physics and Nuclear Engineering, Romania
Halsall, C.	International Atomic Energy Agency
Hart, D.	EcoMetrix Incorporated, Canada
Korolevych, V.	Canadian Nuclear Laboratories, Canada
Kwamena, N.-O.	Canadian Nuclear Safety Commission, Canada
Le Dizes-Maurel, S.	Institut de Radioprotection du Sûreté Nucléaire, France
Melintescu, M.A.	“Horia Hulubei” National Institute of Physics and Nuclear Engineering, Romania
Ota, M.	Japan Atomic Energy Agency, Japan
Patryl, L.	Commissariat à l'Energie Atomique, France
Proehl, G.	Consultant, Germany
Shaw, P.	International Atomic Energy Agency
Walker, J.	Consultant, Canada
Yankovich, T.	International Atomic Energy Agency

---

<sup>†</sup> Deceased.



## LIST OF PARTICIPANTS

Aulagnier, C.	Electricité de France, France
Avramov, V.	Kozloduy Nuclear Power Plant (NPP) Plc, Bulgaria
Berkovskyy, V.	Ukrainian Radiation Protection Institute, Ukraine
Bezhenar, R.	Institute of Mathematical Machines and System Problems, Ukraine
Brown, J.	International Atomic Energy Agency
Bugai, D.	Institute of Geological Sciences, Ukraine
Chen, J.	Health Canada, Canada
Czerniczyniec, M.	Autoridad Regulatoria Nuclear, Argentina
Dolin, V.	Institute of Environmental Geochemistry, National Academy of Sciences, Ukraine
Galeriu, D. <sup>†</sup>	“Horia Hulubei” National Institute of Physics and Nuclear Engineering, Romania
Guetat, P.	Commissariat à l'Energie Atomique, France
Kim, H.R.	Ulsan National Institute of Science and Technology, Republic of Korea
Kim, S.B.	Canadian Nuclear Laboratories, Canada
Kim, W.Y.	Korea Atomic Energy Research Institute, Republic of Korea
Korolevych, V.	Canadian Nuclear Laboratories, Canada
Kwamena, N.-O.	Canadian Nuclear Safety Commission, Canada
Le Dizès-Maurel, S.,	Institut de Radioprotection et de Sûreté Nucléaire, France
Lukashenko, S.	Institute for Radiation Safety and Ecology, Kazakhstan
Maro, D.	Institut de Radioprotection et de Sûreté Nucléaire, France
Melintescu, M.A.	“Horia Hulubei” National Institute of Physics and Nuclear Engineering, Romania

---

<sup>†</sup> Deceased.

Nagai, H.	Japan Atomic Energy Agency, Japan
Ota, M.	Japan Atomic Energy Agency, Japan
Pastor, L.	Electricité de France, France
Patryl, L.	Commissariat à l'Energie Atomique, France
Proehl, G.	Consultant, Germany
Siclet, F.	Electricité de France, France
Walker, J.	Consultant, Canada
Wellings, J.	Public Health England, United Kingdom
Willemsen, S.	Nuclear Research and Consultancy Group, Netherlands
Yankovich, T.	International Atomic Energy Agency
Yu, C.	Argonne National Laboratory, United States of America

**MODARIA Technical Meetings, IAEA Headquarters, Vienna**

19–22 November 2012, 11–15 November 2013, 10–14 November 2014,  
9–13 November 2015

**Interim Working Group Meetings, MODARIA Working Group 7**

Cherbourg, France, 10–13 June 2014, Vienna, Austria, 22–26 June 2015



**IAEA**

International Atomic Energy Agency

No. 26

## ORDERING LOCALLY

IAEA priced publications may be purchased from the sources listed below or from major local booksellers.

Orders for unpriced publications should be made directly to the IAEA. The contact details are given at the end of this list.

### NORTH AMERICA

***Bernan / Rowman & Littlefield***

15250 NBN Way, Blue Ridge Summit, PA 17214, USA

Telephone: +1 800 462 6420 • Fax: +1 800 338 4550

Email: [orders@rowman.com](mailto:orders@rowman.com) • Web site: [www.rowman.com/bernan](http://www.rowman.com/bernan)

### REST OF WORLD

Please contact your preferred local supplier, or our lead distributor:

***Eurospan Group***

Gray's Inn House

127 Clerkenwell Road

London EC1R 5DB

United Kingdom

***Trade orders and enquiries:***

Telephone: +44 (0)176 760 4972 • Fax: +44 (0)176 760 1640

Email: [eurospan@turpin-distribution.com](mailto:eurospan@turpin-distribution.com)

***Individual orders:***

[www.eurospanbookstore.com/iaea](http://www.eurospanbookstore.com/iaea)

***For further information:***

Telephone: +44 (0)207 240 0856 • Fax: +44 (0)207 379 0609

Email: [info@eurospangroup.com](mailto:info@eurospangroup.com) • Web site: [www.eurospangroup.com](http://www.eurospangroup.com)

### Orders for both priced and unpriced publications may be addressed directly to:

Marketing and Sales Unit

International Atomic Energy Agency

Vienna International Centre, PO Box 100, 1400 Vienna, Austria

Telephone: +43 1 2600 22529 or 22530 • Fax: +43 1 26007 22529

Email: [sales.publications@iaea.org](mailto:sales.publications@iaea.org) • Web site: [www.iaea.org/publications](http://www.iaea.org/publications)



**International Atomic Energy Agency  
Vienna**